Future-Proof Research Vessels

Analysis of Decarbonisation Strategies under Market Uncertainty

MSc Marine Technology - Thesis

Charlotte S. Wirooks

Delft University of Technology

TU Delft

FASSMER

This page is left blank intentionally.

Thesis for the degree of Master of Science (MSc) in Marine Technology
in the specialization of Ship Design

Future-Proof Research Vessels

Analysis of Decarbonisation Strategies under Market Uncertainty

By

Charlotte S. Wirooks

Performed at

Fassmer GmbH & Co. KG

This thesis (MT.25/26.008.M) is classified as confidential in accordance with the general conditions for projects performed by the TU Delft.

28th of October 2025

Company supervisor
Responsible supervisor: Dipl.-Ing. T. Funk

Thesis exam committee
Chair/Responsible Professor: Dr. ir. A. A. Kana
Staff Member: Ir. A. Souflis-Rigas
Staff Member: Dr. ir. R. de Winter
Staff Member: Dr. ir. M. A. Zagorowska
Company Member: Dipl.-Ing. T. Funk

Author Details:
Studynumber: 6038875

Cover:
Research vessel *Atair* by Fr. Fassmer GmbH & Co. KG

TU Delft

FASSMER

This page is left blank intentionally.

Preface

I am proud and delighted to present my master thesis. Writing it did not involve the sleepless nights that so many warn about - in fact, I enjoyed most of the process.

Seven years ago, I began my dual studies, learning how to weld and work with steel. Now, I find myself here, close to finishing my Master's degree in Marine Technology. Along the way, my path has taken from Germany to the Netherlands and back again, from practical shipbuilding to academic research, and from working with steel to writing about future-proof vessels. This thesis feels like the point where all these experiences come together - and while it concludes my studies, it also marks the beginning of what lies ahead.

My motivation for the topic came from a strong interest in sustainability and the conviction that the maritime industry must play its part in creating a cleaner future. Ships are vital to our world, but their impact on the environment cannot be ignored. Through my work at Fassmer, research vessels naturally became the focus of this thesis. And of course, I should also admit that my strong will to graduate was, in its own way, a motivation too.

I would especially like to thank my academic supervisor, Austin Kana. His continuous, constructive feedback and patience have guided me through this work. Your support has been essential, and I am deeply grateful for the time and energy you dedicated to my work.

I am also very thankful to Fassmer, not only for making this thesis possible but also for supporting my studies over the past years. Being able to combine academic research with practical shipbuilding experience has been a great opportunity. I would also like to thank my company supervisor Tobias Funk, for his support and for accompanying me through the company side of this project.

My warm thanks also go to the TU Delft. I am grateful to have had the chance to study here - for the, honestly sometimes hard, academic challenges, but also for the amazing student life that made these years so enjoyable. Special thanks go to the friends I found there, who turned stressful weeks into something lighter, and shared countless bike rides, coffee breaks, and study sessions. You made Delft not just a place to study, but a place to feel at home.

I am deeply thankful for my family - especially my parents, who have been there for me from the very beginning, and my sister, who joined a little later. Thank you for always believing in me, encouraging me to even higher jumps, and celebrating every success with me. I couldn't have done it without you.

I would also like to thank my boyfriend, Tim. We both expected this thesis to be a very stressful time, but it turned out differently. By filling our days with so many other moments, you gave me the chance to rest, to laugh, and to enjoy this period far more than I imagined - and for that, I am especially grateful.

With this, I kindly invite you to read and enjoy my thesis.

Charlotte S. Wirooks
Bremen, October 2025

This page is left blank intentionally.

AI Acknowledgement

During the preparation of this work the author used ChatGPT (OpenAI, https://chatgpt.com) in order to check grammar and spelling, and for support with the writing style. After using this tool, the author reviewed and edited the content as needed and takes full responsibility for the content of the publication.

This page is left blank intentionally.

Summary

This thesis investigates how alternative fuels and energy reduction technologies influence the technical and economic viability of research vessels under market uncertainties and varying operational profiles. The study addresses the growing need for decarbonisation in the maritime sector, where research vessels face particular possibilities due to limited regulatory requirements, and constraints due to their demanding mission requirements.

Research vessels, which are exempt from many regulatory emission frameworks, operate under highly variable mission profiles that challenge conventional decarbonisation approaches. The review identifies a significant gap in existing studies, which typically overlook the unique operational demands of these vessels.

The literature analysis evaluates a wide array of fuels - including fossil based fuels with lower carbon intensity such as LNG and LPG, renewable, diesel like fuels as HVO, hydrogen carriers as ammonia, hydrogen, and sodium borohydride, alcohol fuels as methanol, as well as metal-based fuels like iron powder -, wind assisted propulsion systems, and energy reduction methods as exhaust heat recovery and solar systems. Assessment is done on physical and chemical properties, emissions, safety, technological readiness and availability, and costs.

To handle the complex and uncertain decision environment, the study proposes the Many Objective Robust Decision Making Framework combined with an Epoch-Era Analysis that models the most important uncertainty, namely the various operational profiles. This methodological foundation allows for evaluating the technical and economic feasibility of many different propulsive combinations across a wide range of plausible futures.

The subsequent analysis shows that no single configuration is universally optimal across all conditions. Fossil and diesel-like fuels such as LNG and HVO remain technically feasible but offer only slight emission reductions. Methanol-ICE configurations emerge as the most robust low-carbon option, offering technical feasibility across all scenarios and significant emission reduction potential. Ammonia-ICE solutions perform well under lower requirements and can approach carbon neutrality if sustainably produced. The integration of energy reduction technologies such as exhaust heat recovery and wind-assisted propulsion improves performance, but effects remain context-specific and do not fundamentally alter the main trade-off's between cost and emissions.

The analysis further shows that blended fuels (e.g., grey/green methanol or ammonia) can serve as transitional pathways, enhancing economic viability while preparing vessels for a green fuel future. A design-oriented iteration of the MORDM indicate that hull form adjustments can improve robustness, however, more detailed calculations need to be done.

In conclusion, the findings underline that future-proof research vessels will need to adopt technically feasible, robust fuel strategies that enable compliance with long-term climate goals. Methanol, and to a slightly lesser extent ammonia, currently offer the most promising pathways, while fossil and diesel-like fuels cannot ensure sustainability under future conditions.

This page is left blank intentionally.

Contents

List of Figures

List of Tables

This page is left blank intentionally.

Nomenclature

Abbreviations and Acronyms

AWI	Alfred Wegener Institute
Bft.	Beaufort
BSH	Federal Maritime and Hydrographic Agency - Bundesamt für Seeschifffahrt und Hydrographie
CapEx	Capital Expenditure
CCRV	California Coastal Research Vessel
CII	Carbon Intensity Indicator
DAP	Dynamic Adaptive Planning
DAPP	Dynamic Adaptive Policy Pathways
DLR	German Aerospace Center - Deutsches Zentrum für Luft- und Raumfahrt
DNV	Det Noske Veritas
DP	Dynamic positioning
DS	Decision Scaling
ECA	Emission Control Area
EEA	Epoch-Era Analysis
EEDI	Energy Efficiency Design Index
EHR	Exhaust heat recovery
EOA	Engineering Options Analysis
ETS	Emission Trading Scheme
FC	Fuel cell
GHG	Greenhouse gas
HVO	Hydrotreated Vegetable Oil
ICE	Internal combustion engine
IG	Info-Gap Decision Theory
IGF	International Code of Safety for Ships Using Gases or Other Low-Flashpoint Fuels
IMO	International Maritime Organization
Inst.	Installation
L	Policy Levers
LBSI	Lean burn spark ignited engines
LH_2	Liquefied hydrogen
LNG	Liquefied Natural Gas
LPG	Liquefied Petroleum Gas
LR	Lloyd's Register
M	Measures of performance
Main.	Maintenance
MARPOL	International Convention for the Prevention of Pollution from Ships
MCFC	Molten carbonate fuel cell
MDO	Marine diesel oil
MDP	Markov Decision Process
MORDM	Many Objective Robust Decision Making

n/a	not available
NPV	Net Present Value
OpEx	Operational Expenditure
PEMFC	Polymer electrolyte mebrane fuel cell
PV	Photovoltaic
PV	Present Value
R	Relationships
RDM	Robust Decision Making
ROA	Real Option Analysis
SEEMP	Ship Energy Efficiency Management Plan
SOFC	Solid oxide fuel cell
SOLAS	International Convention for the Safety of Life at Sea
TtW	Tank to wake
WASP	Wind-assisted ship propulsion
WtT	Well to tank
WtW	Well to Wake
X	Exogenous uncertainties

Chemical Symbols

CH_3OH	Methanol
CH_4	Methane
CO_2	Carbon dioxide
Fe	Iron
Fe_2O_3	Iron Oxide
H_2	Hydrogen
H_2O	Water
KOH	Potassium hydroxide
N_2O	Nitrous oxide
$NaBH_4$	Sodium borohydride
$NaBO_2$	Sodium metaborate
NaOH	Sodium hydroxide
NH_3	Ammonia
NO_x	Nitrogen oxides
O_2	Oxygen
SO_x	Sulphur oxides

Subscripts

a	Above waterline
BCV	Base case vessel
c	Converter
$conf$	Configuration
E	Effective
e	Epoch
G	Gravimetric
i	Part of mission
j	Greenhouse gases CO_2, CH_4, and N_2O
M	Midship

nR	Normal research mode
o	Outfitting
oa	Over all
pp	Between perpendiculars
pR	Precise research mode
St	Steel
$ST1$	Unprocessed steel
$ST2$	Man-hour
t	Tank
tw	Wall thickness
u	Below waterline
u	Useable space
V	Volumetric

Symbols

Δ	Difference/Change	-
η	Efficiency	%
∇	Displacement	m^3
$^L/_B$	Length-to-beam ratio	-
ρ	Density of Water	kg m^{-3}
ρ	Energy density, in combination with subscripts G or V	kW/m^3
φ_G	Power Density of Converter, in combination with subscripts G or V	kW t^{-1}
A	Area	m^2
B	Beam	m
C	Cost factor	EUR kW^{-1}; EUR t^{-1}; EUR kWh^{-1}; EUR h^{-1}
c	Factor	-
c_B	Block Coefficient	-
c_f	Tank to wake greenhouse gas emission factor	g/g
c_M	Midship area coefficient	-
C_{FR}	Specific production time	h t^{-1}
c_{slip}	Non-combusted fuel coefficient	%
$CapEx$	Capital expenditure	EUR
$CarbonEx$	Expenditure due to carbon costs	EUR
$CO_{2eq\,WtT}$	Emission factor well to tank	g kWh^{-1}
D	Draught	m
E	Energy	kWh
E	Total emission from the production and use of the fuel	g_{CO_2eq} MJ^{-1}
F	Feasibility fraction	%
f	Time fraction	-
f_j	Factor of global warming potential compared to CO_2	-
Fn	Froude number	-
$FuelEx$	Fuel expenditure	EUR
g	Gravity of earth	m s^{-2}
K	Outfitting Weight Density	t m^{-3}
K	Steel factor	-
L	Length	m
LCV	Lower Calorific Value	kWh kg^{-1}
$MaintEx$	Maintenance Expenditure	EUR

n	Number	-
N_{PoB}	Number of people onboard	-
$OpEx$	Operational expenditure	EUR
P	Power	kW
PV	Present Value	EUR
r	Discount factor	%
S	Wetted surface	m^2
T	Total Time of One Mission	d
t	Time	d
V	Volume	m^3
v_s	Transit speed, service speed	kn
W	Weight	t
x	Uncertainty deviation	%

Units

°C	Degree Celsius	
d	Day	86 400 s
EUR	Euro	
g	Gram	10^{-3} kg
GJ	Gigajoule	10^9 kg m^2 s^{-2}
knts	knots	0.5144 m s^{-1}
kW	Kilowatt	10^3 kg m^2 s^{-3}
kWh	Kilowatt-hour	3600 kg m^2 s^{-2}
l	Litre	10^{-3} m^3
MJ	Megajoule	10^6 kg m^2 s^{-2}
mm	Millimetre	10^{-3} m
MPa	Mega-Pascal	10^6 m^{-1} kg s^{-2}
MW	Megawatt	10^6 kg m^2 s^{-3}
nm	nautical mile	1 852 m
t	ton	10^3 kg
US-$	US-Dollar	

1 Introduction

1.1. Background

Research vessels are important for exploring our planet. However, they should not destroy any habitats in the process. This is why more and more research vessels are being built using low-emission fuels, such as those built at the Fassmer shipyard in Berne, northern Germany, in recent years. Examples of those ships include the *Uthörn*, a 35 m vessel powered by methanol (Fr. Fassmer GmbH & Co.KG, n.d.-a), and the *Atair*, a 75 m vessel driven by diesel and Liquefied Natural Gas (LNG) engines (Fr. Fassmer GmbH & Co.KG, n.d.-b). However, in addition to changing the fuel, wind-assisted ship propulsion (WASP) should also be considered, as it can reduce carbon dioxide (CO_2) emissions.

While international agreements like the International Convention for the Prevention of Pollution from Ships (MARPOL) of the International Maritime Organization (IMO) regulate air pollution, research vessels are exempt from certain provisions of Annex VI, Regulations for the Prevention of Air Pollution from Ships (IMO, 1978). For instance, requirements such as the Energy Efficiency Design Index (EEDI) and Carbon Intensity Indicator (CII) primarily apply to commercial vessels like containerships and cruise ships, which are responsible for transporting cargo and passengers (IMO, 1997). The EU Emissions Trading Scheme (ETS), which now also includes maritime transport (European Parliament & European Council, 2023b), is also not applicable to research vessels, as it is only designed for the commercial transport of cargo and passengers (European Parliament, 2015). This means that, unlike cargo or passenger ships, research vessels may not be subject to the same regulatory and financial pressures associated with implementing new technology and carbon pricing. However, independent sustainability efforts and future regulatory developments will influence decarbonisation strategies. The transition to alternative fuels and WASP for research vessels is not primarily driven by regulatory compliance, but rather by institutional, scientific, and operational sustainability goals.

The economic viability of such transitions remains uncertain due to fluctuating fuel prices, technological advancements, and operational variability. Research vessels have unique and highly variable operational profiles. These range from transit voyages to slow speed or stationary periods for sampling, often in diverse environments such as polar regions, coastal areas, and open oceans. Their significant onboard energy demands for laboratory equipment, acoustic systems, and environmental controls further differentiate them from transport vessels.

1.2. Research Gap

Despite significant advances in low-emission technologies for the maritime sector, there remains a lack of studies addressing the integration of decarbonisation strategies onboard of research vessels. Existing research primarily focuses solely on alternative energy carriers (Streng, 2021; Terün, 2020) or WASP for specific types of vessels, such as cruise ships (Lange, 2024) or cargo ships (Kisjes, 2017), often neglecting the unique operational requirements of research vessels.

Despite ongoing efforts in research and development of carbon-reducing technologies for the maritime

sector, significant uncertainties remain regarding their practical implementation. Key uncertainties include fluctuating fuel prices, the (long-term) availability of alternative fuels, and evolving regulations. Technically, the scalability of alternative fuels, the weight of WASP, and the varying operational profiles of research vessels add another layer of uncertainties.

The thesis aims to address these gaps by providing an evaluation of the influence of alternative fuels, and WASP on CO_2 emissions, focusing on different operational profiles of research vessels. By bridging between theoretical potential and practical implementation, this research will offer valuable insights into optimizing design choices for sustainable maritime operations in the research sector.

1.3. Project Task

The thesis aims to assess the technical and economic viability of alternative fuels, such as hydrogen, ammonia, methanol, and biofuels, as well as WASP, like Flettner Rotors, sails, and kites. The analysis will be conducted with a focus on deep-sea research vessels, considering their operational requirements and mission types. In this way, the impact of different fuel and propulsion system choices can be assessed for different applications.

The thesis will estimate fuel consumption and bunkering requirements for various decarbonisation strategies, ensuring that technical feasibility is taken into account alongside economic factors. A market analysis will be conducted under uncertainties to evaluate how fluctuating fuel prices, supply chain challenges, and regulations influence design decisions.

1.4. Research Question

The main research question is as follows:

How do alternative fuels and energy reduction technologies influence the technical and economic viability of research vessels under market uncertainties and different operating profiles?

Sub-questions address the operational profiles of research vessels, efficiency of WASP, regulatory framework, and uncertainties. Sub-questions 1 to 3 will be answered in the literature research, while sub-questions 4 to 8 will be answered in the research period.

1. *What is the current state-of-the-art in the design of research vessels, considering regulatory requirements, operational profiles, and fuel consumption patterns?*
2. *What energy reduction methods and alternative energy options are technically feasible, including alternative fuels and WASP?*
3. *Which research methods, concerning parametric modelling, uncertainty analysis, and economic evaluation, are best suited to assess the feasibility of alternative fuels and WASP for research vessels?*
4. *How do operational profiles of research vessels impact the feasibility and performance of alternative fuels and WASP?*
5. *How does the efficiency of WASP and exhaust heat recovery systems influence the overall decarbonisation potential of research vessels?*
6. *What is the economic impact of the introduction of alternative fuels and WASP for research vessels, taking into account investment costs, operating costs and market uncertainties?*
7. *What are the emission reduction potentials of combined decarbonisation strategies?*
8. *How can the model and results be verified and validated to ensure their reliability for real-world application in research vessel decarbonisation?*

1.5. Expected Outcomes

The thesis aims to provide an analysis of the economic and technical feasibility of alternative energy carriers for research vessels. Key aspects of this market analysis are the operational pattern of research vessels, current and future fuel prices, and the influence of regulatory framework.

A key outcome of this thesis will be the elaboration and categorization of operational profiles of research vessels, helping to understand how different voyage durations, speeds and fuel consumption affect the selection of alternative fuels and WASP. Furthermore, international and EU directives will be analysed to ensure compatibility with these laws, as well as to assess the economic impacts of measures such as carbon taxes and other financial incentives.

Finally, by identifying and modelling the key uncertainties that affect the market for alternative fuels and WASP, this study will develop a decision-making framework. This thesis aims to help identify decarbonisation strategies and ensure that both technical feasibility and economic viability are taken into account.

This page is left blank intentionally.

2

Design of Research Vessels

Chapter 2 provides an overview of the design of research vessels, answering the first sub-question:

What is the current state-of-the-art in the design of research vessels, considering regulatory requirements, operational profiles, and fuel consumption patterns?

The chapter begins with an overview of the classification of different vessel types (Section 2.1). It outlines typical operational profiles and fuel consumption patterns, which are fundamental for evaluating decarbonisation potential under real-world conditions (Section 2.2). This is followed by a survey of current alternative fuel systems used in modern research vessels and typical geometric properties (Section 2.3). Lastly, an analysis of relevant international, European, classification, and national regulations that influence vessel design and decarbonisation strategies is given (Section 2.4).

2.1. Operational Profiles

While regulations define the technical envelope for ship design, the actual decarbonisation potential depends heavily on how vessels are operated. Following Nieuwejaar et al., 2019, research vessels can be classified in 4 different classes, namely the global class, the ocean class, the regional class, and the coastal and local class.

Global-class research vessels operate worldwide, and accommodate more than 25 scientists (Nieuwejaar et al., 2019). They support diverse scientific missions with extensive deck space, advanced laboratory facilities, and specialized equipment. Some are ice-strengthened for polar operations, others support deep-submergence vehicles or multi-channel seismic survey equipment. Examples are the French *Pourquoi pas?*, the German *Sonne* (Figure 2.1a), or the Norwegian *Dr. Fridtjof Nansen*. 18 % of the European research vessel fleet are classified as Global.

Ocean-class research vessels, while sharing many features with their global counterparts, are typically confined to a single ocean and support interdisciplinary research and surveys (Nieuwejaar et al., 2019). They accommodate more than 20 scientists. Examples are the Dutch *Pelagia* (Figure 2.1b) and the Danish *Dana*. Ocean-class research vessels make up the smallest group, accounting for 15 % of the European research vessel fleet.

Regional-class research vessels operate in a specific geographic region, closely to the coast and in deep waters, and are designed to withstand seasonal and local conditions (Nieuwejaar et al., 2019). Nieuwejaar et al. classify 36 % of the European Research Vessel fleet as regional. Examples include the Polish *Oceanograf* (Figure 2.1c) or the Swedish *New Skagerak*.

Coastal-class vessels play a central role in scientific activities where human activity and resource use have the greatest impact (Nieuwejaar et al., 2019). Missions are primarily guided by local and regional demands. Coastal-class vessels are equipped for conducting night operations. Local-class vessels operate in nearby waters with a very small scientific team and typically return to port daily due to a lack

(a) Global Class: *Sonne*, (Federal Ministry of Research, Technology and Space, 2022).

(b) Ocean Class: *Pelagia* (Eurofleets, n.d.).

(c) Regional Class: *Oceanograf* (Seatech Engineering, 2017).

(d) Coastal and Local Class: *CRV Leonardo* (Baltic Shipping, n.d.).

Figure 2.1: Examples of Vessels for Each Class.

of overnight facilities. 31 % of the European research vessel fleet are classified as local and coastal. Examples are the Greek *Aegaeo*, or the Italian *CRV Leonardo* (Figure 2.1d).

The list of European research vessels provided by Nieuwejaar et al. is not complete, as it only includes vessels that are publicly available for research purposes. Furthermore, vessels operating on a daily basis were excluded.

This thesis further narrows its focus to global- and ocean-class vessels. Although they make up only a third of the European research fleet, there are several reasons for this choice. First, due to their longer mission durations, greater onboard power demands, and larger size, the vessels likely account for a big share of total fuel consumption and emissions. Targeting these high-consumption vessels offers the greatest potential for meaningful emission reductions. Second, the integration of alternative fuels and energy systems presents the most critical challenges on these vessel types. Their operational range limit opportunities for refuelling. Therefore, physical limitations of low-energy-density fuels are more pronounced on global- and ocean-class vessels than on smaller ships with a smaller range. Third, a detailed engine load profile is only available for the relatively large research vessel *Sonne*. Including smaller vessel classes would introduce inconsistency in the comparative assessment of decarbonisation technologies, as no equivalent operational data exists for those classes. Finally, global and ocean-class research vessels are often used in missions that are the subject of international media attention. As such, they carry strategic and symbolic weight in demonstrating technological leadership and environmental responsibility. For these reasons, the global and ocean classes are considered the most relevant and technically demanding vessels for investigating the feasibility of low- and zero-emission propulsion systems.

Understanding the classification and operational scope of research vessels is a key factor in assessing their energy requirements. However, vessel class alone does not determine fuel consumption. The nature of missions - transit, station-keeping, or active research - directly influences power demand and engine load. To evaluate the decarbonisation potential of these vessels, the examination of typical operational fuel consumption patterns is therefore fundamental.

2.2. Operational Fuel Consumption Patterns

The operational fuel consumption pattern of research vessels is heavily influenced by mission-specific tasks. Unlike commercial shipping, where transit is the primary activity, research vessels alternate between transit, station-keeping, and scientific operations, each with distinct fuel demand characteristics.

According to Meinders, 2025, the German research vessels *Sonne* and *Maria S. Merian* spend approximately 40 % of their time in transit, 44 % on different research stations, and 16 % in ports or shipyards.

An example of different engine loads can be seen in the load profile of the *Sonne* under various conditions as shown in Figure 2.2. The *Sonne* is a 116-metre research vessel equipped with a diesel-electric propulsion system and capable of missions lasting up to 52 days, with accommodation for up to 40 scientists (Deutsche Forschungsgemeinschaft e. V., n.d.). Her primary research regions are the Indian and Pacific Oceans.

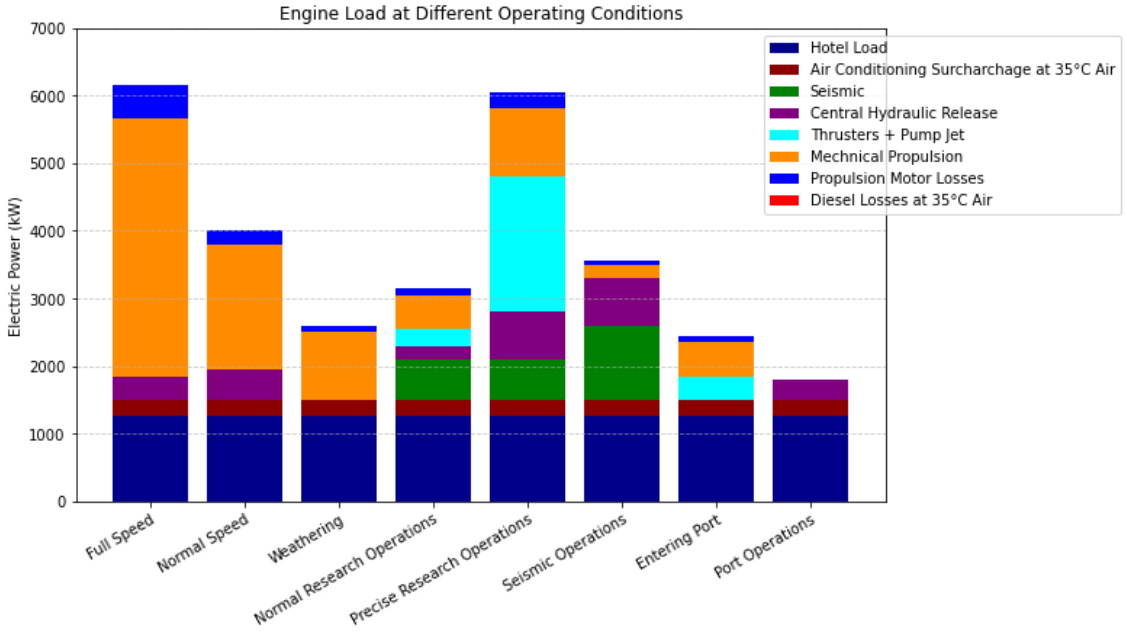

Figure 2.2: Engine Load at Different Operating Conditions (Meinders, 2025), translated.

At full speed (15 knots), the vessel experiences its highest total power demand of about 6 100 kW. The majority of this load comes from mechanical propulsion. A significant but smaller proportion of the load also comes from the hotel systems, which remains consistent across all operating conditions. This driving condition is only used in exceptional cases.

At the normal transit speed of 12 knots, the vessel's power demand decreases significantly to around 4 000 kW. Mechanical propulsion remains the largest contributor, but the overall demand is much lower compared to full speed. Auxiliary systems, such as air conditioning and hotel load, continue to provide a stable base load.

During weathering - dynamic positioning (DP) at station - the power demand drops further to about 2 600 kW. Propulsion requirements are reduced significantly.

In normal research operations, where DP is maintained with precision up to 3 metres and wind forces of up to 4 Beaufort (Bft.), power demand is about 3 100 kW. This is due to the possible activation of the seismic equipment, but as well due to hydraulic systems and the thrusters and pump jets for the positioning system.

Precise research demands nearly as much power as full speed (6 000 kW). This is largely due to the intense use of thrusters and the pump jet, which holds the vessel in position with 0.5 metre accuracy - even under wind forces higher than Bft. 4.

During seismic operations, the vessel travels at slow speeds (around 4 knots) while running compressors for seismic data collection. Although thrusters and pump jets are inactive in this mode, the vessel still consumes a considerable amount of power (approximately 3 500 kW) due to the high energy requirements of the seismic systems.

When entering the port, the power load drops to about 2 500 kW. Mechanical propulsion is minimal, thrusters and pump jet support manoeuvring at low speeds. At these speeds, the propulsion motor operates inefficiently, leading to additional motor losses.

Finally, during port operations, the power demand is at its lowest, at approximately 1 800 kW. Only essential systems such as the hotel load, air conditioning, and hydraulic systems are active. There is no propulsion or seismic activity, as the vessel is docked and not engaged in any demanding operations.

These highly variable power demands illustrate the complexity of energy provisioning on research vessels. Any shift to low- or zero-emission technologies must account not only for peak and average loads, but also for how propulsion and hotel and research systems interact across different operational states. Actual energy use can vary due to changing mission demands and environmental conditions, adding uncertainty to future performance predictions. The following section examines how current vessel designs have responded to these demands - particularly those that have already begun integrating alternative fuels and hybrid propulsion systems.

2.3. Current Designs

While the majority of research vessels are still powered by conventional diesel engines, the sector is beginning to transit towards more sustainable propulsion systems. Although these vessels remain exceptions within the global research fleet, several notable examples have successfully integrated alternative fuels such as biofuels, LNG, hydrogen, and methanol. This section presents a selection of such vessels. The *Atair*, described in Section 2.3.1, has a hybrid system that combines diesel with LNG, while the *CCRV* (Section 2.3.2), combines diesel with hydrogen fuel cells (FCs). The *Uthörn* (Section 2.3.3), on the other hand, uses a methanol-electric configuration avoiding diesel propulsion.

A more special case is a vessel under construction for the German Aerospace Center (Deutsches Zentrum für Luft- und Raumfahrt, DLR). Instead of researching the environment, the purpose of the vessel is to research the integration of low-carbon hydrogen-based fuels and battery systems (DLR, 2025). Building of the 48 m long vessel was contracted at the beginning of 2025 to the Lloyd Werft Bremerhaven.

A few research vessels equipped with diesel-electric propulsion plants utilize Hydrotreated Vegetable Oil (HVO) as alternative to diesel fuel as the Swedish *R/V Svea* and the British *Sir David Attenborough* (British Antarctic Survey, 2023; Swedish University of Agricultural Sciences, 2024). While these alternative-fuelled vessels are promising in terms of emissions reduction and sustainability, they remain the exception in today's research fleet.

The following sections give an impression of research vessels using alternative fuels. Only a few research vessels have been described in greater detail, as these vessels specifically utilize propulsion systems based on alternative fuels which are not diesel like. These vessels were selected because their design requirements represent more complex challenges compared to the relatively straightforward transition from conventional diesel to renewable diesel-like fuels.

2.3.1. Atair

The survey, wreck-search and research vessel *Atair* (Figure 2.3a) is equipped with a dual-fuel system using LNG and diesel (BSH, n.d.; Fr. Fassmer GmbH & Co.KG, n.d.-b). Commissioned on the 27th of April 2021, it operates primarily in the North Sea, Baltic Sea, and the North-East Atlantic (BSH, n.d.). Measuring 75 metres in length, the vessel accommodates up to 15 scientists.

Due to its 130 cubic metre LNG tank, the Atair can be operated entirely on LNG for up to 10 days (BSH, n.d.). The Federal Maritime and Hydrographic Agency (Bundesamt für Seeschifffahrt und Hydrographie, BSH) states, that CO_2-emissions are reduced by around 20 %. Next to LNG, the dual-fuel system can also be driven with high quality diesel. In combined diesel and gas operation, the vessel has a range of around 8 000 nautical miles (nm) (Pospiech, 2019).

Table 2.1: Overview of Research Vessels (AWI, n.d.; BSH, n.d.; Fr. Fassmer GmbH & Co.KG, n.d.-a, n.d.-b; Klebanoff et al., 2021; Pospiech, 2019). Note: Data that the author was unable to find is indicated with 'n/a'.

Vessels Name	Propulsion System	Cruise Speed	Range
Atair	Diesel-Gas-Electric	13 kn	8 000 nm
CCRV	Hybrid: Diesel/Hydrogen	10 kn	2 400 nm
unnamed vessel for DLR	Hydrogen-based + Battery	n/a	n/a
Sir David Attenborough	Diesel-Electric (HVO)	13 kn	13 000 nm
RV Svea	Diesel-Electric (HVO)	11 kn	n/a
Uthörn	Methanol-Electric	10 kn	1 200 nm

2.3.2. California Coastal Research Vessel (CCRV)

In 2020, Madsen et al. published a feasibility study for a coastal research vessel called *Zero-V*, designed to be fully powered by hydrogen FCs (Madsen et al., 2020). This initial concept featured a trimaran hull optimized for stability and efficiency. However, the vessel was never constructed.

Building on this idea, Klebanoff et al., 2021, presented a new vessel concept intended to replace the *R/V Robert Gordon Sproul*. This design, called *CCRV* (Figure 2.3b), employs a hybrid propulsion system that combines hydrogen FCs with a diesel-electric drivetrain. Unlike the earlier trimaran design of *Zero-V*, the revised concept opted for a monohull due to its larger internal volume and cost-effective construction. The design includes liquefied hydrogen (LH_2) storage tanks positioned above the waterline, decreasing the working space.

The vessel is designed to store LH_2 rather than high-pressure hydrogen gas, thereby taking advantage of the similar physical and combustion properties of LH_2 and LNG. This similarity permits Klebanoff et al. the application of the International Code of Safety for Ships Using Gases or Other Low-Flashpoint Fuels (IGF) originally developed for LNG-powered vessels (Klebanoff et al., 2021). Moreover, of the 34 possible mission types, the 25 one-day missions can be carried out exclusively with the hydrogen FC system. A suitable shipyard is currently being searched for to build this monohull research vessel (Duran, 2025).

2.3.3. Uthörn

The research vessel *Uthörn* (Figure 2.3c) of the Alfred Wegener Institute (AWI), a German research centre, is one of the smaller research vessels with a length of 35 m and a range of 1 200 nm (AWI, n.d.; Fr. Fassmer GmbH & Co.KG, n.d.-a). According to the AWI, the *Uthörn* is the "first seaworthy ship powered by green methanol". The ship is equipped with two diesel engines of combined output of 600 kW being refitted to run on methanol. The ship will perform research in the German Bay.

While these early examples of research vessels with low-carbon fuels demonstrate that implementation of alternative fuels is possible on research vessels, their implementation remains limited, as their long-term viability of these designs is uncertain due to evolving fuel prices, infrastructure, and regulations. Another reason for the slow uptake is the relatively weak regulatory pressure compared to commercial shipping, which will be analysed in later sections. However, research vessel design is currently undergoing a transition, marked by the early but increasing implementation of alternative propulsion systems. Although conventional diesel propulsion remains predominant, recent developments demonstrate a shift towards integrating more sustainable technologies. The next section examines the hull proportions of existing research vessels in greater detail, analysing their typical length-to-beam ratios to better understand geometric constraints relevant to vessel design.

(a) *Atair* (Fr. Fassmer GmbH & Co.KG, n.d.-b).

(b) *CCRV* (Klebanoff et al., 2021).

(c) *Uthörn* (Jann, 2022).

Figure 2.3: Vessels described in Section 2.3.

2.3.4. Hull Proportions of Research Vessels

Besides propulsion concepts and fuel systems, the fundamental proportions of a vessel's hull strongly influence performance and feasibility. The length-to-beam ratio (L/B) is particularly important, as it affects resistance, propulsion efficiency and stability (Schneekluth & Bertram, 1998) and constrains available deck area and internal volume. While textbooks on ship design often provide indicative ranges for merchant ship types, such as 6.0 to 7.0 for cargo vessels and 6.5 to 7.5 for passenger vessels (Molland, 2008), research vessels are not usually covered as a distinct category. Their design priorities differ from those of cargo or passenger ships, since they must combine accommodation and laboratory space with diverse operational requirements. For this reason, a closer look at existing research vessels is necessary to understand their typical hull proportions. Table 2.2 shows length (L) and beam (B) of research vessels introduced earlier in this chapter and lists their corresponding L/B-ratio:

Table 2.2: Dimensions and calculated L/B ratios of selected research vessels. L/B rounded to first decimal place.

Vessel	Length [m]	Beam [m]	L/B [-]	Reference
Aegaeo	61.5	9.6	6.4	Eurofleets, n.d.
Atair	75.0	16.8	4.5	Fr. Fassmer GmbH & Co.KG, n.d.-b
CRV Leonardo	28.0	9.0	3.1	Baltic Shipping, n.d.
Dana	78.0	17.0	4.6	Nieuwejaar et al., 2019
Dr. Fridtjof Nansen	74.1	17.4	4.3	Institute of Marine Research, 2024
Maria S. Merian	95.0	19.0	5.0	Nieuwejaar et al., 2019
New Skagerak	49.0	16.0	3.1	Nieuwejaar et al., 2019
Oceanograf	49.5	14.0	3.5	University of Gdansk, 2023
Pelagia	66.0	12.8	5.2	Eurofleets, n.d.
Pourquoi pas?	107.6	20.0	5.4	Ifremer, 2020
RV Svea	69.0	16.0	4.3	Nieuwejaar et al., 2019
Sir David Attenborough	129.0	24.0	5.4	Nieuwejaar et al., 2019
Sonne	116.0	20.6	5.6	Meinders, 2025
Uthörn	35.7	9.2	3.9	Fr. Fassmer GmbH & Co.KG, n.d.-a

The values span a range from about 3.1 to 6.4, with most vessels clustering around 4.3 to 5.6. Compared to the ranges for cargo and passenger ships reported by Molland, 2008, research vessels thus exhibit generally bulkier hulls, although some exceptions, such as the *Aegaeo*, show more slender

proportions. The next section reviews the current regulatory landscape at international, European, and national levels to assess how these frameworks enable or limit the adoption of decarbonisation technologies.

2.4. Regulatory Requirements

Research vessels must comply with international and national norms and regulations in terms of safety, emissions, and operating standards. This thesis only analyses regulations for emissions, energy reduction methods, and alternative energy options, as it is assumed that other regulations are the same for all forms of propulsion.

2.4.1. International Maritime Organization Regulations

International Convention for the Prevention of Pollution from Ships (MARPOL), Annex VI

In Annex VI, Regulations for the Prevention of Air Pollution from Ships, of MARPOL, emissions of nitrogen oxides (NO_x) and sulphur oxides (SO_x) are regulated specifically in Emission Control Areas (ECA) (IMO, 1997). Marine diesel engines need to comply with Tier III (IMO, 1997, Regulation 13), in which the sulphur content of fuel oil is limited below 0.10 % of the weight (IMO, 1997, Regulation 14).

The EEDI and CII are frameworks for evaluating and reducing a vessels carbon footprint. These regulations target primarily commercial transport vessels as bulk carriers, combination carriers, container ships, and cruise passenger ships (IMO, 1997, Chapter 4).

Vessel owners need to provide a Ship Energy Efficiency Management Plan (SEEMP) (IMO, 1997, Regulation 26). For the SEEMP, the energy consumption of an individual vessel - not a fleet - is to be estimated. Various measures should be implemented to reduce this particular consumption. Ships greater than a gross tonnage of 5 000 need to provide annually carbon intensity reduction targets. Research vessel owners need to comply with this, but there are no direct restrictions, especially for ships below 5 000 gross tonnage.

Research vessels are currently exempt from certain MARPOL Annex VI instruments, such as EEDI and CII. However, the broader regulatory landscape is evolving rapidly. In April 2025, during its 83rd session (MEPC 83), the IMO approved the Net-Zero Framework, aiming for net-zero greenhouse gas (GHG) emissions from international shipping by or around 2050 (DNV, 2025b). This framework introduces mandatory emissions limits and a global GHG pricing mechanism, marking the first such comprehensive approach in the maritime sector. The regulations are set to be formally adopted in October 2025 and may take effect from 2028, becoming mandatory for ocean-going ships over 5 000 gross tonnage.

While research vessels may remain exempt from specific measures, the overarching goals of the IMO's Net-Zero Framework signal increasing pressure on all vessel types to align with global decarbonisation efforts. This highlights the importance of proactive adaptation and the consideration of alternative fuels and energy-efficient technologies in the design and operation of research vessels.

International Code of Safety for Ships Using Gases or Other Low-Flashpoint Fuels (IGF)

The IGF provides regulations for vessels using fuels with a low flashpoint (IMO, 2016, 2017b). In the International Convention for the Safety of Life at Sea (SOLAS), this flashpoint is set at 60 °C. These are, for example, methanol (Methanol Institute, n.d.), hydrogen (MAN Energy Solutions, n.d.-b), and LNG (IMO, 2017b). These fuels require specific handling, storage, and challenges addressed under the IGF Code. The code does not handle pollution matters as the majority of the mentioned regulations. Instead, it focuses on the mitigation of risks associated with the use of low-flashpoint fuels.

International Code for Ships Operating in Polar Waters (Polar Code)

The International Code for Ships Operating in Polar Waters (also referred to as Polar Code) aims to protect ships from the harsh environment in polar regions, but as well to protect the pristine environments (IMO, n.d.-a). The code is mandatory through SOLAS and MARPOL and applicable to all ships operating in Arctic and Antarctic. Non-commercial ships solely used for governmental operations can be exempted, however, SOLAS encourages governmental vessels to act consistent to the Polar Code (IMO, 1974, Chapter XIV). In conclusion, the code is mandatory for all research vessels operating in polar areas.

Vessels must be structurally reinforced and able to handle sea ice and low temperatures. These requirements include redundant systems, but also the capability for engines to be capable of working in extreme cold, including coping with cold inlet air and seawater. Environmental standards as the prohibition of discharge of sewage and garbage are set (IMO, 2017a).

2.4.2. European Regulations

EU Emission Trading Scheme (ETS)

The EU ETS is a cap-and-trade mechanism established in 2005 to reduce GHG emissions cost-effectively by setting a limit on total emissions, which decreases annually (European Comission, n.d.-a). Companies buy emissions allowances. In the maritime sector, the system is restricted to transport vessels, exempting research vessels (European Parliament, 2015).

FuelEU Maritime

Next to the ETS, the FuelEU Maritime Regulation as part of the "Fit for 55" package aims to reduce GHG emissions in the maritime sector by promoting the use of renewable and low-carbon fuels (European Comission, n.d.-b). The regulation came into force in January 2025. The regulation sets emission reduction targets of up to 80 % compared to 2020 levels by 2050 (European Parliament & European Council, 2023b). Additionally, from 2030, passenger and container ships are required to use onshore power supply or zero-emission technologies while at berth in major EU ports.

The regulations scope include ships "[...] of above 5 000 gross tonnage that serve the purpose of transporting passengers or cargo for commercial purposes [...]" (European Parliament & European Council, 2023b). Therefore, research vessels are exempted.

The regulation offers default emission factors to determine the GHG intensity for specific fuels (European Parliament & European Council, 2023b, Annex II). Section 3.2 describes multiple fuels taken into account for this thesis. The GHG intensity factors given in (European Parliament & European Council, 2023b, Annex II) will be used to estimate emissions during this thesis.

2.4.3. Classification Societies

Classification societies fulfil a significant part in the implementation of novel marine technologies. Although many leading classification societies have published their own guidelines and notations, a focus will be set on rules by Det Norske Veritas (DNV) and Lloyd's Register (LR), as many European research vessels are certified under these two societies.

The **LR** has published frameworks for the installation of FCs (Lloyd's Register, 2024c, Part 5, Chapter 26) and for ships using gases or other low-flashpoint fuels (Lloyd's Register, 2024d). Next to that, guidance notes for WASP (Lloyd's Register, 2024a), methyl and ethyl alcohol fuels (Lloyd's Register, 2024b), LH_2 systems (Lloyd's Register, 2025), and the installation of FCs (Lloyd's Register, 2023) are provided.

Also **DNV** has developed dedicated rules and guidelines for alternative propulsion. Those are incorporated into DNV's classification of ships (DNV, 2024, Chapter 2, Section 16 and 17). Next to that, the society offers specific guidelines for a variety of tank concepts.

While these guidelines address detailed technical and safety aspects - such as structural integration, load effects, and operational risks - they do not evaluate the environmental performance or emission reduction potential of the technologies. Consequently, although these regulations are essential for ship design and approval of the ship, they are of limited relevance for the analysis of decarbonisation strategies.

2.4.4. National Regulations

In addition to international regulations, several national authorities have established frameworks that support the integration of carbon reducing technologies. Germany's **Blue Angel** is a voluntary environmental certification for products and services, including maritime vessels. For ships, the certification includes requirements around usage of low sulphur fuels, installation of WASP and FCs, but also structural requirements (Federal Ministry for the Environment, Nature Conservations, and Nuclear Safety et al., 2021). The Netherlands offer incentives under the **Green Deal Maritime**, with the goals of reduc-

ing carbon with 20 % in 2020, being carbon neutral in 2030, and being fully climate neutral and resilient in 2050 within the state fleet (Nederland Maritiem Land, 2024). In 2020, already 25 % CO_2 reduction compared to the level of 2008 was archived, surpassing the original target (Berger, 2025).

Together, these international, regional, and national frameworks create a patchwork of regulatory influence, where research vessels often operate under exemptions or voluntary standards. This mixed landscape reinforces the need for proactive, technology-driven solutions that are not solely dependent on regulatory mandates.

2.5. Conclusion

The current design landscape of research vessels is at a transitional stage. While diesel propulsion remains dominant across the global fleet, a growing number of vessels are implementing low- and zero-emission technologies. Hybrid systems incorporating hydrogen, methanol-electric configurations, and dual-fuel LNG systems illustrate the potential for cleaner propulsion, but these vessels still represent exceptions rather than the norm.

Regulatory frameworks have begun to support this transition, particularly through national initiatives like Germany's Blue Angel and the Dutch Green Deal. However, many international and European emissions regulations, such as MARPOL's EEDI and the EU ETS, exempt research vessels, reducing the immediate regulatory pressure to decarbonise. Classification societies, while essential in setting technical and safety standards, also do not currently assess the environmental impact of new technologies.

The operational profile of research vessels significantly complicates the decarbonisation challenge. Unlike commercial vessels, their fuel consumption is highly variable, depending on mission-specific activities such as station-keeping, DP, or seismic surveying. This uncertainty added by the variability in class, purpose, and actual mission demands flexible energy systems capable of maintaining efficiency across a wide range of conditions.

Despite increasing interest in low-emission propulsion lines, existing literature lacks a structured evaluation of how different operational profiles influence the feasibility of alternative fuel and propulsion systems. While a few alternative propulsion solutions have been designed, no literature could be found that acknowledges the great mission-specific difficulties compared to merchant vessels. As a result there is a lack of analysis of decarbonisation strategies for research vessels. The next chapter (Chapter 3) will explore available decarbonisation technologies.

This page is left blank intentionally.

3

Energy Reduction Methods and Alternative Energy Options

Chapter 3 answers the second sub-question:

What energy reduction methods and alternative energy options are technically feasible, including alternative fuels and WASP?

In the context of this thesis, a technology or configuration is considered **technically feasible** if it can be installed and operated safely on board a research vessel in the near term - either already available or realistically deployable within the next few years. It must meet the fundamental operational requirements (energy demand and compatibility with the ship's space and weight constraint) and be supported by at least a minimum level of technological readiness demonstrated in maritime environments. This definition does not imply economic viability. Rather, it focuses on the technology's functional integration, meaning its ability to be effectively embedded into the vessel's existing systems, and its technical operability under realistic conditions. This includes the physical integration, the compatibility with onboard systems (e.g. a fuel cell cannot be operated with diesel), and safety of the system and the vessel as a whole.

The chapter examines a broad spectrum of energy converters (Section 3.1), as well as a variety of alternative fuels ranging from biofuels and hydrogen to emerging options like iron powder and sodium borohydride (Section 3.2). It also investigates WASP (Section 3.3) and onboard energy-saving measures such as solar power and exhaust heat recovery (EHR) (Section 3.4). By evaluating each solution through key criteria, this chapter lays the basis for identifying viable decarbonisation pathways for research vessels.

3.1. Energy Converters

Energy converters deliver mechanical or electrical energy by converting chemical energy contained in fuels (Klein Woud & Stapersma, 2019). Section 3.1 describes various energy converters as electric motors and generators (Section 3.1.1), internal combustion engines (ICEs, Section 3.1.2), FCs (Section 3.1.3), and steam turbines (Section 3.1.4).

Nuclear propulsion is not considered in this analysis. Research vessels regularly accommodate changing crews and visiting scientists. Due to the high safety and security requirements of nuclear systems, nuclear reactors are considered unsuitable for this specific application and will not further be considered.

3.1.1. Electric Motors and Generator

Electric motors convert electrical energy to mechanical energy. Generators work similarly, but the other way round (Klein Woud & Stapersma, 2019). Many research vessels are propulsed by a diesel-electric drive. Electric generators are needed to cope with hotel and research load.

3.1.2. Internal Combustion Engine (ICE)

The vast majority of prime movers installed on ships are ICEs, specifically diesel engines (Klein Woud & Stapersma, 2019). These engines generate mechanical energy through the combustion of fuel. Medium speed diesel engines operate with a thermodynamic efficiency ranging from 40 % to 50 % (Stapersma, 2010). In a four-stroke cycle, commonly used on research vessels, the process involves air intake, compression, combustion during the expansion phase, and exhaust (Klein Woud & Stapersma, 2019; Stapersma, 2010).

ICEs have low power densities (φ) and high specific emissions, which depend on the fuel utilized (Klein Woud & Stapersma, 2019). Power density can be expressed on a gravimetric (φ_G) and a volumetric (φ_V) basis. Representative values are summarised in Table 3.1. At present, no four-stroke hydrogen engines for marine application are commercially available. While prototype and demonstration projects are ongoing, they have not reached market maturity. Therefore, the lowest value within the reported diesel engine range was taken from Stapersma, 2010.

Table 3.1: Power Densities of ICEs for Different Fuels, Rounded.

Fuel	Gravimetric Power Density [kW/t]	Volumetric Power Density [kW/m³]	Reference
MDO	150	97	Wärtsilä, 2024a
Ammonia	92	52	Wärtsilä, 2024b
Hydrogen	50	36	Stapersma, 2010
LNG	110	87	Wärtsilä, 2024a
Methanol	107	82	Wärtsilä, 2023

3.1.3. Fuel Cell (FC)

A FC converts chemical energy directly into electrical energy (Klein Woud & Stapersma, 2019). It consists of two electrodes — an anode and a cathode — separated by an electrolyte. A continuous supply of fuel, such as hydrogen, is delivered to the anode, while oxygen is supplied to the cathode. Chemical reactions within the cell allow ions to pass through the electrolyte, while electrons generate an electric current that can be utilized.

FCs are highly efficient, produce only clean water as an emission, and operate silently, making them an environmentally friendly energy converter (Klein Woud & Stapersma, 2019).

Not every FC is applicable to maritime operations. Fu et al., 2023, state that the polymer electrolyte membrane fuel cell (PEMFC), molten carbonate fuel cell (MCFC), and solid oxide fuel cell (SOFC) are promising candidates for the implementation of FCs in propulsion lines. An important aspect for the application of FCs is their durability. Mylonopoulos et al., 2024, reports typical lifetime values of around 25 000 operating hours for maritime FC systems, after which significant stack degradation requires replacement.

FCs for maritime application are technologically ready, but not installed on many vessels. In 2025, FCs will be installed on two Norwegian ferries with a power output of 6.4 MW (PowerCell Group, 2023). For this power, several FCs need to be stacked. Every cell has dimensions as shown in Table 3.2.

Table 3.2: Properties of Fuel Cell “Marine System 225” from PowerCell Group, 2025.

Width	Depth	Height	Weight	Net Output Power	Efficiency
1165 mm	915 mm	2035 mm	1220 kg	225 kW	42 % - 57 %

Capital costs of hydrogen FCs are today estimated at 1 600 US-$/kW and may fall to 425 US-$/kW by 2030 (IEA, 2019).

3.1.4. Steam Turbine

Steam turbines convert thermal energy from pressurized steam - typically around 40 bar - into mechanical energy (Klein Woud & Stapersma, 2019). They have traditionally been used in marine propulsions systems due to their ability to deliver high power output.

However, conventional steam plants have a very low thermal efficiency of 30 % and come with high installation costs, approximately 600 $^{EUR}/_{kW}$ (Stapersma, 2010). These factors, combined with the rise of more efficient engines, led to a decline in their use for commercial shipping. Despite this, steam turbines are regaining interest in the context of iron powder as to be seen in Section 3.2.7.

3.2. Alternative Fuels

This section investigates a range of alternative fuels, using marine diesel oil (MDO, Section 3.2.1) as benchmark.

The selected fuels represent a broad spectrum of approaches to reduce GHG emissions in maritime applications. These include fossil-based fuels with lower carbon intensity such as LNG (Section 3.2.8) and Liquefied Petroleum Gas (LPG, Section 3.2.9), renewable, diesel-like fuels such as HVO (Section 3.2.4), hydrogen (Section 3.2.5) and hydrogen carriers like ammonia (Section 3.2.2) and sodium borohydride (Section 3.2.6), alcohol fuels as methanol, as well as metal-based fuels like iron powder (Section 3.2.7), and solutions such as batteries (Section 3.2.3).

Each fuel is evaluated against the following criteria to ensure that its suitability for research vessel operations is assessed from a holistic perspective.

- **Physical and Chemical Properties** determine the compatibility of a fuel with engine systems and space on board. A key factor is energy density (ρ), which influences onboard storage requirements. Fuels with low volumetric (ρ_V) or gravimetric energy density (ρ_G), such as hydrogen, can significantly affect the vessels design by increasing tank size or weight.
- **Emissions** are central to the decarbonisation goal of this thesis. A fuel's GHG profile affects both its environmental footprint and its compliance with international maritime regulations.
- **Technological Readiness** reflects how mature and proven a fuel or energy system is for maritime use. Technologies at lower readiness levels may be promising but often lack real-world validation, making their near-term adoption uncertain.
- **Fuel Availability** is crucial for operational feasibility, particularly when considering global supply chains and port infrastructure. For research vessels, this port infrastructure may be less restrictive than for commercial shipping, since these vessels are often refuelled via tank trucks at home ports. This logistical flexibility allows the use of fuels not yet widely available at standard terminals. However, limited availability often results in higher costs due to increased transportation effort and supply chain uncertainty. In this way, availability directly influences economic viability.
- **Safety** is a fundamental concern due to the hazardous nature of several alternative fuels. Properties such as toxicity (e.g. ammonia), flammability (e.g. hydrogen), or high-pressure storage (e.g. LNG) significantly influence the design. This criterion is especially critical for research vessels, which carry scientists who are not trained for maritime operations. Ensuring a safe environment for all crew and passengers is essential for operational approval and mission success.
- **Costs**, both in terms of capital expenditure ($CapEx$) for installation or retrofitting and operational expenditure ($OpEx$) for fuel price and maintenance, are decisive factors for long-term feasibility. For publicly funded research operations, economic sustainability is essential.

These criteria were chosen to reflect the key practical, environmental, and operational challenges involved in decarbonising research vessels. While all six criteria are relevant, some are especially important in the context of decarbonisation of research vessels. Physical and chemical properties - especially energy density - act as boundary conditions, since they have main influence on the size of the vessel. Emissions remain the foremost concern, since reducing GHG is the core objective of this thesis.

3.2.1. Marine Diesel Oil (MDO)

Many research vessels are utilizing diesel as explained in Section 2.3. To compare alternative fuels, the following section gives the physical and chemical properties of MDO as a baseline.

Diesel yields 39.6 $^{MJ}/_{l}$ and 44.9 $^{GJ}/_{t}$ (IOR energy Pty Ltd, 2010). To determine the GHG intensity index, the European Parliament and European Council provide emission factors for various fuels (European Parliament & European Council, 2023a, Annex II). For MDO, these factors are shown in Table 3.3. Values are shown for well to tank (WtT), as well as tank to wake (TtW) emissions. C_f are the TtW GHG emission factors, c_{slip} is the non-combusted fuel coefficient.

Table 3.3: MDO Emissions from European Parliament and European Council, 2023a, adapted.

WtT	$CO_{2eq\,WtT}$	$\left[\frac{gCO2eq}{MJ}\right]$	14.4
	Fuel Consumer		All ICEs
TtW	$c_{f\,CO_2}$	$\left[\frac{gCO_2}{gFuel}\right]$	3.206
	$c_{f\,CH_4}$	$\left[\frac{gCH_4}{gFuel}\right]$	0.00005
	$c_{f\,N_2O}$	$\left[\frac{g\,N_2O}{gFuel}\right]$	0.00018
	c_{slip}	As % of the mass of the fuel used by the engine	-

Costs for engine and storage can be estimated at 636 $^{EUR}/_{kW}$ and 27 $^{EUR}/_{GJ}$, respectively (TNO, 2020).

3.2.2. Ammonia

Ammonia (NH_3) is a compound composed of nitrogen and hydrogen that has garnered significant interest as an alternative fuel in maritime applications (Bora et al., 2024). Ammonia is an indirect storage medium for hydrogen (Valera-Medina et al., 2018), offering a higher hydrogen density compared to LH_2, which can be advantageous for energy storage and fuel efficiency (Chai et al., 2021).

Physical and Chemical Properties

With an energy density of about 22.5 $^{MJ}/_{kg}$, ammonia can be stored in liquid form by either compressing it to 0.8 MPa at 20 °C or cooling it to -33 °C at atmospheric pressure (Al-Aboosi et al., 2021). The volumetric energy density of liquid ammonia at -33 °C is 14.4 $^{MJ}/_{l}$ (Chatterjee et al., 2021).

Emissions

As a carbon-free molecule, ammonia does not produce CO_2 during combustion, thereby offering the potential for reduced GHG emissions (Hansson et al., 2020). When produced using renewable energy, so-called “green ammonia” becomes carbon-neutral (Bora et al., 2024). Green ammonia production involves extracting nitrogen from the air and combining it with hydrogen produced using renewable power. This process effectively eliminates the GHG emissions associated with conventional fossil-based ammonia production (Bora et al., 2024; MAN Energy Solutions, n.d.-d). However, most current ammonia production relies on fossil-fuel-based hydrogen, contributing significantly to CO_2 emissions (Hansson et al., 2020). According to Wärtsilä, 2024a, GHG emissions are reduced by at least 70 % when using sustainable alternative fuels compared to a diesel engine.

Technological Readiness

Ammonia can be utilized in ICEs with only minor modifications, as well as in FCs (Al-Aboosi et al., 2021; Bora et al., 2024). A 4-stroke engine, being able to combust ammonia is e.g. the Wärtsilä 25 Ammonia (Wärtsilä, 2024a).

Ammonia can also be directly used in SOFCs and PEMFCs (Seddiek & Ammar, 2023). Several projects are undergoing, in which vessels are designed to operate on FCs using ammonia. One of these is ShipFC, co-funded by the European Union (ShipFC, 2020). This project aims to demonstrate the

Table 3.4: Ammonia Emissions from Seddiek and Ammar, 2023 and European Parliament and European Council, 2023c, adapted.

WtT	$CO_{2eq\,WtT}$	$\left[\frac{gCO2eq}{MJ}\right]$	132 Grey	0.231 Blue	0.168 Green
TtW	$c_{f\,CO_2}$	$\left[\frac{gCO_2}{gFuel}\right]$	-		
	$c_{f\,CH_4}$	$\left[\frac{gCH_4}{gFuel}\right]$	-		
	$c_{f\,N_2O}$	$\left[\frac{g\,N_2O}{gFuel}\right]$	-		
	c_{slip}	As % of the mass of the fuel used by the engine	-		

feasibility of long-range, zero-emission voyages by retrofitting the offshore vessel *Viking Energy* with a 2 MW ammonia FC. The project was temporary suspended in February 2025 due to supply challenges in ammonia-compatible SOFCs (ShipFC, 2025).

Fuel Availability

Ammonia is already manufactured on an industrial scale and is globally traded, with its annual production reaching approximately 150 million tonnes in 2019 (Al-Aboosi et al., 2021; MAN Energy Solutions, n.d.-d). However, most ammonia production today relies on fossil-fuel based hydrogen, resulting in high CO_2 emissions (Hansson et al., 2020).

Safety

Ammonia is a toxic and hazardous gas at room temperature (IRENA, 2024b). It is corrosive, harmful to health, and dangerous if inhaled. Leakages can damage both the environment and human health, so careful handling is essential. The flammability of NH_3 is limited by a high ignition temperature (Cheliotis et al., 2021).

Safety measures like proper materials, inspection routines, and emergency protocols are essential to manage the risks (Cheliotis et al., 2021).

Costs

In 2023, Seddiek and Ammar concluded, that SOFC operation with green ammonia is able to reduce total costs by 5.7 % compared to conventional diesel operation.

Capital and installation costs for ammonia engines are estimated at 500 and 25 US-$/kW (Seddiek & Ammar, 2023). For the system, 5 % of capital costs can be set. A generator is needed (400 US-$/kW), as well as a cracker (50 US-$/kW).

For FCs, capital and installation costs are estimated at 950 and 42.5 US-$/kW, 5 % of the capital costs should be planned for the system (Seddiek & Ammar, 2023). Auxiliary costs for motor, cracker, batteries and converter are estimated at 1000 US-$/kW. Costs for cryogenic tanks can be estimated at 0.7 US-$/kg (Schreuder et al., 2025).

Bunker costs of green ammonia in Northwest Europe were averaged at 924.05 US-$/t in February 2025 (S&P Gobal, 2025). In regions with optimal solar and wind resources, ammonia costs around 720 US-$/t, estimated to decline to 480 US-$/t by 2030 and 310 US-$/t by 2050 (IRENA, 2024b). In contrast, costs of grey ammonia are around 300 US-$/t (Yang & Lam, 2023).

3.2.3. Battery Systems

As hotel and research loads on research vessels are high, they are typically already equipped with battery packages. This section will dive deeper into batteries as energy provider.

Physical and Chemical Properties
Heavy-duty marine lithium ion batteries in a system with cooling, racks, etc. have a specific weight of 11 to 30 $^{kg}/_{kWh}$, and a specific volume of 12 - 38 $^{l}/_{kWh}$ (MAN Energy Solutions, 2019). This results in energy densities of 0.12 to 0.33 $^{GJ}/_{t}$ and 0.1 to 0.3 $^{GJ}/_{m^3}$.

Emissions
The emissions associated with battery-electric propulsion depend on the WtT emissions of the electricity used for charging. If electricity is generated from renewable energy sources such as wind or solar power, battery systems enable zero-emission operation.

Technological Readiness
Battery systems for vessels are technologically ready and commercially available. An increasing number of ships are being equipped with diesel-electric propulsion systems. Some ferries, such as the *Aurora*, operate entirely on battery power (MAN Energy Solutions, 2019). While current battery technology is sufficient for short-sea shipping and port operations, further advancements in energy density are expected in the coming years.

Energy Availability
Currently, only a limited number of ports offer on-shore power supply infrastructure. However, beginning in January 2030, container ships and other seagoing vessels will be required to connect to shore-side electricity while at berth in European ports (European Parliament & European Council, 2023a, 2023c). It can be assumed, that by 2030, a sufficient number of berths equipped with shore power supply will be available across European ports to meet this regulatory demand. Renewable energy supply is increased year by year (IRENA, 2024a).

Safety
One of the primary safety risks associated with battery systems on board of vessels is thermal runaway, a process in which a battery cell self-heats uncontrollably, leading to a rapid increase in temperature and the potential for fire or explosion (EMSA, 2023). To mitigate this risk, battery systems must be equipped with high-temperature alarms and effective thermal monitoring systems. Additionally, the battery room should be physically separated from other onboard spaces. This separation not only protects the battery system from external fires but also prevents fire from spreading to other areas of the vessel. When appropriate safety measures are in place, battery systems are considered safe and reliable for maritime use.

Costs
According to MAN Energy Solutions, 2019, system prices of at least 500 $^{US\text{-}\$}/_{kWh}$ need to be considered. Potentially, prices can decrease to 250 $^{US\text{-}\$}/_{kWh}$. Operational costs depend on the actual energy prices, renewable energy cost in 2023 differed from 0.033 $^{US\text{-}\$}/_{kWh}$ (onshore wind) to 0.075 $^{US\text{-}\$}/_{kWh}$ (offshore wind) for different energy sources (IRENA, 2024a). Margins can be estimated by 6 % (IEA, 2024b), leading to renewable energy prices of 0.022 $^{US\text{-}\$}/_{MJ}$.

3.2.4. Biofuels - Hydrotreated Vegetable Oil (HVO)
Biofuels are derived from biomass, offering a renewable and more sustainable alternative to conventional fossil fuels (Laursen et al., 2023). Following current literature, HVO produced from fats, oils, and greases shows the greatest potential for replacing traditional fuels. Several research vessels are (e.g. *Sir David Attenborough* (British Antarctic Survey, 2023) since 2023, *R/V Svea* (Swedish University of Agricultural Sciences, 2024)) or can be (e.g. *R/V Skagerak* (University of Gothenburg, 2024)) fueled by HVO.

Physical and Chemical Properties
HVO exhibits energy content values of approximately 43 $^{MJ}/_{kg}$ and 32 $^{MJ}/_{l}$ (Laursen et al., 2023). Its properties closely resemble those of heavy fuel oil, making them a viable substitute for existing maritime and industrial applications (DNV GL, 2019; Laursen et al., 2023).

Table 3.5: HVO Emissions from European Parliament and European Council, 2023a, adapted.

WtT	$CO_{2eq\,WtT}$	$\left[\frac{gCO2eq}{MJ}\right]$	$E - \frac{C_{fCO_2}}{LCV}$
	Fuel Consumer		All ICEs
TtW	$c_{f\,CO_2}$	$\left[\frac{gCO_2}{gFuel}\right]$	3.115
	$c_{f\,CH_4}$	$\left[\frac{gCH_4}{gFuel}\right]$	0.00005
	$c_{f\,N_2O}$	$\left[\frac{g\,N_2O}{gFuel}\right]$	0.00018
	c_{slip}	As % of the mass of the fuel used by the engine	-

Emissions
HVO has the potential to reduce emissions by about 20 %. Table 3.5 gives the emissions from the European Parliament and European Council.

The WtT emission of HVO is given as a function of the total emission from the production and use of the fuel E, the CO_2 TtW emission factor $C_{f\,CO_2}$, and the lower calorific value LCV. European Parliament, 2018, specifies a default value of E of 50.1 g_{CO_2eq}/MJ for HVO from rape seed, and a LCV of 44 MJ/kg.

Technological Readiness
One of the key advantages of biofuels is their compatibility with existing combustion systems. They can be used as a drop-in fuel without requiring significant modifications to current infrastructure (DNV GL, 2019).

Fuel Availability
Despite their potential, the widespread adoption of biofuels faces challenges due to a lack of global infrastructure and dedicated bunkering facilities (DNV GL, 2019). However, HVO can be transported efficiently using existing fuel distribution networks.

Safety
With properties similar to heavy fuel oil, biofuels do not present any known safety concerns.

Costs
Prices in February 2025 were 131.43 $EUR/100\,l$ of HVO in Germany (Argus O.M.R., 2025). Costs for engine and storage are the same as for MDO in Section 3.2.1.

3.2.5. Hydrogen
Hydrogen (H_2) offers significant promise as an alternative fuel due to zero carbon emissions during combustion (Atilhan et al., 2021; Sazali, 2020).

Physical and Chemical Properties
Hydrogen is the lightest of all gases, delivering an energy density of 122 MJ/kg. However, its low volumetric density means that for practical storage, hydrogen must be either highly compressed (5.6 MJ/l at 700 bar) or liquefied (8 MJ/l) (Center for Sustainable Systems, University of Michigan, 2024; MAN Energy Solutions, n.d.-b; Xing et al., 2021).

Emissions
Hydrogen can be used either in FCs for electricity generation or directly in ICEs, all while emitting no toxic by-products (Sazali, 2020). However, the environmental benefit of hydrogen depends heavily on its production pathway. Currently, around 95 % of global hydrogen is produced from fossil fuel reforming (MAN Energy Solutions, n.d.-a). To ensure low lifecycle emissions, “green hydrogen”, produced via electrolysis powered by renewable energy or gasification of biomass, must be prioritized (Kayfeci et al.,

2019). The European Parliament and European Council, 2023a, indicate the TtW emissions with zero for both ICEs and FCs. Solely the N_2O emissions in combustion engines need to be measured. The WtT emissions for fossil hydrogen are 132 g_{CO_2eq}/MJ and not applicable for green hydrogen.

Technological Readiness

Hydrogen is currently being deployed in a small number of short-sea and inland waterway vessels (MAN Energy Solutions, n.d.-b), demonstrating a growing technological maturity in controlled, nearshore environments. However, this does not necessarily translate to readiness for high-sea or long-range research operations. Deep-sea applications present additional challenges, including larger energy demands, limited refuelling infrastructure, and stricter safety requirements due to the extended duration and remoteness of missions. Additionally, no four-stroke hydrogen engines for marine applications are commercially available. Therefore, while hydrogen is considered technologically ready for short-sea shipping, its readiness for high-sea research vessels remains limited and is still in the early stages of development and demonstration.

Fuel Availability

Global hydrogen demand reached 97 million tonnes in 2023, predominantly used in the chemical sector (IEA, 2024a). As mentioned, only a very small percentage is green hydrogen. Hydrogen is available worldwide, though port infrastructure is not developed (MAN Energy Solutions, n.d.-b).

Safety

Liquid hydrogen has a very low flashpoint, requiring adherence to the IGF Code (MAN Energy Solutions, n.d.-b). To ensure safety, a double-hull tank, double walled piping, and hydrogen detection systems are necessary. Additionally, the maximum filling level of the tanks is limited to 69 %.

Costs

Cryogenic storage is essential for the transport of LH_2, with associated costs estimated at 1 180 EUR/GJ (TNO, 2020). Additionally, the costs of FCs are approximately 1 600 $US\text{-}\$/kW$ and may fall to 425 $US\text{-}\$/kW$ in 2030 (Section 3.1.3).

Although completely renewable, green hydrogen production is highly endothermic and energy-intensive (Kayfeci et al., 2019). Hydrogen costs will be largely dependent on electricity and gas costs (IEA, 2019). DNV, 2022b, estimates the costs of renewable hydrogen to 5 $US\text{-}\$/kg$ in 2020 and 2 $US\text{-}\$/kg$ in 2050.

3.2.6. Sodium Borohydride

According Kaya, 2024, sodium borohydride ($NaBH_4$) is a promising hydrogen storage option for marine fuel due to its ability to be stored at room temperature and atmospheric pressure.

Physical and Chemical Properties

Sodium borohydride is a chemical storage medium for hydrogen (Kaya, 2024). When it comes into contact with water, it undergoes a spontaneous, exothermic, and irreversible hydrolysis reaction that releases hydrogen. As shown in Equation 3.1, half of the released hydrogen originates from water (H_2O) (Muir & Yao, 2011). After release, the by-product sodium metaborate ($NaBO_2$) needs to be stored before discharged at a port.

$$\mathrm{NaBH_4} + 2\,\mathrm{H_2O} \longrightarrow \mathrm{NaBO_2} + 4\,\mathrm{H_2} \tag{3.1}$$

To prevent premature reactions with moisture, sodium borohydride can be stored in a dry state under an inert atmosphere or in a stabilized wet form using additives like sodium hydroxide (NaOH) or potassium hydroxide (KOH) (Kaya, 2024). Wet storage offers the added benefit of acting as a thermal buffer, though it requires additional water to be stored onboard (Kaya, 2024; Muir & Yao, 2011). Storage temperatures ranges between 15 and 25 °C (Kaya, 2024). In wet storage systems, at least 10 % of free volume is required to accommodate any hydrogen that might be released. $NaBH_4$ as future marine fuel benefits from its high gravimetric (10.7 wt%) and volumetric (114 kgH_2/m^3) hydrogen content. The system itself is increased by a fresh water generator, a purifier, the catalyst, etc. Furthermore, the solid rest product needs to be stored.

Emissions
Kaya, 2024, states, that hydrogen storage via $NaBH_4$ does not cause any airborne emission. Further emissions are the same as for H_2 (see Section 3.2.5).

Technological Readiness
$NaBH_4$ as a hydrogen carrier in marine applications is still under development. Research is ongoing to optimize storage, reaction efficiency, and safety measures (Kaya, 2024).

Fuel Availability
Sodium borohydride is not available in ports.

Safety
The flashpoint of sodium borohydride is at 69 °C (Kaya, 2024; Sigma-Aldrich, 2025). In dry storage, flammable H_2 can be liberated if $NaBH_4$ comes in contact with water or moisture. This gas can be ignited by the heat of the exothermic hydrolysis reaction. Despite the relative stabilization, also in wet storage flammable hydrogen may be liberated.

Costs
Unlike compressed or liquefied hydrogen, $NaBH_4$ hydrolysis is exothermic and occurs under moderate conditions, avoiding the high costs and challenges of extreme storage methods (Kaya, 2024). However, regeneration of sodium borohydride is energy-intensive and inefficient compared to other storage methods, leading to high costs. Energy is also consumed in hydrolysis-related processes such as water purification, heating, and hydrogen release control. Wet storage requires cooling to 4 °C to prevent uncontrolled hydrogen release, increasing energy demand. Catalyst deactivation further adds to costs due to replacement needs. Additionally, the by-products of hydrolysis require costly and energy-intensive regeneration, making sodium borohydride a less economical option unless an efficient, low-cost regeneration process is developed.

3.2.7. Iron Powder
Iron fuel is a novel, recyclable energy carrier that uses iron (Fe) powder as a medium to store and release energy, when burned (TU/e, n.d.). With its high energy density, cost-effectiveness, and safety, iron fuel is a promising solution for energy storage, transport, and industrial application.

Physical and Chemical Properties
Iron fuel has a volumetric energy density of about 16 $^{kWh}/_{l}$ and a gravimetric energy density of about 2 $^{kWh}/_{kg}$ (Bergthorson et al., 2015). While the volumetric energy density is relatively high, making it efficient in terms of storage space, the low gravimetric energy density means that a large mass of fuel is required to store a given amount of energy. This results in a higher onboard fuel weight compared to conventional marine fuels. Next to its energy characteristics, iron fuel has the advantage of producing a single, solid by-product. The only by-product of the reaction shown in Equation 3.2 is iron oxide (Fe_2O_3, i.e. rust, which can be recycled back into iron fuel. Both fuel and by-product are solids, making them less easy to store compared to liquids (De Kwant, 2021).

$$\mathrm{Fe} + \mathrm{O_2} \longrightarrow \mathrm{Fe_2O_3} + \mathrm{heat} \tag{3.2}$$

Emissions
Under the assumption, that all iron oxide can be filtered out the exhaust, iron powder is a zero-emission fuel (De Kwant, 2021).

Technological Readiness
According to De Kwant, 2021, many systems required for an iron-fuelled vessel remain untested. For instance, while solid iron powder could be stored in silos, its feasibility for use on ships and the challenges of storing large quantities in a salty marine environment have not been studied. In terms of energy conversion, the system would require a boiler capable of combusting iron fuel-technology that does not yet exist at an industrial scale - along with a turbine, which is already well-established and thoroughly tested (De Kwant, 2021). To mitigate particulate emissions, exhaust gases would need to be treated using baghouse and cyclone filters. However, these filtration methods have not yet been tested on vessels (De Kwant, 2021).

Fuel Availability
According to Scherpenhuijsen Rom, 2023, iron is highly available as its the 4th most common element in the earth crust. However, iron powder as fuel is not available in ports.

Safety
According to TU/e, n.d., iron powder has the potential of being safe and transportable. Iron powder is stable, not toxic, and as being a solid less prone to spills or leaks (Carl Roth, 2024b).

Costs
De Kwant, 2021, estimated costs of iron fuel on 0.12 US-$/kWh, twice as expensive as MDO.

3.2.8. Liquefied Natural Gas (LNG)
Physical and Chemical Properties
LNG is liquefied by cooling natural gas to -162 °C (MAN Energy Solutions, n.d.-d; Shell Deutschland Oil GmbH, 2019). It is a mixture which exact composition depends on its place of origin (Klebanoff et al., 2021). It consists of around 93 % methane and 5 % ethane, with small proportions of propane, butane, nitrogen and other trace gases. LNG has a gravimetric energy density of around 45 MJ/kg, and a volumetric energy density of 21 MJ/l (Shell Deutschland Oil GmbH, 2019). LNG needs to be stored in tanks for cryogenic liquids (Shell Deutschland Oil GmbH, 2019).

Emissions
By utilising LNG instead of diesel, emissions can be significantly reduced (Fun-sang Cepeda et al., 2019). Sulphur oxides are completely eliminated and nitrogen oxides are significantly reduced. However, LNG consists mainly of methane (CH_4). Methane slip (unburnt methane) limits the benefits of LNG, as methane has up to 30 times the GHG effect of CO_2.

Emissions from LNG will be estimated using EU regulation 2024/1805 (FuelEU Maritime) as stated in section 2.4.2, shown in Table 3.6.

Table 3.6: LNG Emissions from European Parliament and European Council, 2023a, adapted.

WtT	$CO_{2eq\,WtT}$	$\left[\frac{gCO2eq}{MJ}\right]$	18.5	
TtW	Fuel Consumer		LNG Otto (dual fuel medium speed)	LBSI
	$c_{f\,CO_2}$	$\left[\frac{gCO_2}{gFuel}\right]$	2.750	
	$c_{f\,CH_4}$	$\left[\frac{gCH_4}{gFuel}\right]$	0.0	
	$c_{f\,N_2O}$	$\left[\frac{g\,N_2O}{gFuel}\right]$	0.00011	
	c_{slip}	As % of the mass of the fuel used by the engine	3.1	2.6

Technological Readiness
LNG is a highly mature alternative fuel already used in the maritime industry. It is increasingly adopted for vessels, including the German research vessel *Atair* (Section 2.3.1). LNG dual fuel engines, such as those provided by Wärtsilä, 2024a, are commercially available, and ongoing developments aim to further reduce methane slip.

According to DNV, there are currently 642 LNG-powered vessels in operation, excluding LNG carriers, additionally 264 new orders for LNG-fuelled vessels were placed in 2024 (DNV, 2025a).

Fuel Availability

The LNG market has seen substantial expansion, driven by the development of new liquefaction facilities in the United States, Russia, and Australia (SEA-LNG, n.d.). The number of markets is growing, with 26 import terminals currently under construction. LNG now represents approximately 11 % of global gas consumption.

Safety

LNG is generally considered non-toxic, but its extremely low temperature poses significant hazards, including cold burns and frostbite (Bernatik et al., 2011). Due to its low viscosity, LNG can quickly penetrate porous materials such as clothing, and its cryogenic temperature can embrittle materials such as carbon steel and rubber, potentially leading to cracking failures. As LNG is colourless, it is undetectable when it evaporates and can cause asphyxiation. Finally, LNG is highly flammable.

Costs

As of March 2025, LNG bunker prices in Rotterdam were approximately 750 $^{EUR}/_{t}$ (SEA-LNG, 2025). For capital investment, cryogenic storage costs are estimated at 100 $^{EUR}/_{GJ}$ (TNO, 2020), while engine costs are around 923 $^{EUR}/_{kW}$.

3.2.9. Liquefied Petroleum Gas (LPG)

LPG is composed of Butane and Propane (Ryste, 2019). Fossil LPG is a by-product of oil and gas extraction or the refining process. Additionally, LPG can be derived from renewable sources, such as a by-product of renewable diesel production.

Physical and Chemical Properties

LPG has a volumetric energy density between 25.3 (propane) and 27.7 $^{MJ}/_{l}$ (butane), and a gravimetric energy density between 49.1 (butane) and 49.6 $^{GJ}/_{t}$ (propane) (IOR energy Pty Ltd, 2010). With an density of 1.898 $^{kg}/_{m^3}$, the gas is heavier than air (1.225 $^{kg}/_{m^3}$) (Hahn, 2024). The flashpoint of LPG is at -104 °C (Ryste, 2019).

Emissions

Using LPG, emissions can be reduced by 10 % to 30 % (Wang et al., 2022). Emission factors provided from European Parliament and European Council, 2023a are shown in Table 3.7.

Table 3.7: LPG Emissions from European Parliament and European Council, 2023a, adapted.

WtT	$CO_{2eq\,WtT}$	$\left[\frac{gCO2eq}{MJ}\right]$	7.8
TtW	Fuel Consumer		All ICEs
	$c_{f\,CO_2}$	$\left[\frac{gCO_2}{gFuel}\right]$	3.03 (Butane) 3.00 (Propane)
	$c_{f\,CH_4}$	$\left[\frac{gCH_4}{gFuel}\right]$	TBM
	$c_{f\,N_2O}$	$\left[\frac{g\,N_2O}{gFuel}\right]$	TBM
	c_{slip}	As % of the mass of the fuel used by the engine	N/A

Technological Readiness

Currently, there are no 4-stroke combustion engines available running on LPG. However, 2-stroke engines are available and are primarily used by LPG gas carriers, which utilize their own cargo as fuel (MAN Energy Solutions, n.d.-c).

Fuel Availability
LPG import- and export-terminals are available worldwide (Ryste, 2019). The lack of bunkering infrastructure for ships remains a challenge for its adoption as a fuel. However, according to DNV GL, 2019, bunkering infrastructure can easily be developed at existing LPG storage locations.

Safety
LPG is a non-toxic fuel. It can ignite at temperatures as low as -104 °C (Ryste, 2019). Vessels operating on LPG must comply with the IGF Code.

Costs
According to Argus O.M.R., 2024, LPG is one of the least expensive fuels. In October 2024, LPG bunker prices were averaged at 577 US-$/t.

3.2.10. Methanol
Methanol is increasingly being adopted by the shipping industry as an alternative fuel to meet decarbonisation goals (DNV, 2023). It is considered a promising alternative for reducing emissions and the carbon footprint of ship operations (Ellis & Tanneberger, 2015). Production is done in three steps: First, syngas is produced, either from natural gas, or from gasification of biogas, biomass, residual waste, or coal. Syngas is compressed to yield crude methanol. Finally, the crude methanol is distilled, to get methanol on chemical level (Riaz et al., 2013). In a second method, methanol can be produced from synthesis of captured CO_2 and H_2, which is produced via synthesis of water (H_2O) using (green) electricity (Xing et al., 2021).

Physical and Chemical Properties
Methanol is a type of alcohol with the chemical structure CH_3OH (Svanberg et al., 2018; Tian et al., 2022; Zhen & Wang, 2015). It remains in liquid form under normal temperature and pressure and can be used in both ICEs and FCs (Tian et al., 2022). The gravimetric energy density of methanol is 20 MJ/kg (Zhaka & Samuelsson, 2024), the volumetric energy density is 15.8 GJ/m³ (Kang et al., 2021). The flashpoint of methanol is at 12 °C (Methanol Institute, n.d.).

Emissions
Methanol is a clean-burning fuel that does not produce sulphur emissions (Svanberg et al., 2018). Although it is primarily produced from natural gas and coal, it can also be derived from renewable sources. Svanberg et al. describe methanol as potentially carbon-neutral fuel when produced from renewable sources. However, the European Parliament and European Council, 2023a provide specific emission factors depending on the production pathway shown in Table 3.8.

Table 3.8: Methanol Emissions from European Parliament and European Council, 2023a, adapted.

WtT	$CO_{2eq\,WtT}$	$\left[\frac{gCO2eq}{MJ}\right]$	$\frac{E - C_{fCO_2}}{LCV}$
			Green: 31.3 / Grey
	Fuel Consumer		All ICEs
TtW	$C_{f\,CO_2}$	$\left[\frac{gCO_2}{gFuel}\right]$	1.375
	$C_{f\,CH_4}$	$\left[\frac{gCH_4}{gFuel}\right]$	TBM
	$C_{f\,N_2O}$	$\left[\frac{g\,N_2O}{gFuel}\right]$	TBM
	C_{slip}	As % of the mass of the fuel used by the engine	-

Also for methanol, the WtT emissions are given as a function. European Parliament, 2018, specifies a default value of E of 10.4 g_{CO_2eq}/MJ for methanol from black-liquor gasification and 16.2 g_{CO_2eq}/MJ for farmed wood methanol, and a LCV of 22 MJ/kg.

Technological Readiness

Methanol can be utilized in current ICEs with minimal modifications (DNV, 2023). It is easy to handle regarding storage (MAN Energy Solutions, n.d.-e). No cryogenic or pressurized tanks are required. However, around 2.5 times the tank size compared to diesel is needed.

Methanol-combustion engines are technological ready. 4-stroke engines are for example available from Wärtsilä (Wärtsilä, 2023).

Methanol can also be utilized in FCs. The first system enabling power of one MW will be installed on a vessel of Maersk in 2026 (Blue World Technologies, 2024). The plant is expected to be commercially ready in 2027.

Fuel Availability

The characteristics of methanol allows it to be integrated into existing fuel storage and bunkering infrastructure. Currently, methanol is available at more than 120 ports worldwide (DNV, 2023). Methanol bunker and storage facilities can be seen in Figure 3.1. In 2021, global methanol production reached approximately 107 million tons (Statista, n.d.), but the production of green methanol remains limited (DNV, 2023). However, ongoing investments aim to expand production capacity.

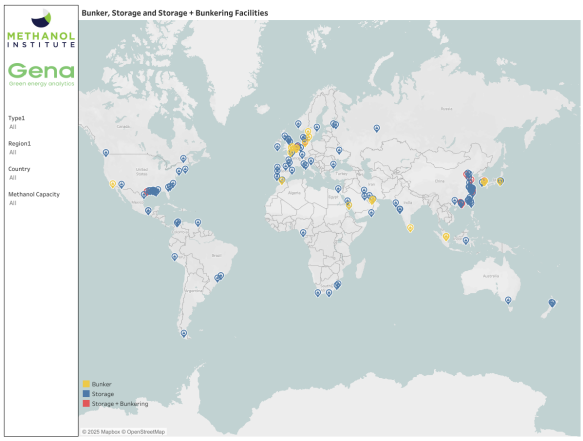

Figure 3.1: Methanol Bunker and Storage Facilities (Methanol Institute, 2025).

Safety

The flashpoint of methanol is at 12 °C, so the IGF Code, including its annex for methyl alcohol needs to be followed (MAN Energy Solutions, n.d.-e).

Next to that, methanol is toxic if swallowed, however, the risk is mitigated by proper handling (Carl Roth, 2024a).

Costs

One of the advantages of methanol is its relatively low production cost (Tian et al., 2022). Average bunker costs in February 2025 of grey methanol were 382.27 $^{\text{US-\$}}/_{\text{t}}$ in Rotterdam or 1025 $^{\text{US-\$}}/_{\text{t}}$ of sustainable methanol in Singapore (S&P Gobal, 2025). Kang et al., 2021, estimate costs of renewable methanol at 500 $^{\text{US-\$}}/_{\text{t}}$ in 2050. Engine costs of methanol can be estimated at 655 $^{\text{EUR}}/_{\text{kW}}$, storage costs at 45 $^{\text{EUR}}/_{\text{GJ}}$ (TNO, 2020).

3.2.11. Comparison

A wide range of alternative fuels was assessed based on their physical and chemical profiles, technological readiness, availability, safety, and costs. Table 3.9 provides a comparative summary using colour-coded indicators, offering a visual overview of their relative performance across key criteria. If cryogenic tanks are needed, depending on the temperature 5 to 20 % of the actual size are added on top of the tank size. Costs are converted from US-Dollar at an exchange rate from 09th of April 2025 of 1 US-$ = 0.90 EUR (European Central Bank, 2025a). Cost estimations are primarily compared on the basis of ICE configurations, wherever applicable. In cases where FCs are employed, operational fuel costs are expected to decrease due to their higher efficiencies. This advantage is offset by significantly higher installation costs.

HVO offers immediate emissions reduction to a certain extent but faces supply limitations. Ammonia, hydrogen, and methanol appear as a midterm option due to their compatibility with existing systems and growing availability. It can be expected, that supply of sustainable fuel options will increase. While battery systems are technologically mature and well-suited for auxiliary and peak-shaving applications,

Table 3.9: Summary of Fuels.

	Tank Size Compared to MDO	Emissions	Technological Readiness	Fuel Availability	Safety	Costs Fuel EUR/kWh	Costs Engine EUR/kW	Considered
Ammonia	2.8	WtT emissions	currently no ships	yes, but fossil	toxic	0.029	900	yes
Battery	200	zero emission	already in use	shore supply expected from 2030	safe with sufficient measures	0.071		no, huge storage volume required
HVO	1.2	reduced compared to MDO	already in use	no, but MDO infrastructure can be used	safe	0.148	640	yes
Hydrogen	8.0	zero emissions	used in short sea shipping	yes, but fossil	low flashpoint	0.591	920	yes
Iron Powder	0.7	zero emissions	in research	not available	safe	0.108		no, insufficient readiness
LNG	2.1	reduced compared to MDO	already in use	available	low temperature	0.060	920	yes
LPG	1.7	reduced compared to MDO	no 4-stroke engines available	lack of bunkering infrastructure	low temperature	0.047		no, 4-stroke engines not available
Methanol	3.0	zero emissions	already in use	yes, but fossil	low flashpoint	0.062	655	yes
Sodium Borohydride	0.8	zero emissions	in research	not available	Hydrogen liberation possible			no, insufficient readiness

their high weight and low energy density limit their feasibility as a primary propulsion source for long-range research missions. Therefore, batteries will not be further considered as a stand-alone propulsion solution, but remain essential for onboard energy storage and supporting hybrid configurations.

Novel fuels such as iron powder and sodium borohydride show conceptual promise but remain in early development stages and are not yet practical for maritime use. Similarly, LPG is not currently viable for research vessels due to the absence of compatible 4-stroke engines. Those fuels will not further be investigated. Further investigated will be HVO and LNG, ammonia, hydrogen, and methanol.

3.3. Wind-assisted Ship Propulsion (WASP)

WASP offers a practical and energy-efficient way to reduce fuel consumption and emissions in the maritime environment. By using wind as a complementary energy source, various technologies can lower engine load and support decarbonisation. This section introduces key WASP systems as Flettner Rotors (Section 3.3.1), kite sails (Section 3.3.2), rigid sails (Section 3.3.3), suction-based foils (Section 3.3.4), and wind turbines (Section 3.3.5) with a focus on their applicability to research vessels.

3.3.1. Flettner Rotor

The Flettner rotor, a vertical installed cylinder rotated by a motor, was already invented in the 1920s by Anton Flettner (Traut et al., 2014). The rotor utilizes the Magnus Effect and produces a thrust, that pulls the vessel forward. Due to the economical crisis, the technology was not investigated any further. During the shipping crisis (1980s), Bergeson and Greenwald, 1985, studied WASP, including Flettner rotors, again. Furthermore, from 2010 some vessels were equipped with rotors, as the cargo ship *Enercon E-Ship 1* shown in Figure 3.2, the retrofitted Ro-Ro carrier *M/V Estraden*, or, for test purposes, the cruise vessel *Viking Grace* (Lu & Ringsberg, 2020; Traut et al., 2014; Viking Line, 2021).

Figure 3.2: *E-Ship 1* Equipped with 4 Flettner Rotors (Lu & Ringsberg, 2020).

The rotor on the *Viking Grace* was decommissioned after three years. T. Riski, CEO of Norsepower, the company that supplied the Flettner Rotor, stated that fuel savings of up to 20 % could potentially be achieved (Viking Line, 2021).

In 2014, Traut et al. studied the impacts on a slow-steaming general cargo carrier, equipped with three Flettner rotors. Their numerical performance model demonstrated an average power contribution ranging from 193 kW to 373 kW. On the route between Varberg (Sweden) and Gillingham (Great Britain), the rotors could generate more than half of the power needed by the main engine.

Lu and Ringsberg, 2020, compared three different WASP, namely Flettner rotors, DynaRigs, and Wingsails, on an oil tanker and two different routes. All three technologies resulted in fuel savings of between 5.6 % and 8.9 %, with the Flettner rotor providing the highest savings while requiring the smallest sail area on the analysed route. Installation costs of a Flettner rotor with the size of 18 metre height and a diameter of 3 metre can be accounted for with 750 000 EUR, monthly maintenance costs are 1 208.33 EUR (Chica et al., 2023; Interreg, n.d.).

3.3.2. Kites

Kite-based WASP has been explored since the 1980s as an alternative means of reducing fuel consumption in shipping (Duckworth, 1985; Traut et al., 2014). In 1985, Duckworth proposed parachute kites, being more stable and easy to manage.

Kites have a few advantages to other WASP: Kites require fewer modifications to existing vessels, making them a relatively easy solution to implement (Duckworth, 1985). A key advantage of kite propulsion is its ability to generate a higher driving force per unit of sail area compared to traditional sails. This

efficiency is attributed to the windmill apparent effect, which enhances aerodynamic performance. Additionally, kites operate by flying in front of the ship rather than being mounted on the deck, thereby preserving valuable space onboard (Traut et al., 2014).

Traut et al. demonstrated that kites achieve optimal performance in crosswind conditions. Their calculations indicate that kite-assisted propulsion can lead to fuel savings of up to 32 %, depending on the vessel's route and wind conditions. The company Airseas projects an average fuel reduction of approximately 20 % with their kite technology (airseas, n.d.; Traut et al., 2014).

Kites are technological ready. First kites were tested between 2004 and 2012 by the German company SkySails (SkySails Marine, n.d.), one of the first ships equipped with a kite was the MS Beluga Skysails (length of 132 m (VesselFinder, 2025)) with a size of 160 m^2 (BBC, 2008). Further applications were, e.g., installed for test purposes on the ro-ro vessel *Ville de Bordeaux* (airseas, 2021). Modern kite systems are typically computer-controlled and automated, improving their ease of operation and reliability. Costs of a kite with an area of 160 m^2 can be estimated to 280 000 US-$ (IMO, n.d.-b).

Kites as electricity generator

SkySails shifted focus from marine propulsion to electric power generation. In 2024, they presented an externally verified power curve (SkySails Power GmbH, 2024).

The system consists of a kite, a control pod, a tether, the launch and landing mast, the ground station, namely a container, the drive train, and a tripod with ring mount (SkySails Power GmbH, n.d.-a).

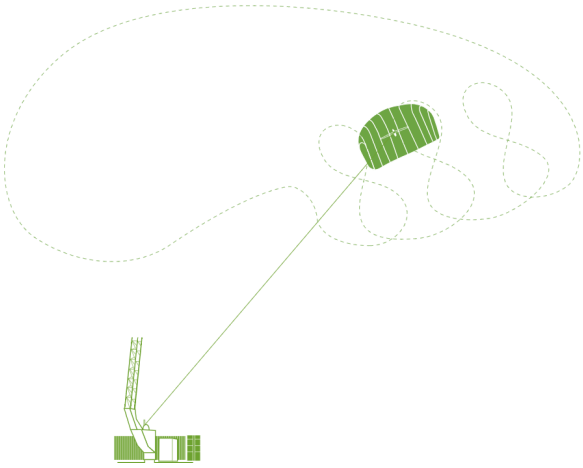

Figure 3.3: Working Principle of Power Generating Kite (SkySails Power GmbH, n.d.-a).

The power kite, controlled automatically, generates electricity by flying in figures of eight, pulling up to 800 metres of a tether from a winch on the ground (SkySails Power GmbH, n.d.-a). This motion drives a generator in the ground station, producing power during the "work phase". Once fully extended, the kite shifts to a neutral position and the generator, now working as a motor, reels in the tether using minimal energy. This circle repeats. The generated energy can be fed into the grid or stored. The kite can land docking to a mast before being stored inside the ground station. The system has a weight of about 40 t and archives power production of 100 to 200 kW per cycle (SkySails Power GmbH, n.d.-b; Taphorn, 2024). The system is technological ready and supposed to work on- and offshore, but is not meant for working on vessels.

3.3.3. TwinFoil Wingsails

TwinFoil wingsails are rigid, aerodynamic sail systems designed to harness wind power more efficiently than traditional sails (Barbu et al., 2024). The most well-known and commercially advanced example is the OceanWing system, developed by VPLP Design (VPLP Design, n.d.). These wingsails operate on the same aerodynamic principles as aeroplane wings, using a vertical foil with an oval-shaped cross-section and an adjustable trailing flap to generate lift and thrust (Barbu et al., 2024).

OceanWings are modular in design and can be installed in tiltable or lower-able configurations. Each sail has a surface area of 363 m^2, stands 33 m high (with a total height of 38 m above deck), and spans 11 m in width (OceanWings, 2024b, 2024c). An unit weighs approximately 45 t and can deliver a maximum equivalent engine power of 2 400 kW.

Figure 3.4: *Canopée* equipped with 4 OceanWings (arianeGroup, 2023).

Fuel savings of up to 30 % have been reported under favourable wind conditions (Barbu et al., 2024), with wind power contributions ranging between 15 % and 35 % (OceanWings, 2024a). A key milestone for this technology was the installation of four Oceanwings sails on the cargo vessel *Canopée* in 2023, marking the first application on a commercial ship.

Comparable twin-foil systems (9 m height, 3 m width) cost 250 000 EUR per unit and monthly another 500 EUR for maintenance (Chica et al., 2023; Interreg, n.d.).

3.3.4. VentoFoil

Suction wings, as the VentoFoil, were first investigated in the 1980s (Smeets, 2024), with sea trials on board the *Moulin a Vent I* in 1983 (Charrier et al., 1985). VentoFoils use aerodynamic physics. The foils have holes in the shell, in which fans blow air producing a suction side (Smeets, 2024). Holes on the lee side are covered with flaps.

The VentoFoil produces thrust as shown in Figure 3.5. The figure depicts a VentiFoil, whose fundamental working principle is the same as that of a VentoFoil, with modifications.

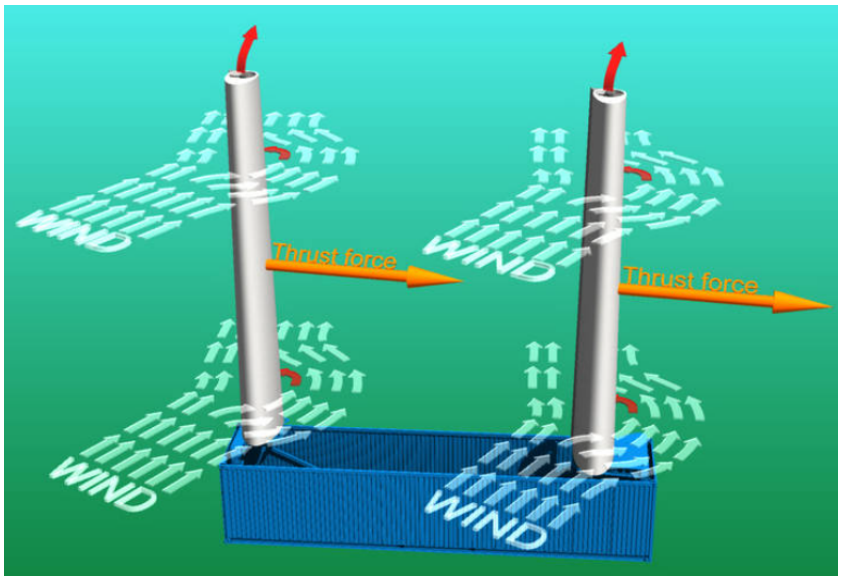

Figure 3.5: Aerodynamics of VentiFoils (Econowind, n.d.-c).

Econowind offers VentoFoils with various mounting options. For newbuilds, they can be seamlessly integrated, while smaller versions come in containerized formats or can be installed on flatracks (Econowind, n.d.-b; Smeets, 2024). Generally, they are tiltable.

The system is technically ready and installed on several ships, as the *MV Chemical Challenger* (Econowind, n.d.-a). Econowind aims to reduce fuel consumption by up to 60 % (Econowind, n.d.-b). It should be noted that VentoFoils reduce fuel consumption and they cannot be used to produce electricity. Installations costs for two suction wings of 11 m height can be considered with 325 000 EUR,

monthly maintenance costs with 535 EUR (Chica et al., 2023; Interreg, n.d.). The weight of a system with similar size can be assumed to be 9 600 kg (Conoship International, n.d.).

3.3.5. Wind Turbine

Wind turbines are widely used for energy generation both on- and offshore. In 2011, Bøckmann and Steen examined the use of a wind turbine for propulsion, specifically analysing a route between Bremerhaven, Germany, and Peterhead, United Kingdom. This route was selected due to its strong winds and their study found that a wind turbine with optimized blades achieved minimal greater energy savings compared to wing sails. The main advantage of wind turbines is their ability to generate electricity even when the vessel is stationary. However, wind turbines require significantly greater altitude compared to other forms of WASP. The turbine being studied had a height of 40 metres (Bøckmann & Steen, 2011). Vessels of this size are unable to access many inland ports or pass under bridges. Given that research vessels are smaller and typically stationed near research facilities, wind turbines will no longer be considered for the decarbonisation of research vessels.

3.3.6. Comparison

WASP - including Flettner rotors, kites, and suction-based foils - demonstrate solid potential to reduce fuel consumption and emissions. These systems can serve as effective supplements to conventional propulsion. Table 3.10 gives a summary of the main data of the introduced WASP. Not further investigated will be wind turbines due to their height and high centre of gravity as well as Flettner Rotors due to their high installation (Inst.) and maintenance (Main.) costs.

Table 3.10: Summary of WASP.

	Expected Savings	Size	Weight	Costs		Considered
			t	Inst. 10^3 EUR	Main. $\frac{\text{EUR}}{\text{month}}$	
Flettner Rotor	up to 50 %	height: 18 m, diameter: 3 m	n/a	750	1 208	no
(Power) Kite	100 - 200 kW per cycle	30 ft container	40	250		no
TwinFoil Wingsail	15 % to 30 %	height: 33 m, width: 11 m	45	250	500	no
VentoFoil	up to 60 %	40 ft container, foilheight: 10.3 m	9.6	325	535	yes
Wind Turbine	n/a	height of 40 m	n/a	n/a		no

Due to the limited number of vessels currently equipped with WASP, performance data vary significantly across and inside academic literature and manufacturer sources. Reported savings often differ depending on vessel type, device size, operational profile, and of course wind conditions. Additional uncertainty is added due to high dependency on wind speed and direction, which can vary significantly

by region and season, which must be considered when evaluating their overall feasibility. To address this uncertainty and ensure consistency in the modelling process, this thesis will consider only one representative WASP, namely the VentoFoils. This choice is based on the relatively large amount of publicly available performance data.

3.4. Further Energy Reduction Methods

In addition to alternative propulsion systems, there are various onboard technologies and operational strategies that can further reduce a vessel's overall energy demand. This section focuses on technologies such as EHR (Section 3.4.1) and solar power (Section 3.4.2).

Design-related optimizations - such as hull form adjustments or propeller optimizations - are not considered here, as research vessels are typically purpose-built and already optimized for their specific scientific missions.

3.4.1. Exhaust Heat Recovery (EHR)

Waste heat recovery, especially from exhaust heat offers significant potential for reducing fuel consumption and emissions. Especially for research vessels, which often operate in remote regions, optimizing energy usage is of particular importance.

Depending on type and configuration of the machinery, considerable amounts of waste heat are generated (Klein Woud & Stapersma, 2016). In medium speed diesel engines, exhaust gas temperatures reach up to 350 °C. Recovered waste heat can be utilized for onboard heating or for electricity generation (Klein Woud & Stapersma, 2016). Different principles are possible to achieve that. During the last years, a lot of research was done on this topic.

Mondejar et al., 2018, conducted a study, showing that Organic Rankine Cycles are promising for maritime applications. They often perform better at smaller scales, lower temperatures, and are more compact. Specific costs can be assumed with 2000 US-$/kW for units with around 500 to 1 000 kW. Mondejar et al. calculated fuel savings of up to 10 %.

3.4.2. Solar Power

Solar power is gaining increasing attention as a sustainable energy source. In 2016, Jacobson et al. conducted a study on the replacement of Washington State's energy consumption with renewable sources, proposing that solar energy should account for 10 % of total energy consumption by 2050. However, solar energy is not confined to land-based applications, it also holds potential for usage onboard vessels.

Diab et al., 2016, compared a hybrid system, which consists of a photovoltaic (PV) setup with a battery and a diesel generator, feeding a converter and distributing electrical load both on a ship and on land. A key difference from land installations is, that the PV system on a vessel experiences a load, which varies depending on the vessel's operation. Furthermore, the radiation level is dependent on the longitude and latitude the ship is sailing on. Efficiency is dependent on green water.

Since a research vessel solely powered by solar energy is unlikely, the variability in the electrical load on the PV system is not a significant issue, as there will be an additional electricity source.

In 2020, Karatuğ and Durmuşoğlu designed a PV system for a Ro-Ro vessel, utilizing PS335M-24/T Premium Panels by Solar Energy Company. With 1 274 solar panels placed on the foredeck for optimal sun availability, the system had a peak power of 426.8 kW. On a route from Pendik, Turkey, to Trieste, Italy, the system generated 334.06 MWh, contributing to 7.38 % reduction of the fuel consumption. Unsurprisingly, the ship, sailing in the northern hemisphere, achieved its highest energy production between May and August. The solar panels used in this study were of monocrystalline type with the measurements shown in Table 3.11.

Taking a look at the research vessel *Sonne*, the bulwark of the deckhouse and a small area on the upper part of the vessel can be assumed to be suitable for solar panel installation. Approximately 55 solar panels of the size given in Table 3.11 can be fitted on these areas, resulting in a peak power of

$$W_{Solar} = 55 \cdot P_{Peak} \cdot \eta_{Solar} = 3.18\,kW \tag{3.3}$$

Table 3.11: Measurements and Energy Capacity of Solar Panels (Karatuğ & Durmuşoğlu, 2020).

Length	Width	Height	Weight	Peak Power	Efficiency
1956 mm	992 mm	40 mm	22.5 kg	335 W	17.26 %

This corresponds to only about 0.05 % of the vessel's maximum power demand. While RoRo vessels may provide sufficient deck area for photovoltaic installation, research vessels typically need the space for research operations. Considering these spatial limitations as well as the uncertainties of this study, solar power is therefore considered negligible and will not be further taken into account.

3.5. Conclusion

Chapter 3 explored energy reduction strategies and alternative fuels for research vessels, focusing on technical feasibility.

FCs offer high efficiency (up to 57 %), silent operation, and zero emissions, but they remain costly and limited implemented in maritime use. ICEs are currently dominant due to reliability and fuel flexibility, but they emit GHG emissions, making them unsuitable for long-term decarbonisation unless used with low-emission or carbon-neutral fuels.

Alternative fuels were evaluated based on physical and chemical properties, emissions, technological readiness, availability, safety, and costs. HVO and LNG provide some immediate reductions in emissions, though HVO is limited by supply constraints. Ammonia, hydrogen, and methanol show strong potential as medium-term alternatives.

WASP such as Flettner rotors, kites and suction based foils can reduce fuel consumption and emissions. This thesis focuses on VentoFoils as WASP, given the high availability of relevant data. While power-generating kites are not viable for shipboard use, they could contribute to shore-based energy generation.

Onboard energy-saving devices such as EHR provide further efficiency improvements for auxiliary loads.

Throughout this chapter, uncertainty has emerged as a central issue. Performance data for novel technologies and alternative fuels is often limited, context-dependent, or inconsistent across sources. Pricing of sustainable fuels remain volatile and dependent on external factors. These uncertainties affect the reliability of the analysis and must be incorporated into modelling efforts.

4

Research Methods

To identify and evaluate decarbonisation strategies for research vessels, a decision making approach is required. This chapter addresses the third sub-question:

Which research methods, concerning parametric modelling, uncertainty analysis, and economic evaluation, are best suited to assess the feasibility of alternative fuels and WASP for research vessels?

The complexity of this task arises from the high level of uncertainty surrounding future developments in fuel and converter technologies, vessel operations, regulatory requirements, and operational and capital expenses.

Therefore, the chosen modelling framework must be capable of

- **Integrating technical, operational, and economic aspects**
  Decarbonisation strategies for research vessels must consider not just propulsion technologies but also how these technologies interact with vessel operations and life-cycle costs. A model ensures that the interdependencies between fuel choice, onboard systems, mission profiles, and economic viability are fully captured.
- **Accounting for deep uncertainty**
  Future developments in fuel technologies, infrastructure, and regulations are highly unpredictable and cannot be forecast with confidence. The model must therefore accommodate a wide range of plausible futures rather than rely on fixed assumptions or probabilities.
- **Comparing many different scenarios**
  To evaluate decarbonisation strategies effectively, it is essential to simulate a broad set of operational and technological scenarios.
- **Finding a robust rather than an optimal strategy**
  Rather than identifying a single “best” solution for a specific future, the goal is to find strategies that perform acceptably across many possible futures. This robustness ensures long-term viability and reduces the risk obsolescence.

4.1. Uncertainties

Decarbonisation of research vessels is a complex topic, holding certainties, but also a high number of uncertainties. The certainties - the things we already know - were explored in Chapters 2 and 3.

Assessing the feasibility of alternative fuels and propulsion technologies requires not only technical analysis but also a deep understanding of the uncertainties that shape long-term outcomes. Terün, 2020, described three types of uncertainties, namely the technological, economic, and regulatory one. In case of research vessel, a fourth layer - operational uncertainty - needs to be added.

Technological uncertainty refers to the unknowns associated with the development and deployment

of alternative propulsion technologies (Terün, 2020). Key concerns are the performance and durability of FCs under maritime conditions, especially over extended periods of operation, as well as the performance of EHR systems and WASP. The availability of supporting infrastructure further adds to the uncertainty, particularly given the global and remote operational scope of many research vessels.

Economic uncertainties stem primarily from the volatility of prices for alternative fuels, which are influenced by fluctuating demand, evolving production methods, and inconsistent supply chains as also stated by Terün, 2020. The long-term availability of these fuels, especially in remote or underdeveloped regions, remains difficult to predict. Capital expenditure ($CapEx$) and operational expenditure ($OpEx$) for new propulsion technologies are also difficult to estimate with precision due to rapidly changing market conditions and limited historical data. Furthermore, there is a considerable risk that early investments in specific technologies may become obsolete as standards evolve or more efficient alternatives emerge.

Regulatory uncertainty arises from the evolving nature of maritime emission policies at both international and regional levels (Terün, 2020). While current frameworks, such as those established by the IMO, provide some direction, the timeline and exact scope of future regulations remain unclear. This lack of predictability poses a challenge for shipowners and operators seeking to make long-term investment decisions aligned with compliance requirements. Additionally, the certification processes for emerging technologies, such as hydrogen FCs or WASP, are not yet fully standardized, further complicating regulatory planning.

Research vessels differ significantly from commercial ships in that each voyage is typically unique and driven by scientific mission objectives rather than fixed routes. This introduces substantial **operational uncertainty**, as energy requirements, system loads, and voyage durations can vary widely between expeditions depending on the research goals, environmental conditions, and geographic regions involved. The dynamic nature of these missions - ranging from stationary sampling to long transits - makes it difficult to predict fuel consumption patterns. Unlike commercial operations, which allow for standardization and forecasting, research missions require flexible propulsion and energy systems.

4.2. Level of Uncertainty

Widely adopted, next to others by Terün, 2020, and Suy, 2022, in the context of decision making under uncertainty is the classification of Marchau et al., 2019. As in Figure 4.1, Marchau et al., 2019, introduce different levels of uncertainty.

	Complete determinism	Level 1	Level 2	Level 3	Level 4 (deep uncertainty)		Total ignorance
					Level 4a	Level 4b	
Context (X)		A clear enough future 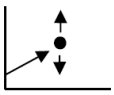	Alternate futures (with probabilities) 	A few plausible futures 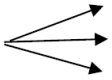	Many plausible futures 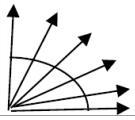	Unknown future 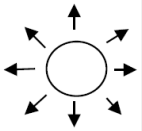	
System model (R)		A single (deterministic) system model	A single (stochastic) system model	A few alternative system models	Many alternative system models	Unknown system model; know we don't know	
System outcomes (O)		A point estimate for each outcome	A confidence interval for each outcome	A limited range of outcomes	A wide range of outcomes	Unknown outcomes; know we don't know	
Weights (W)		A single set of weights	Several sets of weights, with a probability attached to each set	A limited range weights	A wide range of weights	Unknown weights; know we don't know	

Figure 4.1: Levels of Uncertainty by Marchau et al., 2019.

Level 1 and 2 uncertainties are relatively certain. A system is well defined, for level 1 uncertainties, historical data is assumed as predictors of the future. Level 2 uncertainties can be described by stochastic and probabilistic properties. Potential outcomes of the future are attached by probability weights. In the case of decarbonising research vessels, this is not feasible. For example, no universally accepted

timeline exists for green hydrogen becoming cost-competitive or available at scale in ports. Assigning probabilities to technological breakthroughs or regulatory decisions is not possible with current knowledge.

Level 3 uncertainty implies a limited set of possible future scenarios, systems, outcomes and weights. Probabilities cannot be assigned to them. However, the complexity of the topic contradicts this simplification. Although the complexity of decarbonising research vessels initially suggests that the number of relevant parameters - such as port infrastructure availability, performance of FCs, WASP, and EHR, prices or policy levers - is too large to be captured by a limited set of scenarios, some aspects can be effectively scoped. Mission uncertainty - the main uncertainty differencing research vessels from commercial vessels - can be represented by a manageable set of distinct futures. As such, within the modelling framework, mission profiles can be treated in a more structured way, allowing them to be analysed as a discrete set of possible outcomes.

Level 4b would suggest an absence of any knowledge to guide decision-making. Also this level does not apply, as existing studies, and prototypes of alternative fuelled engines or FCs do provide partial knowledge and a basis for structured exploration.

The overall uncertainty associated with the decarbonisation of research vessels is best categorized as level 3 to 4a described by many plausible futures. This level captures situations in which a wide range of plausible futures must be considered simultaneously. Decarbonisation of research vessels is characterized by interdependent and evolving uncertainties across technological, regulatory, economic, and operational domains, which cannot be reduced to a limited number of discrete or predictable scenarios. Uncertainty levels associated with each uncertainty are described in Table 4.1.

Table 4.1: Levels for Each Uncertainty.

Uncertainty	Level	Explanation
Performance of FCs	3	FC systems for use in shipping are still under development, but individual projects are in the making (PowerCell Group, 2023). There is insufficient certainty to establish probabilities for future results, yet the possible directions are identifiable and describable.
Infrastructure	3	The construction of bunkering and loading facilities for environmentally friendly fuels depends on international investment, political incentives and technological restrictions. However, there is a range of possible futures, that can be thought of.
Availability of Fuels	4a	Production capacities for green ammonia, hydrogen and e-fuels are in the early stages and will be determined by global politics, market acceptance and geopolitics - there are no agreed scenarios or reliable probability limits (IRENA, 2024b). However, a wide range of future outcomes can be thought of.
Volatility of Prices	4a	Literature provides current prices and some long-term projections for alternative fuels (e.g. DNV, 2022b; IRENA, 2024b; Kang et al., 2021). However, prices are determined by many different influencing factors. It is not possible to draw up a probability calculation.

(Continued on next page)

(Continued from previous page)

Uncertainty	Level	Explanation
Capital and Operational Expenses	4a	While some estimates of capital and operational expenses are available (Chica et al., 2023; IEA, 2019), the cost of installing and operating novel technologies is driven by emerging technique, volatile supply chains and evolving markets - factors that introduce uncertainty and make reliable modelling or scenario planning difficult.
Evolving regulations	3	A number of policy instruments (carbon taxes (European Comission, n.d.-c), zero-emission mandates (DNV, 2025b)) are conceivable, but the timing and inclusion of research vessels cannot be credibly estimated.
Unique Missions	3 - 4a	Missions are highly unique. However, taking simplifications into account, a few scenarios can be thought of.
Transit Speed	3	Transit speed varies due to differences in missions, vessel characteristics, or operational practices. Based on the data for European research vessels provided by Nieuwejaar et al., 2019, a range of transit velocities can be defined.
Number of People Onboard	3	The number of onboard personnel, including crew and scientific staff, varies with vessels and operators. However, typical values can be derived from Nieuwejaar et al., 2019, allowing for a limited number of representative scenarios.

4.3. Decision Making Methods

Five approaches are provided by Marchau et al., 2019, the list is extended by Moallemi et al., 2020, and Terün, 2020. An overview of these, sorted into the different levels of uncertainties, is shown in Table 4.2.

Table 4.2: Decision Making Methods for Different Levels of Uncertainty Based on Terün, 2020, and Suy, 2022.

Level 2	Level 3	Level 4a	Level 4b
Real Option Analysis (ROA)	Engineering Options Analysis (EOA)	Dynamic Adaptive Planning (DAP)	Info Gap Decision Theory (IG)
Markov Decision Process (MDP)	Epoch-Era Analysis (EEA)	Dynamic Adaptive Policy Pathways (DAPP)	
		Decision Scaling (DS)	
		Robust Decision Making (RDM)	
		Many Objective Robust Decision Making (MORDM)	

As outlined in Section 4.2, the decarbonisation of research vessels is best characterized by level 3 to 4a uncertainty. Therefore, the focus of this section on decision-making methods is set specifically on these higher levels.

Engineering Options Analysis (EOA) offers a quantitative analysis for planning, design, and management of engineering systems over time (Marchau et al., 2019; Moallemi et al., 2020). A key strength of EOA is its explicit treatment of flexibility: It assesses the value of preserving multiple implementation pathways and informs decision-makers of trade-offs in terms of technical performance, cost, and risk.

Epoch-Era Analysis (EEA) decomposes and combines the contextual aspects on a group of scenarios (Gaspar et al., 2015). It distinguishes between short-term epochs and longer term eras. Several epochs, each defined by a static set of key factors, define a dynamic interval of time, an era, which can represent the lifetime of a vessel.

Dynamic Adaptive Planning (DAP) is a approach designed to maintain flexibility in face of uncertainty and changing environments (Marchau et al., 2019). It prioritizes flexibility, adaptability, and continuous learning to cope with uncertainty and complexity. The method typically unfolds in two main phases: design and implementation. During the design phase, robust strategies are developed that can perform well across a wide range of possible futures. In the implementation phase, these strategies are put into action, supported by monitoring systems that enable timely adjustments.

Dynamic Adaptive Policy Pathways (DAPP) is a planning approach that integrates the principles of DAP with the concept of adaptation pathways (Marchau et al., 2019). Originally developed to support climate-resilient strategies in water management, DAPP provides a structured method for decision-making that emphasizes flexibility within an overarching plan. The method addresses long-term strategic planning challenges under changing conditions by enabling a sequence of actions over time. These plans typically consist of initial actions and long-term options, allowing for adjustments as the context evolves. At the core of this approach is the recognition that policies have a limited design life and may become ineffective as conditions change.

Decision Scaling (DS), especially developed for climate risk assessment, uses a decision-analytic framework and structured sensitivity analysis to guide decision-making (Marchau et al., 2019). It focuses first on the decision context, identifying key objectives and thresholds. Then, through a climate stress test, the system is exposed to a wide range of climate conditions to reveal vulnerabilities. Finally, climate-informed risks are estimated using relevant projections, allowing decision-makers to evaluate which climate scenarios are most critical. DS ensures that decisions remain effective under diverse and uncertain climate futures.

Robust Decision Making (RDM) is a scenario-based, iterative approach designed to support strategic decision-making. Rather than seeking an optimal solution based on predicted outcomes, RDM emphasizes the identification of robust strategies - those that perform well compared to alternatives across a wide range of plausible future scenarios. This method involves running computational models thousands of times to stress-test proposed decisions against diverse futures. The results are then analysed using statistical tools and visualizations to help to identify robust strategies. RDM was used by Terün, 2020, to assess alternative fuel types of Ultra Large Container Vessels and Suy, 2022, to examine the feasibility of zero-emission walk to work vessels.

Many Objective RDM (MORDM) is used, when multiple objectives - as for example technical viability and economic rentability - are in contrast to each other. MORDM uses the RDM structure, but integrates concepts from multi-objective optimization to address complex decision problems involving multiple, often conflicting, objectives.

After a comparative evaluation of decision making methods, MORDM emerges as the most appropriate approach for the underlying topic. As part of this thesis, it is proposed to integrate the approach with an EEA to address the uncertainty surrounding potential future missions of research vessels.

In the maritime sector, the selected propulsion systems are cost-intensive installations that will be in operation for several decades. Considering the deep uncertainties with regard to technological developments, legal framework conditions, mission profiles, and costs, the strategies must remain viable across a wide range of future scenarios. The ability to operate satisfactorily in many highly uncertain

scenarios is a key factor in the decision to prioritise robustness over identifying a single optimal solution. Even if uncertain, a few plausible scenarios with the parameters of fraction of precise research and range can be thought of. To do so, an EEA will be included in the MORDM. Furthermore, the decarbonisation of research vessels is inherently a multi-objective problem, requiring an approach that can address and balance competing priorities, as the minimization of GHG emissions and the minimization of lifecycle costs.

MORDM provides a structured and flexible framework for evaluating these objectives in parallel, enabling the identification of robust, non-dominated strategies that support long-term decision-making under deep uncertainty.

4.4. Methodology

The MORDM framework was selected to evaluate the feasibility of decarbonisation strategies for research vessels under deep uncertainty. As presented in Section 4.3, this method enables a structured exploration of many possible futures, supporting the identification of vessel configurations that remain robust across a wide range of conditions. This section describes the steps of this method, which are shown in Figure 4.2, more in detail based on Marchau et al., 2019, Chapter 2.

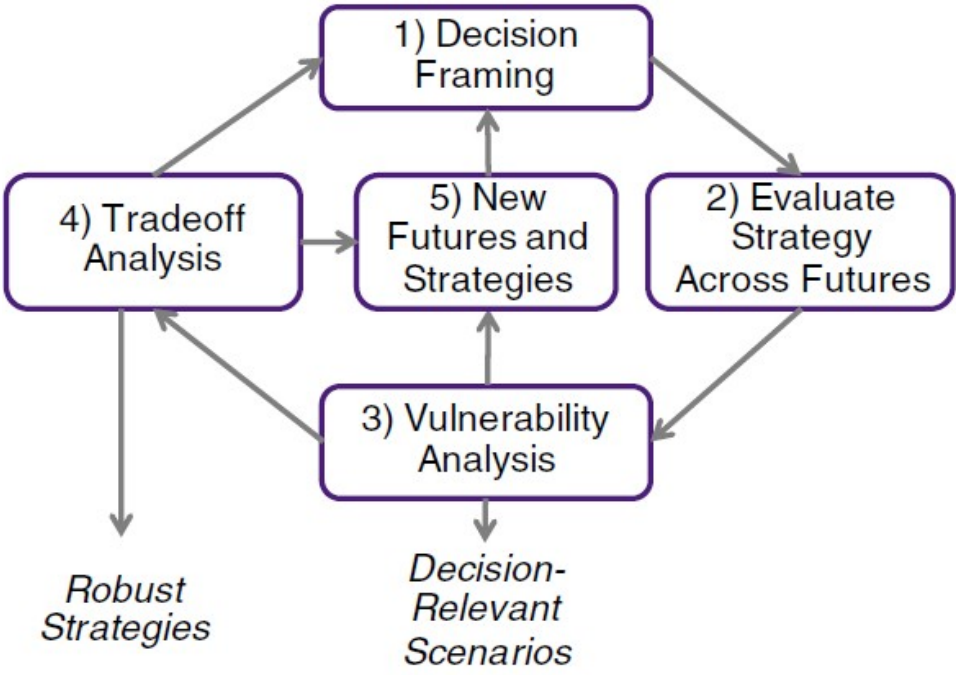

Figure 4.2: Steps in a RDM Analysis by Marchau et al., 2019, Chapter 2.

The method begins with **step 1** by establishing the decision context, often defined in a so-called “XLRM” matrix. Properties are exogenous uncertainties (X), policy levers (L), relationships (R), and measures of performance (M).

4.4.1. Exogenous Uncertainties (X)

Exogenous uncertainties are uncertainties, that come from outside the system and are not influenced by the choice of propulsion system.

The most important uncertainty in the context of decarbonisation of research vessels is the uncertainty of the missions. To address this, an EEA, as introduced in Section 4.4, is applied. This section defines the final set of eras proposed and used in this thesis to structure that uncertainty. The method helps to reduce the possible missions to a range of possible futures.

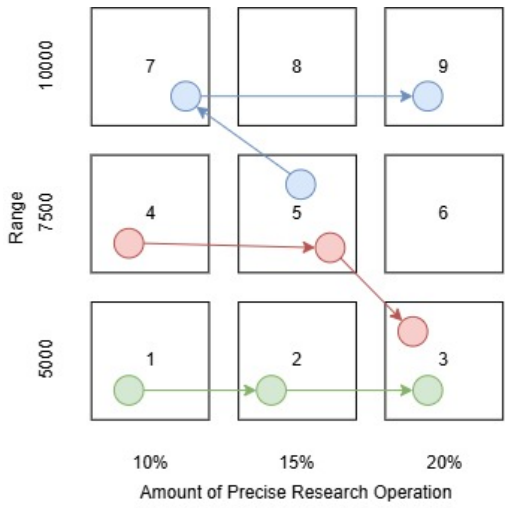

Figure 4.3: Epoch-Era-Diagram Based on a Figure by Gaspar et al., 2015.

The epoch-era diagram used is based on the methodology described by Gaspar et al., 2015, and already used by van Lynden, 2021. Figure 4.3 illustrates different research vessel types across various operational profiles, referred to as “eras”. The diagram is used to systematically cover plausible operating profiles. Each era represents a unique combination of range and the amount of precise research operation, thereby capturing the diversity in mission demands that a vessel may encounter. Unlike as in Gaspar et al., 2015, the diagram is not based on market forecasts, but attempts to cover as many different ship designs as possible. As research missions are dependent on current research projects, the author believes that these cannot be predicted but should remain diverse. This is why those eras are selected at representative low/medium/high levels of mission requirements to achieve a broad coverage of mission cases. Three epochs per era capture gradual changes over time. Each era has the length of a ships lifetime, which is assumed to be 30 years. Each epoch has a duration of 10 years. Consistency and validity is ensured by constraining the combinations to meet the statistically determined time budgets of the missions (fixed proportions for transit and port time as stated in Section 2.2), and by restricting transitions to remain within the same range row or shift between epochs by no more than one row to avoid unrealistic swifts.

$$t_{nr} = T - t_{transit} - t_{port} - t_{pr} \tag{4.1}$$

, where T denotes the total mission duration, and t represents the time allocated to normal research (t_{nr}), transit ($t_{transit}$), port or yard stay (t_{port}), and precise research (t_{pr}).

Figure 2.2 showed the engine load of different operations. Times of entering the port and weathering are assumed to be very low. For simplifying purposes, these operations will be neglected. Normal research, and seismic research will be combined to normal research, as the engine loads are quite similar. Table 4.3 describes the eras shown in Figure 4.3.

Table 4.3: Description of Proposed Eras.

Era	Epochs	Description
1	1 - 2 - 3	The vessel performs research within a range of 5 000 nm. After each ten years, the amount of precise research operations is increased to enable more detailed exploration.
2	4 - 5 - 3	This vessel is performing research within a range of 7 500 nm. After 10 years, it increases its amount of precise research operation. After another 10 years, it is going to support vessel 1.
3	5 - 7 - 9	Vessel 3 starts with a medium percentage of precise research in the range of 7 500 nm. After 10 years, it increases the range from 7 500 to 10 000 nm, while performing with a small fraction of time precise research. After another 10 years, the fraction is doubled.

Transit Speed

Transit speed v_s can vary due to differences in missions, vessel characteristics, or operational practices. Table 2.1 showed transit velocities ranging between 10 and 13 knots for various research vessels. For

this study, a reference transit speed of 12 knots is assumed, with an uncertainty factor x_V of 25 %, resulting in a velocity range from 9 to 15 knots. This approach not only accounts for the inherent uncertainty in transit velocity but also allows for evaluating the influence of speed variation on technical feasibility and economic performance.

Number of Crew and Scientific Staff

The number of people onboard, including both crew and scientific staff, can vary due to differences in mission profiles. The *Sonne* has accommodation for up to 72 people (Briese Research, n.d.). The majority of the European deep sea going research vessels have capacities for 20 to 40 scientists (Nieuwejaar et al., 2019). With crew, a standard number of people onboard N_{PoB} is assumed to be at 60, with a deviation (x_N) of 50 %.

Fuel Cell Performance

The performance of FCs represent a critical exogenous uncertainty in the assessment of low-emission propulsion systems. The technology is still undergoing rapid development and have yet to reach full technological maturity in maritime applications. Including FC performance uncertainty in the model allows for a more realistic appraisal of energy system viability across diverse futures. PowerCell Group, 2025, gives the efficiency with 42 to 57 %. To reflect long-term performance, an efficiency (η_{FC}) of 50 % is used with a deviation (x_{FC}) of 20 %.

WASP Performance

The performance of VentoFoils depends highly on the external factor of wind condition. In this study, WASP efficiency (η_{WASP}) is treated as a continuos uncertainty parameter, representing the relative reduction in fuel consumption. Based on literature and manufacture estimates shown in Section 3.3, the saving potential is modelled to range between 5 and 15 %, reflecting both pessimistic, conservative, and optimistic scenarios. The uncertainty factor is called x_{WASP}.

EHR Performance

The baseline efficiency for EHR (η_{EHR}) is set at 10 %, based on calculations from Mondejar et al., 2018. To reflect variability in technology, an uncertainty factor x_{EHR} of $\pm$ 50 % is applied. This yields a 5 - 15 % efficiency range and keeps the value consistent with the second energy reducing technology of WASP.

Fuel Prices

Energy carrier prices are subject to volatility. Fuel costs have a substantial influence on both the operational expenditure and the overall economic feasibility of alternative propulsion systems. However, these prices are difficult to predict due to their dependence on a range of external factors, including fluctuations in global energy markets, geopolitical developments, and technological progress in fuel production and distribution.

Closely linked to fuel price is the uncertainty surrounding future fuel availability. As already described, research vessels are only bound to a limited extent to the availability of fuel in ports, as they are typically refuelled by tank trucks, but this nevertheless has an impact on fuel costs.

Based on literature review and actual port price data, plausible base prices for the years 2025 and 2050 were described in Section 3.2, summarized in Table 4.4. Prices for ammonia, hydrogen, and methanol are forecasted to decrease, however, forecasts of HVO and LNG are not available, so they will be priced as in 2020.

Suy, 2022 defined an uncertainty range of $\pm$ 30 % for fuel prices, while also defining a range for fuel availability. In this thesis, they are combined, as it is assumed, that the measurable influence of fuel availability is shown in the price. For this reason, a deviation (x_{fuel}) of 40 % of the base price is assumed. As in Suy, 2022, short-term volatility is neglected to not further complicate the analysis.

Capital Expenditure

Unlike fuel prices and political parameters, capital costs can be traced back to literature as indicated in Section 3.2. Therefore, a range (x_{CapEx}) of $\pm$ 25 % is used, which is narrower than for other exogenous factors, while it still follows a modest approach.

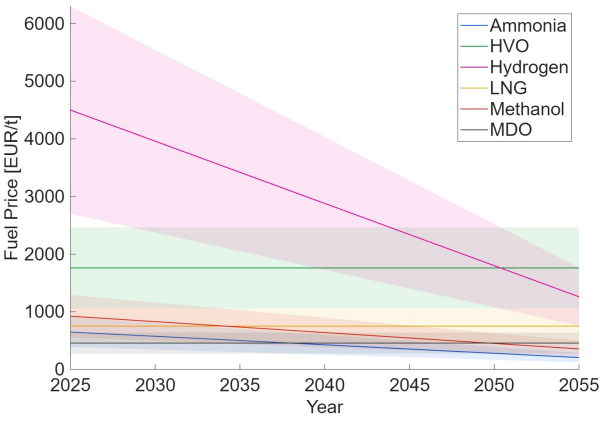

Figure 4.4: Projected Fuel Prices with $x_{Fuel} = 0.4$ Based on Figures by Suy, 2022.

Table 4.4: Summary of Fuel Prices Based on Section 3.2 (Argus O.M.R., 2025; DNV, 2022a; IRENA, 2024b; Kang et al., 2021; SEA-LNG, 2025; S&P Gobal, 2025).

Fuel	Price 2025 [EUR/t]	Price 2050 [EUR/t]
Ammonia	648	279
HVO	1 760	1 760
Hydrogen	4 500	1 800
LNG	750	750
Methanol	923	450
MDO	456	456

4.4.2. Policy Levers (L)

In the context of decarbonising research vessels, the most likely policy lever is a carbon trading scheme, such as the EU ETS. As with many current regulations, non-commercial vessels are often exempted, therefore, the introduction of a zero-carbon mandate for research vessels is considered unlikely.

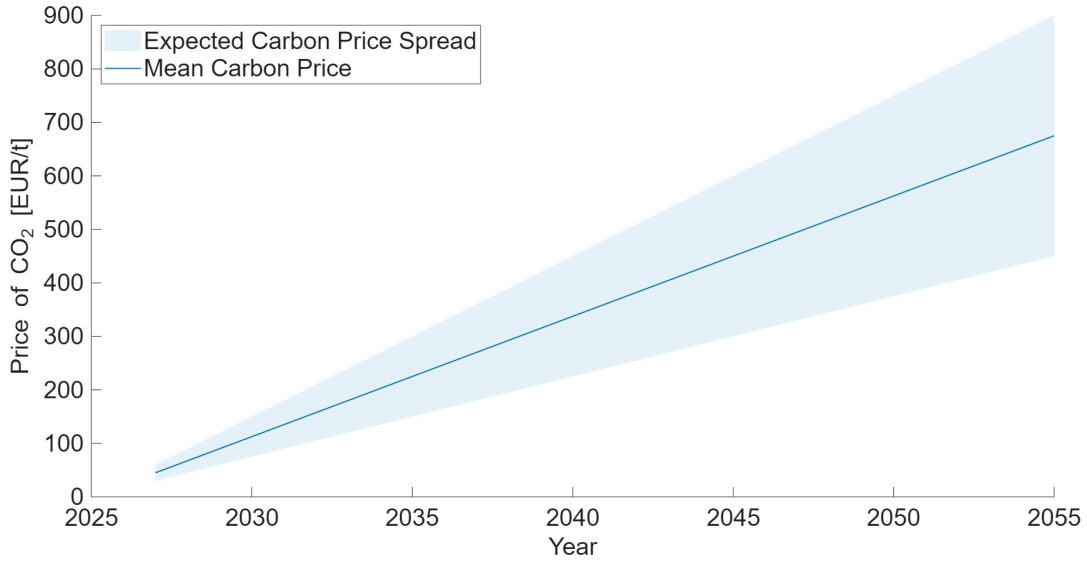

Figure 4.5: Projected Price of CO_2 under the EU ETS Based on Figures by Suy, 2022.

Within the EU ETS, a cap is placed on total emissions, and companies must hold allowances equal to their emissions. These allowances can be traded, creating a market-based price for carbon (see also Section 2.4.2). To ensure a smooth introduction of the expanded system (ETS2), a soft price cap of 45 EUR/t may be introduced (European Comission, n.d.-c). However, market analysts expect the actual starting price in 2027 to be closer to 60 EUR/t CO_2 (BloombergNEF, 2025), reaching 150 EUR/t CO_2 by 2030.

To estimate the long-term cost implications, a linear extrapolation from this forecast suggests a potential price of 900 EUR/t CO_2 by 2055. This extrapolated value is used as a conservative upper bound in the analysis, representing the potential cost impact if this policy lever is applied to research vessels. The assumed price range is illustrated in Figure 4.5.

4.4.3. Relationships (R)

The relationships R of the XLRM matrix are the links between the uncertainties and levers as input of a scenario and the measures as output (Lempert et al., 2003).

A state-of-the-art research vessel as described in Section 2.3, namely the *RV Sonne*, is selected to assess technical feasibility. This approach relies on using a representative baseline vessel, rather than designing a vessel from scratch for each scenario. While this method may yield different outcomes compared to a full vessel design process, it significantly simplifies the modelling task given the limited availability of detailed public data and research on this specific type of vessels. Moreover, it allows for a more practical and transparent evaluation of current technological capabilities within varying operational contexts.

The *RV Sonne* is selected, as she is the vessel with the greatest data available. Nieuwejaar et al., 2019, classified her as a global vessel, however, her main research area is the Indic and Pacific. Main technical data is shown in Table 4.5.

Table 4.5: Technical Data of *RV Sonne* (Briese Research, n.d.; Meinders, 2025).

Length over all	L_{oa}	116.00	m
Length between perpendiculars	L_{pp}	102.86	m
Beam	B	20.60	m
Draught	D	6.40	m
Service Speed	v_S	12	kn
Range		7 500	nm
Endurance	T	50	d
Power	P	6 000	kW
max. number of persons onboard	N_{PoB}	80	

4.4.4. Measures of Performance (M)

To evaluate the decarbonisation strategies, two measures of performance are applied: GHG emissions and expenses associated specifically with the propulsion system. These represent the “M” component of the XLRM matrix. Emissions are calculated on a life-cycle basis, covering Well to Wake (WtW) contributions of each fuel type. This way, the analysis provides insight into the effectiveness of each decarbonisation strategy. This enables a fair comparison between fossil and renewable fuels, as well as an understanding of how auxiliary technologies such as WASP or EHR contribute to GHG reduction. Expenses include both capital and lifecycle operational costs of the propulsion system. The detailed formulations of these measure are provided in Chapter 6, where they form the basis of the performance evaluation.

In **step 2**, simulation models are used to test the proposed strategies across a wide range of possible futures, creating a large database of results. These strategies may originate from public debate, optimization routines, or a broad initial set that is refined into more viable options. In this thesis, the parametric model utilizing the XLRM-matrix, will be used to create many plausible futures.

Table 4.6: Possible Propulsion Configurations. Red: Technically not Plausible.

		EHR	no EHR	EHR	no EHR
Fuel	**Converter**	WASP		no WASP	
Ammonia	ICE				
HVO					
LH_2					
LNG					
Methanol					
Ammonia	FC				
HVO					
LH_2					
LNG					
Methanol					

A total amount of 40 propulsion configurations could be constructed, however, some are technically implausible, as shown in Table 4.6. For instance, EHR is only useful, if exhaust heat is produced, so only in combination with ICEs. Furthermore, HVO and LNG cannot be utilized in FCs. In total, 26 configurations are plausible, although they do not necessarily have to be technically feasible. Each configuration is examined across all combinations of uncertainties shown in Table 4.7. Hence, the parametric model evaluates 128 304 unique possible futures.

Table 4.7: Uncertainty Factors.

Uncertainty	Factor	Range or Scenario Option	Number of Scenarios
Mission Profile		Era 1, Era 2, Era 3	3
Transit velocity	x_V	-25 %, +0 %, +25 % (from base velocity)	3
Number of personnel on board	x_N	-50 %, 0 %, +50 % (from base number)	3
Fuel Cell Performance	x_{FC}	-20 %, 0 %, 20 % (relative to baseline efficiency)	3
WASP Performance	x_{WASP}	-50 %, 0 %, 50 % (relative to baseline efficiency)	3
EHR Performance	x_{EHR}	-50 %, 0 %, 50 % (relative to baseline efficiency)	3
Fuel Prices	x_{Fuel}	-40 %, 0 %, 40 % (from base price)	3
CapEx Uncertainty	x_{CapEx}	-25 %, 0 %, 25 % (from estimate)	3
Emission Trading Scheme	l_{ETS}	Not introduced, -33 %, 0 %, 33 % (from base price)	4

In contrast to the approach taken by Suy, 2022, where the parametric model was constructed and analysed before introducing uncertainty through RDM, this thesis integrates uncertainty already in the examination of the technical feasibility. Due to the critical influence of uncertainty factors such as the operational profiles of research vessels and the technological performance of FCs, these uncertainties will be considered already during the parametric model setup.

In **step 3**, the dataset is explored using statistics and visualised through box and scatter plots. The objective is to identify configurations that exhibit vulnerabilities, such as exceeding geometric constraints, limited robustness across operational profiles, and sensitivity to fuel price assumptions, or that perform consistently well across uncertainty scenarios. Uncertainty drivers are analysed regarding their influence on the results. To identify the most influential uncertainty parameters, the data set is divided according to the parameters. For each subdivision, the shifts in the boxes across parameter settings are compared and the stability of the fuel ranking is checked.

For the visualization of distributions, mainly two approaches are available: box plots, as used by Terün, 2020, and violin plots, as applied by Suy, 2022. Box plots provide a summary of the distribution by indicating the median, quartiles, and potential outliers, making them a precise tool for identifying the spread and extreme values (Yi, n.d.-a). Violin plots, by contrast, extend box plots with a mirrored kernel

density curve, which visualizes the shape of the distribution (Yi, n.d.-b). They are based on a kernel distribution function rather than the actual data points. This smoothing may exaggerate the tails of the distribution, making configurations that are fully robust appear less reliable. Since the optimistic and pessimistic scenarios in this thesis are already conservatively defined, a direct visualization of the available data points is more appropriate. For this reason, box plots are chosen as the visualization method.

Figure 4.6 illustrates the structure of a boxplot. The central box represents the interquartile range, which covers the middle 50 % of the data. The line inside the box indicates the median (Q2). The whiskers extend to the smallest and largest values within 1.5 times the interquartile range, thereby capturing the main spread of the data. Any points beyond this range are classified as outliers and shown individually as dots. This visualization provides insights into both the central tendency and the variability of the results, while also showing extreme cases.

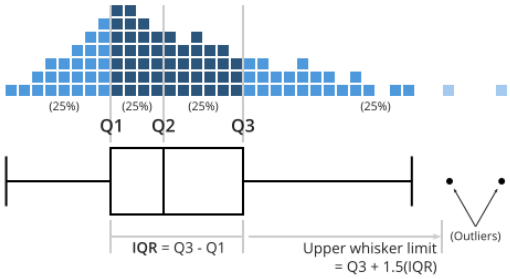

Figure 4.6: Visualization of box plots from Yi, n.d.-a.

Trade-off's are displayed and evaluated to support decision-making processes in **step 4**. A multi-objective analysis is conducted to assess the two competing criteria, namely lifecycle GHG emissions and costs. Results are visualised as scatter plots to make the trade-offs explicit, and technical robustness is assessed against predefined feasibility constraints. Those that maintain acceptable performance - of technical feasibility, economic and emission-related performance - across most scenarios are identified as robust strategies.

Finally, **step 5** enables to use the scenarios to identify potentially more robust strategies. The iterative process can be started from the beginning.

4.5. Conclusion

Chapter 4 presented the methodology that will be used to evaluate decarbonisation strategies for research vessels in the face of deep uncertainty. Levels were assigned to these uncertainties - described in Section 4.1 - in Section 4.2. From the decision making methods Section 4.3, it was decided to apply the MORDM framework in combination with a parametric model. A structured process was described to generate, simulate and assess a wide range of vessel configurations in Section 4.4. The model incorporates essential technical requirements to ensure that only configurations capable of reliably meeting energy demands for propulsion and hotel loads are considered.

5

Parametric Model

Building on the review of vessel design, energy options, and research methods, the next step is to translate these findings into a tool to evaluate the feasibility of alternative fuels and propulsion systems for research vessels. This chapter contributes to step 1 of the MORDM framework, the problem framing. While developing a parametric model, it links the “X” and “L” specified in Section 4.4 through the “R” to “M” in Chapter 6. Together, Chapters 5 and 6 complete step 1 by specifying the XLRM structure. The model developed links the choice of fuel, converter and auxiliary technologies with hull geometry, displacement and power requirements. By introducing a geometric constraint, the model ensures that only technically consistent and feasible configurations are considered. The following sections describe the main components of the model, starting with the geometric constraints, through the evaluation of the basecase vessel, time calculations, and energy requirements, to the volume and displacement updates.

Figure 5.1 provides an overview of the model structure. Inputs such as vessel data, operational profiles, and fuel properties are processed through the model, which calculates energy demand, additional length, costs, and emissions. Results are expressed as performance measures including technical robustness, lifetime GHG emissions, and associated costs of the propulsion system (Chapter 6). Base values used in this chapter are summarised in Table A.1. The uncertainty deviations x are directly applied to the variables in the model.

5.1. Geometrical Constraint

To ensure that all vessel configurations remain technically realistic and applicable across different ship types, a relative constraint for the hull geometry is introduced. Rather than applying an absolute limit on the added length, the vessel’s length-to-beam ratio ($^{L}/_{B}$) is used as the primary geometric boundary. As summarized in Section 2.3.4, the reviewed research vessels exhibit $^{L}/_{B}$-ratios between 3.1 and 6.4, with most clustering around 4.3 to 5.6. In comparison, cargo ships typically fall in the range of 6 to 7 and passenger vessels in 6.5 to 7.5 (Molland, 2008). To ensure that the parametric model remains consistent with these observed proportions, while still allowing for somewhat more slender hulls than those currently common, a maximum $^{L}/_{B}$ of 7.0 is applied. This threshold lies above the values observed in current research vessels, but it remains within the ranges considered acceptable for both cargo and passenger ships. In this way, the model avoids excluding potential future designs with more slender forms, while at the same time preventing unrealistic hull geometries beyond established practice.

$$\frac{L_{BCV} + \Delta L}{B_{BCV}} \leq 7.0 \tag{5.1}$$

, where the subscript BCV denotes the base case vessel.

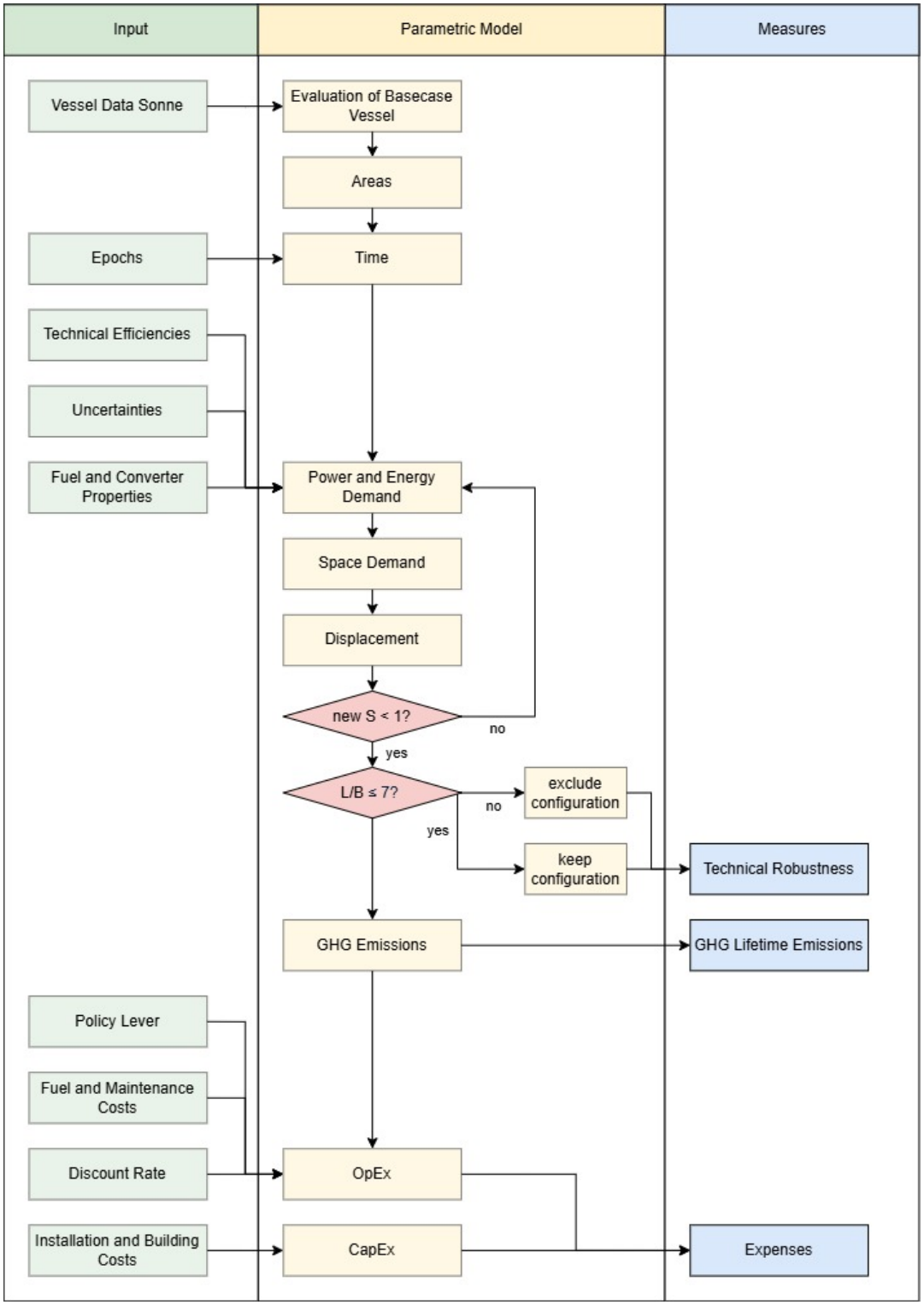

Figure 5.1: Flowchart of Parametric Model.

5.2. Evaluation of Basecase Vessel

The available data for the base ship must be analysed according to the parameters required for the subsequent calculations. Important measures, as c_B, c_M, and Fn equations provided by Schneekluth, 1985, are used. These formulas are relatively old, and mainly used for cargo vessels. Cargo and research vessels share the requirement for large, unobstructed volumes within the hull. In cargo vessels,

this space is needed for holds that can accommodate goods, while in research vessels it is required to integrate laboratories and storage areas for scientific equipment.

$$c_B = \frac{0.14}{Fn} \cdot \frac{L_{pp}/B + 20}{26} \tag{5.2}$$

$$c_M = 0.9 + 0.1 \cdot c_B \tag{5.3}$$

, where

$$Fn = \frac{v_s}{\sqrt{(L_{pp} \cdot g)}} \tag{5.4}$$

, where $g = 9.81 m/s^2$ represents the gravity of earth. Equations 5.2 to 5.4 are applied to the basecase vessel, yielding calculated values of $c_B = 0.6926$, $c_M = 0.9693$, and $Fn = 0.1943$. Barrass and Derrett, 2012, state that medium-form vessels have a block coefficient of around 0.70, so it is assumed that the equations give some good indicates.

To estimate the actual tank size of the basecase vessel, the operational profile introduced in Chapter 2 is applied. 40 % of the time is used for transit, corresponding to a sailing distance of 7 500 nm. A further 15 % of the mission time is spent in port. It is assumed, that the rest of the time is equally used for normal and precise research.

$$T = \frac{Range}{v_s \cdot 40\,\%} \cdot (100\,\% - 15\,\%) = 55\,d \tag{5.5}$$

As shown in Equation 5.5, this yields an endurance of 55 days, which is close to the reported endurance in Table 4.5.

The energy consumption per mission is the sum of the power for each mission part -transit, normal research, and precise research - multiplied by the time for that specific part as in Equation 5.6. The utilized power in the port is neglected, as it is assumed, that the vessel can be fuelled before and after the port stay.

$$E = \sum P_i \cdot t_i \tag{5.6}$$

Where E denotes the total energy consumption, and i is the part of the mission. In all operating modes, propulsion and research power is handled separately from hotel load, to avoid double counting later on. The term $\sum P_i \cdot t_i$ includes all mission components:

$$\sum P_i \cdot t_i = P_{transit} \cdot t_{transit} + P_{nR} \cdot t_{nR} + P_{pR} \cdot t_{pR} + P_{Hotel} \cdot (t_{transit} + t_{nR} + t_{pR}) \tag{5.7}$$

Values as introduced in Figure 2.2 are shown in Table 5.1.

Table 5.1: Estimated Energy Consumption per Mission *RV Sonne*.

i	P	t
transit, normal speed	2 750 kW	0.4 T
normal research	1 950 kW	0.225 T
precise research	4 750 kW	0.225 T
hotel	1 250 kW	0.85 T
Sum E_{BCV}	4 874 634 kWh	

The tank size (V_{Tank}) is calculated with the energy density of the used fuel, namely MDO.

$$V_{Tank} = \frac{E}{\rho_{V,\,MDO}} = 443\ m^3 \tag{5.8}$$

The calculated tank size (Equation 5.8) is 443 m^3, which is close to the 600 m^3 LNG tank for the research vessel *Atair*. Considering the lower energy density of LNG compared to MDO, this indicates that the calculated value is realistic and of representative size.

The vessel will most likely be subject to a lengthening if alternative energy carriers are used, since their lower volumetric energy densities compared to MDO require significantly larger fuel volumes. To accommodate these larger tanks within the geometric constraints of the hull, additional length becomes necessary. Only in a few configuration where the range is reduced to 5 000 nm this effect can be offset. The effective power P_E can be calculated as a function of density of the water, the velocity v_s, the wetted surface S and the coefficient of total resistance c_T (Schneekluth, 1988). Assuming, that only v_s and S are variables, the factor c can be calculated. Please note, that within Equation 5.9 efficiencies of the shaft line ($\eta_D \cdot \eta_S$) are already taken into account.

$$P_B = \eta_D \cdot \eta_S \cdot P_E = \underbrace{\eta_D \cdot \eta_S \cdot \frac{\rho_{sw}}{2} \cdot c_T}_{c} \cdot v_s^3 \cdot S \tag{5.9}$$

$$c = \frac{P_{transit}}{v_s^3 \cdot S} \tag{5.10}$$

The wetted surface area S is estimated using the formula of Danckwardt given in Schneekluth, 1988.

$$S = \frac{\nabla}{B} \cdot \left[\frac{1,7}{c_B - 0.2\,(c_B - 0.65)} + \frac{B}{D} \right] \tag{5.11}$$

, where

$$\nabla = L_{pp} \cdot B \cdot D \cdot c_B \tag{5.12}$$

This formula was originally derived for cargo and passenger ships. While research vessels are designed for different operational purposes, their hulls also fall within the general family of displacement forms. This suggests that the correlation can still provide a useful approximation of wetted surface areas, especially as it is only used here to establish a baseline value. Since relative changes in wetted surface are updated iteratively, the results of these are more sensitive to variations than the absolute baseline itself.

Variations in people onboard lead to in- or decrease of hotel power demand. Based on Figure 2.2, where a hotel load of 1 250 kW is shown, an average value of 16 kW per person is assumed. It is acknowledged that this simplification does not capture the non-linear nature of hotel load scaling with personnel number, since some systems are only partially dependent on occupancy. However, this is the best approximation available to the author, as alternative estimation methods, such as the equations provided by Taen et al., 2016, showed significant deviation from the load diagram of the base case vessel and were therefore deemed unsuitable for this study.

5.3. Available Tank and Converter Midship Areas

Before evaluating configuration-specific space demand, the available installation areas of the vessel must be defined. These represent static geometric constraints that apply to all configurations equally and are directly dependent on the basecase vessel. In the parametric model, geometry changes are expressed through the additional vessel length ΔL. Since the required volumes of fuel and converters are obtained later from energy and power requirements (Sections 5.5 and 5.6), a link is needed to convert these volumes into length increments. This link is provided by the available installation areas of the hull. The following section therefore defines the tank and converter areas available based on the geometry of the *Sonne*.

For the definition of tank areas, two storage cases are considered. For both cases, the additional volume for fuel and converter will be located below the design waterline to allow for scientific workspace and crew area above the waterline. Furthermore, from both bottom and sidewalls a double hull with

$B/20$ is taken into account. Ammonia, hydrogen, and LNG require cryogenic storage, which is represented in the model by circular tanks. Here, three circular tanks are arranged side by side, each with a diameter equal to the draught excluding the double bottom. This layout results in a combined width of approximately 16 m, leaving about 4 m free for corridors and auxiliary systems. The loss of effective tank area due to wall thickness of the cryogenic tank is represented by a factor η_{tw}. This factor is set to 97 %. In contrast, HVO and methanol are stored under ambient conditions. The available area is derived from the midship area and adjusted by an space efficiency factor η_u, accounting for space for corridors, steel structures, and equipment. Suy, 2022, used a coefficient of 85 %, which included the double bottom. Since this double bottom is already taken into consideration, an η_u of 90 % is used.

$$A_{Tank} = \begin{cases} \left(D_{BCV} - \frac{B_{BCV}}{20}\right)^2 \cdot \frac{\pi}{4} \cdot n_{Tanks} \cdot \eta_{tw}, & \text{if fuel is cryogenic} \\ c_{M,\,BCV} \cdot \left(B_{BCV} - \frac{2 \cdot B_{BCV}}{20}\right) \cdot \left(D_{BCV} - \frac{B_{BCV}}{20}\right) \cdot \eta_u, & \text{otherwise} \end{cases} \tag{5.13}$$

For additional converters, the available installation area is likewise derived from the midship section of the basecase vessel.

$$A_M = c_{M,\,BCV} \cdot B_{BCV} \cdot D_{BCV} \cdot \eta_u \tag{5.14}$$

5.4. Time

The duration of a research mission is divided into several operational phases, each with different power requirements. As shown in Section 2.2, research vessel operations typically consist of transit, precise research, normal research, and time in port or shipyard. First, the transit time ($t_{transit}$) is calculated based on the required mission range as part of the epoch and the vessel's average service speed (v_s).

$$t_{transit} = \frac{Range}{v_s} \tag{5.15}$$

As discussed in Section 4.1, the transit speed is subject to uncertainty and can vary depending on mission profiles and vessel characteristics. For this thesis, a baseline value of 12 knots is used, with a variation range of $\pm$ 25 %.

Given the assumed transit fraction ($f_{transit}$), which is 40 % according to operational patterns observed in two German research vessels (see Section 2.2), the total mission duration T is determined according Equation 5.16:

$$T = \frac{t_{transit}}{f_{transit}} \tag{5.16}$$

The time spent in port or shipyard is derived from operational data discussed in Section 2.2, where the *Sonne* and *Maria S. Merian* show average port times of approximately 15 % of their total mission duration.

$$t_{port} = f_{port} \cdot T \tag{5.17}$$

While this phase is not directly relevant for the calculation of the required hull length - as it is assumed that the vessel can bunker before and after the port stays - it is still essential for an accurate assessment of lifecycle emissions in later steps of the analysis.

The time allocated to precise research is defined as a fraction f_{pR} of the total time. These fractions are scenario-dependent and are derived from the epoch-era framework presented in Section 4.1 and visualized in Figure 4.3.

$$t_{pR} = f_{pR} \cdot T \tag{5.18}$$

Finally, the normal research time is derived by subtracting transit, port and precise research time from the total mission time.

$$t_{nR} = T - t_{transit} - t_{port} - t_{pR} \tag{5.19}$$

These time values form the foundation for calculating the vessel's energy demand during each operational mode, enabling an estimation of required fuel volumes, system dimensions, and associated emissions and costs.

5.5. Power and Energy Demand

Building upon the operational time splits calculated in Section 5.4, the vessel's energy requirements are quantified for each operational mode - transit, normal research, and precise research. These values depend not only on the operational duration but also on the type of installed converter and optional technologies like WASP or EHR. The power calculations are integrated into an iteration loop, as changes in hull length and displacement influence resistance, thereby altering transit power requirements.

The transit power is calculated as a function of the vessels resistance. For each configuration, the propulsion power is adjusted to account for the converter efficiency η_c and, if installed, WASP. WASP reduces the propulsion demand by the efficiency η_{WASP}. Transit propulsion power is estimated following the common cubic speed scaling with wetted surface as provided by Schneekluth, 1988:

$$P_{transit} = \begin{cases} \frac{\eta_{c\,BCV}}{\eta_c} \cdot (1 - \eta_{WASP}) \cdot c \cdot v_s^3 \cdot (S_{BCV} + \Delta S)\,, & \text{if WASP is applied} \\ \frac{\eta_{c\,BCV}}{\eta_c} \cdot c \cdot v_s^3 \cdot (S_{BCV} + \Delta S)\,, & \text{otherwise} \end{cases} \tag{5.20}$$

, where

- c: constant derived from the baseline vessel, see Equation 5.10.
- ΔS: added wetted surface due to the hull extension. In the first iteration round, before the geometry has been updated, $\Delta S = 0$.

For normal and precise research operations, power demand is based on fixed loads from the basecase configuration in Figure 2.2 and Table 5.1, scaled with the efficiency of the converter system. These phases are typically conducted at very low transit speed, but with high power demand for winches, positioning systems, and scientific equipment. The following equations are used.

$$P_{nR} = P_{nR\,BCV} \cdot \frac{\eta_{c\,BCV}}{\eta_c} \tag{5.21}$$

$$P_{pR} = P_{pR\,BCV} \cdot \frac{\eta_{c\,BCV}}{\eta_c} \tag{5.22}$$

It should be noted that these power demands are not updated as a function of hull geometry. Since they are mainly determined by scientific equipment and DP requirements, only minor changes would be expected within the geometric constraints considered here. A detailed recalculation would not only require significant computational effort but also operational data that is not available at this stage. Therefore, these loads are kept constant in order to avoid unnecessary model complexity. The hotel load is calculated assuming 16 kW per person, as stated in Section 5.2.

$$P_{Hotel} = 16\,kW \cdot N_{PoB} \cdot \frac{\eta_{c\,BCV}}{\eta_c} \tag{5.23}$$

, where N_{PoB} is the number of people onboard, which varies between scenarios.

The total energy consumption per mission includes all power demands over time - propulsion, research operation, and hotel load - summed across all operational phases. If an EHR system is installed, the entire energy demand can be reduced by the factor η_{EHR}, as exhaust heat is generated in all operation modes where fuel is burned - including transit, normal research, and precise research. Therefore, EHR savings apply globally.

In contrast, WASP only reduces the propulsion power during transit as the aerodynamic thrust provided by WASP can only be used when the vessel is moving. In principle, this thrust could also be used to increase speed at constant power. However, since research vessels are not designed to operate at high speeds, and maintaining a common service speed improves comparability between scenarios, this model considers only power reductions. During normal and precise research operations, the vessel is either stationary or manoeuvring slowly, making WASP infeasible. Likewise, hotel load and auxiliary systems are unaffected by WASP.

$$E = \begin{cases} (1 - \eta_{EHR}) \cdot \sum P_i \cdot t_i, & \text{if EHR is applied} \\ \sum P_i \cdot t_i, & \text{otherwise} \end{cases} \tag{5.24}$$

5.6. Space Demand of Configurations

In the vessel design evaluation, different types of internal volume are required to accommodate additional systems, such as fuel tanks and energy converters, and increased personnel. Equations 5.25 to 5.27 are applied to estimate additional volume requirements. The relations follow directly from design logic: fuel tank volume scales with the required energy content and energy density of the fuel, converter volume depends on the installed power and the specific power density, and additional accommodation space is assumed to increase proportionally with the number of persons on board.

$$\Delta V_{fuel} = \frac{E}{\rho_V} - V_{fuel,\,BCV} \tag{5.25}$$

$$\Delta V_c = max(P_m) \cdot \varphi_v - V_{c,\,BCV} \tag{5.26}$$

$$\Delta V_{PoB} = (N_{PoB} - N_{PoB,\,BCV}) \cdot 30\,m^3 \tag{5.27}$$

When calculating the required hull extension to accommodate additional volumes for fuel, converter and additional person on board, the space demand can be distributed between below and above the waterline. Two lengths are calculated:

- ΔL_u: Required length extension below the waterline, where fuel and converters are installed.
- ΔL_a: Length extension above the waterline, where accommodation and crew space is located.

$$\Delta L_u = \frac{\Delta V_{fuel}}{A_{M,\,t}} + \frac{\Delta V_c}{A_M} \tag{5.28}$$

$$\Delta L_a = \frac{\Delta V_{PoB}}{(H_{BCV} - D_{BCV}) \cdot B_{BCV}} \tag{5.29}$$

If $L_u > L_a$, there is free space available above the waterline. The corresponding free volume is expressed as

$$V_{free} = (\Delta L_u - \Delta L_a) \cdot (H_{BCV} - D_{BCV}) \cdot B_{BCV} \tag{5.30}$$

, where $(H_{BCV} - D_{BCV}) \cdot B_{BCV}$ represents the area that can be used between depth and main deck. In contrast to the hull volume below the waterline, the above-waterline areas are less efficient for technical installations, as they are interrupted by corridors and scientific facilities, and therefore cannot provide the same usable area, as the area below the waterline. Therefore a relocation factor $\eta_{relocation}$ is introduced here, which is set at 50 % and represents the efficiency with which volume can be shifted above the waterline. The updated below-waterline length demand is then expressed as

$$\Delta L'_u = \frac{\Delta V_{fuel}}{A_{M,\,t}} + \frac{\Delta V_c}{A_M} - \frac{V_{free}}{A_M} \cdot \eta_{relocation} \tag{5.31}$$

while the updated above-waterline length demand becomes:

$$\Delta L'_a = \frac{\Delta V_{PoB}}{(H_{BCV} - D_{BCV}) \cdot B_{BCV}} - \frac{V_{free}}{(H_{BCV} - D_{BCV}) \cdot B_{BCV} \cdot \eta_{relocation}} \tag{5.32}$$

This iterative relocation process is repeated until the difference between $\Delta L'_u$ and $\Delta L'_a$ falls below 0.5 m. Finally, the governing added length is taken as the maximum of both and rounded up to the next 0.5 m, corresponding to the typical frame spacing of research vessels. This ensures that the modelled length extensions remain consistent with realistic structural subdivisions and avoids unrealistic partial-frame additions.

5.7. Displacement

The increase in displacement must be evaluated as a consequence of design adaptations required to meet the energy demand of the selected propulsion configurations. This step integrates structural, outfitting and system-related weight contributions into the model to ensure technical feasibility under the given constraint. These values feed back into resistance and power demand calculations.

$$\Delta W = \Delta W_{St} + \Delta W_o + \Delta W_c + \Delta W_{fuel} + \Delta W_{WASP} \tag{5.33}$$

The steel weight added due to hull lengthening is estimated using an empirical formula by Chapman, as reported in Schneekluth, 1985. This formula links steel weight to the principal dimensions of the vessel. Since only the additional length contributes to additional steel weight, the calculation is simplified to:

$$\Delta W_{St} = 0.007 \cdot \Delta L^{1.759} \cdot B_{BCV}^{0.712} \cdot H_{BCV}^{0.374} \tag{5.34}$$

The coefficient 0.007 is an empirically derived constant for the density of conventional steel construction in ocean-going vessels.

The weight of outfitting, which includes systems such as piping, insulation, furniture, and electrical installations, is estimated using a simplified formula (Schneekluth, 1985) based on the added volume.

$$\Delta W_o = K \cdot \Delta L \cdot B_{BCV} \cdot H_{BCV} \tag{5.35}$$

with $K = 0.039\,t/m^3$. The coefficient K reflects an average outfitting weight density. Schneekluth, 1985, suggests a value between 0.036 and 0.039 t/m³. Based on the characteristics of modern research vessels, the installation density is assumed to lie at the upper end of the values reported for passenger ships of that time. Accordingly, the factor K is set at the upper bound.

The converter weight depends on the maximum power required during operation and the gravimetric power density of the converter φ_G:

$$\Delta W_c = \frac{max(P_i)}{\varphi_G} - W_{c,\,BCV} \tag{5.36}$$

Similarly, the fuel weight is computed using the missions total energy demand E, divided by the fuel gravimetric energy density φ_G, and compared to the baseline fuel weight:

$$\Delta W_{fuel} = \frac{E}{\rho_G} - W_{fuel,\,BCV} \tag{5.37}$$

Finally, the additional weight introduced by the WASP, if part of the configuration, is included as a constant:

$$\Delta W_{WASP} = 9.6\,t \tag{5.38}$$

The added weights from hull extension, energy systems, and fuel storage contribute to a change in vessel displacement. These changes are carried forward into the next iteration of the model, where their effects on draught, resistance, and propulsion power are evaluated.

5.8. Iteration Procedure

To ensure consistency between structural adaptions and vessel performance, the parametric model includes an iteration loop. The parametric model starts from the values of the basecase vessel *Sonne*. This provides the first set of values for transit power, energy demand, and added volumes. These results then enter the iterative loop, in which the ships length, displacement, resistance, and required power are successively updated. In this loop, the calculated increase in length and therefore displacement is used to update the ship's draught, wetted surface area, and propulsion power - all of which influence energy demand and space requirements.

First, the new draught D is estimated from the updated displacement and hull dimensions:

$$D = \frac{\Delta_{BCV} + \Delta W}{\rho \cdot (L_{BCV} + \Delta L) \cdot B_{BCV} \cdot c_{B,BCV}} \tag{5.39}$$

, where ρ donates the density of sea water of 1025 kg/m³. This ensures that the effect of added weight or length is directly reflected in the vessel's immersion. Based on this new draught, S is recalculated. The increase in surface comes from two extra areas: the additional length adds extra side and bottom panels, the greater (or smaller) depth increases the side area along the original hull length. This can be expressed as follows:

$$S' = S + \Delta L \cdot (2 \cdot D + B) + 2 \cdot (L_{pp} + B)\,(D - D_{BCV}) \tag{5.40}$$

Since S determines the frictional resistance, the updated value directly influences the propulsion power. A larger D and S therefore lead to higher power and energy demand, which in turn modify the required tank volume and converter size, and thereby the additional length and displacement of the vessel. The cycle is repeated with the updated parameters until convergence is achieved, which is defined here as a change in S of less than 1 m^2. Through this iterative process, the model ensures that structural adaptions remain consistent with vessel performance measures.

5.9. Definition of Feasibility

The iterative procedure described in the previous section provides the basis for assessing how consistently a configurations satisfies the defined technical constraints across a wide range of uncertainty scenarios. In this context, feasibility expresses the proportion of simulations in which a configuration remains technically valid and operationally functional. The feasibility fraction F_{conf} is calculated as

$$F_{conf} = \frac{n_{feasible,\, conf}}{n_{total,\, conf}} \tag{5.41}$$

, where $n_{feasible,\, conf}$ denotes the number of scenarios in which the configuration $conf$ fulfils the geometric constraint, and $n_{total,\, conf}$ is the total number of evaluated scenarios of the same configuration. In line with Lempert et al., 2003, robustness describes the extent to which a configuration maintains its feasibility when exposed to varying and uncertain future conditions. Configurations with a higher F_{conf} are thus more robust, as they remain technically feasible under a larger share of the explored uncertainty space.

5.10. Conclusion

Chapter 5 introduced the parametric model that links operational profiles and power and energy demands with the resulting volume, weight, and structural adaptions. By connecting these requirements to displacement, draught, and wetted surface, the model captures the key interdependencies between ship geometry, system installation, and performance. A central feature is the iterative procedure, which repeatedly updates geometric values and corresponding energy demand.

The model relies on simplifications to remain computationally efficient and transparent. Increase in wetted surface is approximated by flat panels, and power is scaled primarily with wetted surface and velocity, which avoids the need for full hydrodynamic calculations at every step. Furthermore, the energy demand of the research modes is held fixed. Within the geometric constraints considered here, these loads are expected to increase only marginally, whereas detailed recalculations, for example of DP systems, would not only require substantial computational effort but also detailed operational and technical information that is not available at this stage. These simplifications represent a balance between accuracy and practicality: while they reduce the level of detail in absolute predictions, they allow the model to remain consistent, transparent, and effective for comparative scenario analysis.

In the following chapter, the model is extended to include the performance measures.

This page is left blank intentionally.

6

Performance Measures

To evaluate the technical feasible decarbonisation strategies for research vessels within the MORDM framework, two central performance metrics are defined: GHG emissions and total expenses. These measures represent the “M” component of the XLRM matrix and form the basis for comparing vessel configurations across a wide range of uncertain futures.

6.1. Greenhouse Gas Emissions

To quantify the environmental impact of different vessel configurations over time, GHG emissions are calculated using a WtT and TtW approach. The total emissions over the vessel’s operational lifetime of 30 years are derived from summing the emissions of each epoch, as outlined in Equation 6.1:

$$GHG = \sum_{e=1}^{3} (GHG_{WtT,\,e} + GHG_{TtW,\,e}) \cdot \frac{10\ years}{T_e} \tag{6.1}$$

Where

- e denotes the epoch within a vessel’s operational era.
- $GHG_{WtT,\,e}$ and $GHG_{TtW,\,e}$ are the WtT and TtW GHG emission of one mission in each epoch e as in Equation 6.2 and Equation 6.3, respectively.
- 10 years is the duration of one epoch e.
- T is the duration of one mission in epoch e.
- f_j represents the factor of global warming potential compared to CO_2.
- j are the GHG CO_2, CH_4, or N_2O.

Table 6.1: Emission Factors from Climate Change Connection, 2020.

j	f_j
CO_2	1
CH_4	25
N_2O	298

The WtT emissions are determined by the total energy demand E per mission and the associated emission factor $CO_{2eq\,WtT}$ of the chosen fuel (Section 3.2):

$$GHG_{WtT} = CO_{2eq\,WtT} \cdot E \tag{6.2}$$

The TtW emissions account for direct emissions from fuel combustion and slip. These emissions are calculated as a function of the energy demand E, the fuel-specific gravimetric energy density ρ_G, the GHG-specific emission factors $C_{f,\,j}$ presented in Section 3.2, the global warming potential factors f_j, and the methane slip emissions C_{slip}.

$$GHG_{TtW} = \frac{E}{\rho_G} \cdot \sum (C_{f,\,j} \cdot f_j) + C_{Slip} \cdot C_{f\,CH_4} \cdot f_{CH_4} \tag{6.3}$$

6.2. Expenses

Economic performance is the second key measure in the XLRM matrix and represents the total cost of a propulsion strategy over the vessel's lifecycle. The cost assessment is divided into capital and operational expenses.

6.2.1. Capital Expenses (CapEx)

CapEx represent investment required to install and integrate a specific propulsion configuration onboard. In the context of this thesis, these expenses include the energy converter, the onboard storage system, any required structural hull adaptations, and optional auxiliary systems such as WASP and EHR. As shown by Gao et al., 2023, expenditures can be represented as the sum of individual cost components. Following this approach, Equation 6.4 gives the total capital expenditure, which expresses $CapEx$ as the sum of converter, tank, hull extension, and costs of EHR and WASP.

$$CapEx = CapEx_C + CapEx_t + CapEx_{Hull} + CapEx_{EHR} + CapEx_{WASP} \tag{6.4}$$

The investment cost for the energy converter is calculated as:

$$CapEx_C = C_C \cdot (max(P_{i,\,e}) + P_{Hotel}) \tag{6.5}$$

Here, $max(P_{i,\,e})$ is the highest mechanical power demand across all mission phases and epochs of the specific era, while P_{Hotel} refers to the average hotel load. The total installed power must cover both propulsion and non-propulsion loads to ensure reliable operation across all scenarios. The cost coefficient C_C reflects the specific price per installed kilowatt of the selected converter type.

If the required tank and machinery volume exceeds the available internal space of the reference vessel, a hull extension is triggered. To capture the associated cost increase, the steel cost model by Papanikolaou, 2014, shown in Equation 6.6, is applied only to the additional steel weight of each configuration resulting from propulsion-related changes. It should be noted that this thesis does not consider retrofits, but a design adaptation, with the resulting configurations considered as new builds. Consequently, costs for physically cutting and extending an existing vessel are not included.

$$CapEx_{Hull} = C_{ST1} \cdot W_{St} + C_{ST2} \cdot C_{FR} \cdot W_{St} \tag{6.6}$$

, where

- C_{ST1}: Cost of unprocessed steel per ton.
- C_{ST2}: Cost of man-hour.
- C_{FR}: Specific production time.

In 2023, cost of steel was around 1 000 $^{EUR}/_{t}$, however, prices were volatile (Jactio, 2023). Labour costs in the steel industry were reported at 30 $^{EUR}/_{h}$ in the European Union. Kerlen, 1985, provided a specific production time for a vessel of this size with approximately 32 $^{h}/_{t_{steel}}$. Although this values is dated, more recent shipbuilding productivity data could not be identified in the literature and even Papanikolaou, 2014, presents cost relations derived from the 1960s. The value is therefore used here as an indicative estimate, consistent with established practice, while recognising that modern production methods are likely more efficient. Given the structural complexity of research vessels, the number is treated as a conservative estimate, and potential deviations are addressed through the CapEx uncertainty factor.

Tank costs are only explicitly modelled for cryogenic fuels. These fuels require specialised tanks with insulation and pressure containment, resulting in higher cost compared to ambient-pressure fuels. For these fuels, costs are given on a $^{EUR}/_{kg_{fuel}}$ basis as described in Section 3.2, and are applied here in Equation 6.7. For non-cryogenic fuels, tank costs are assumed to be integrated into the hull steelwork and are therefore not considered separately. This simplification avoids the over-estimation of non-cryogenic fuel tank costs. Tank costs are modelled as:

$$CapEx_{Tank} = \begin{cases} C_{Tank} \cdot \frac{E}{\rho_G}, & \text{if fuel is cryogenic} \\ 0, & \text{otherwise} \end{cases} \tag{6.7}$$

, where C_{Tank} represents the cost of the tank per kg of fuel. CapEx for the storage system can be taken into account with 0.7 US-$/kg for ammonia storage, 5 US-$/kg for LNG storage, for hydrogen with 12.5 US-$/kg LNG equivalent (Ryste, 2019; Schreuder et al., 2025).

Where applicable, technologies such as WASP or EHR add extra investment costs. If not used, the corresponding terms are set to zero.

$$CapEx_{EHR} = \begin{cases} \frac{1}{1-\eta_{EHR}} \cdot (max(P_{i,\,e}) + P_{Hotel}) \cdot C_{EHR}, & \text{if EHR is installed} \\ 0, & \text{otherwise} \end{cases} \tag{6.8}$$

, where

- $max(P_{i,\,e}) + P_{Hotel}$: installed power.
- C_{EHR}: cost per kilowatt of EHR installation.

$$CapEx_{WASP} = \begin{cases} C_{WASP}, & \text{if WASP is installed} \\ 0, & \text{otherwise} \end{cases} \tag{6.9}$$

, where C_{WASP} denotes the costs per WASP installation. These costs for EHR and WASP are treated as a one-time investment. WASP expenses do not scale with vessel size or power.

6.2.2. Operational Expenses (OpEx)

Operating costs are the recurring costs incurred during the service life of a ship. Those costs play a critical role in the long-term economic feasibility of decarbonisation strategies. These costs are directly influenced by fuel consumption, converter type, maintenance requirements and potential policy mechanisms such as carbon pricing.

All costs are evaluated over the vessel's 30-year operational lifetime, split into three 10-year epochs, as defined in Section 4.4. The total operational costs for each configuration in each year are calculated as

$$OpEx_{year} = FuelEx_{year} + MaintEx_{year} + CarbonEx_{year} \tag{6.10}$$

distinguishing between fuel, maintenance, and carbon expenses. Each of these components is described in the following subsections.

Fuel costs are a major driver of operational expenditure and a key differentiator between propulsion system configurations. Their impact is determined by both the vessel's energy demand and the market price of the selected energy carrier.

$$FuelEx_{year} = \frac{E}{\rho_G} \cdot C_{fuel} \cdot \frac{365}{T} \tag{6.11}$$

, where

- C_{fuel}: price per kg of the fuel.
- $^{365}/_{T}$: number of missions per year.

This approach assumes that the vessel completes a certain number of missions per year. It enables the model to capture differences in operational patterns and to account for the fuel type.

Maintenance requirements vary depending on the propulsion system. FCs, in particular, have a limited service life and require periodic replacement of the stack. Based on Mylonopoulos et al., 2024, a FC lifetime of 25 000 hours is assumed.

$$\begin{aligned} &MainEx_{year} = \\ &\begin{cases} C_{FC} \cdot (max(P_{i,\,e} + P_{Hotel})), & \text{if FC is installed and replacement is needed} \\ 0, & \text{otherwise} \end{cases} \\ &+ \begin{cases} C_{main,\,WASP}, & \text{if WASP is installed} \\ 0, & \text{otherwise} \end{cases} \end{aligned} \tag{6.12}$$

Although FC replacement is a large investment, it is modelled as OpEx in this thesis, as it recurs at regular intervals and is linked to system usage rather than the initial acquisition.

In scenarios where an emission trading mechanism applies, emissions from onboard fuel consumption are monetised based on a CO_2 price. The cost is calculated from the WtW GHG emissions as

$$CarbonEx_{year} = GHG_{year} \cdot C_{Carbon,\,year} \tag{6.13}$$

, where C_{Carbon} represents the carbon price as in Section 4.4.1. Four scenarios of carbon pricing ranging from no carbon price to a strong pricing scheme are implemented in the model.

To reflect the decreasing economic weight of future expenditures, the model applies a present value (PV) approach to operational expenses. This reflects the principle of the time value of money, whereby financial costs incurred in the future are economically weights less than those occurring today. Discounting ensures that operational configurations with later cost peaks, such as FC stack replacements or rising carbon prices, are assessed consistently alongside alternatives with higher up-front expenditures.

$$PV_{OpEx} = \sum_{year=2025}^{2055} \frac{OpEx_{year}}{(1+r)^{year-2025}} \tag{6.14}$$

, where

- $OpEx_{year}$: total operational expenses in each year as in Equation 6.10.
- r: discount rate.

The discount rate r is set to 3.01 %, based on the average interest rate for 10-year government bonds in the euro zone, as published by European Central Bank, 2025b.

As this study focuses on research vessels, no direct revenue streams are included in the analysis. These vessels are often government-funded or institutionally operated (Chapter 2), so competitiveness in the commercial sense plays only a limited role. Nevertheless, the use of alternative fuels could strengthen their sustainability profile and thereby improve their chances in future funding decisions. However, unlike the technological and economic uncertainties and policy levers discussed earlier, this type of advantage is determined case by case at the level of individual research projects, rather than across a set of possible futures. As such it cannot be represented in the calculations of expenses and is therefore only acknowledged qualitatively. Accordingly, the net present value (NPV) is not used. Instead, the present value of total costs serves directly as the economic performance metric in the MORDM framework.

The resulting lifecycle expenses are defined as the sum of capital and discounted operational expenses.

$$Ex = CapEx + PV_{OpEx} \tag{6.15}$$

This value is used for multi-objective evaluation alongside GHG emissions to identify robust and economically viable decarbonisation strategies under deep uncertainty.

All input parameters used in this section are summarised in Table A.2. With the XLRM structure complete, the MATLAB model is run to evaluate the strategies, which corresponds to step 2 of the framework.

7

Verification and Validation

Chapter 7 aims to answer Sub-question 8.

> *How can the model and results be verified and validated to ensure their reliability for real-world application in research vessel decarbonisation?*

In line with Law, 2015, verification is the process of determining whether the assumptions and conceptual formulations of the model have been correctly translated into the simulation program. In contrast, validation concerns itself with whether the simulation model provides an accurate representation of the real-world system, relative to the specific goals of the study.

7.1. Verification

Verification is a critical step in the simulation modeling process, focused on confirming that the conceptual model has been correctly translated into a functioning computerized simulation. The goal of verification is to detect and eliminate programming errors, logical inconsistencies, and incorrect implementations.

Within this thesis, the conceptual model comprises the parametric relationships and system structure described in Chapter 5. The computer simulation implemented in MATLAB simulates a variety of research vessel configurations under future decarbonisation scenarios. Its core functions include calculating energy requirements, dimensioning tanks, scaling converters, changes to vessel geometry, life cycle emissions and operating costs.

Law, 2015, explained different techniques of verification of programs:

1. **Modular Implementation**
   Simulation programs should be written in modules and subprograms, allowing different parts of the model to be developed and debugged more easily. In this thesis, the MATLAB model was implemented step by step. Each logical component, including energy demand, tank sizing, hull geometry, emissions, and lifecycle costs, was developed in sequence. Although the subprograms were not tested fully independently, their incremental development allowed each step to be visually analysed, making it easier to isolate and correct errors early in the modelling process.
2. **Code Review**
   Having a second programmer review the model can help identify implementation errors and improve reliability. Since this thesis was developed independently, no external review of the code was performed.
3. **Input Variation**
   Running the simulation under a variety of input conditions is a key verification technique to identify implementation errors. In this thesis, both realistic and extreme values were tested to assess whether the outputs responded logically and consistently.

Similar to the approach taken by Suy, 2022, inputs were changed to challenge the model. The applied test cases are summarized in Table 7.1.

Table 7.1: Test Cases for Verification Purposes.

Parameter Modified	Value Used	Expected Behaviour	Result
$\rho_{V,\,Ammonia}$	1000 $^{kWh}/_{m^3}$	Very high values for ΔL, since low volumetric energy density requires large tank volume.	Passed
η_{FC}	100 %	Approximately half of ΔL, because perfect efficiency eliminates converter losses and reduces overall energy demand.	Passed
N_{PoB}	0	P_{Hotel} to 0 and ΔL smaller, as hotel load is eliminated leading to decreased energy demand.	Passed
η_{EHR}	100 %	E for scenarios with EHR and $x_{EHR} = 1$ to zero, since complete recovery of exhaust heat removes the need for additional fuel input.	Passed
η_{WASP}	100 %	$P_{Transit}$ to zero for scenarios with WASP and $x_{WASP} = 1$, because perfect wind assistance fully replaces propulsion power.	Passed
C_{FC}	0	$MainEx$ to 0 for configurations with FCs and without WASP, as instalment for FCs becomes cost-free.	Passed

4. **Trace**
   In a trace, variables are displayed after calculation and checked by hand calculations. In this thesis, tracing was applied by monitoring key variables, for example the evaluation of the basecase vessel. Values like block and midship coefficient, tank volume, and hotel load were compared against hand-written calculations. For example, the tank volume for the base case configuration using MDO was verified manually. With an energy demand of 4 874 219 kWh and an energy density of 39.6 $^{MJ}/_{l}$, the expected volume is:

$$V_{Tank} = \frac{4\,874\,219\,kWh}{39.6\,{}^{MJ}/_{l}} \cdot \frac{3.6\,MJ}{kWh} \cdot \frac{m^3}{1\,000} = 443.11\,m^3 \tag{7.1}$$

   This matches the model output (443 m^3) and confirms the correct implementation of Equation 5.8. Similar checks were carried out for other intermediate results during the model construction.

5. **Simplifying Assumptions**
   Simplifying assumptions can be useful both for testing specific parts of a model in isolation and for managing model complexity. Simplified conditions should be used to trace errors and verify that individual components function as expected. During verification, certain input conditions were deliberately simplified to isolate the effects of specific parameters. For example, $P_{transit}$ was calculated without increasing the resistance, to archive a more linear solution. In addition, parts of the model structure itself remain intentionally simplified. For instance, the power demand during normal and precise research phases is treated as a constant and does not vary with other factors. While this limits detailed realism, it ensures that the model structure remains transparent and verifiable.

6. **Animation**
   Animation can be used as a tool to verify dynamic behaviour in simulation models and detect unexpected changes over time. The model used in this thesis is structured around static yearly outputs, so an animation was not possible. However, Figure 7.1 shows the PV of the fuel expenses over

the years of a randomly selected propulsion configuration and uncertainty composition. It can be observed that within each decade, the fuel expenses decrease linearly due to the expected decrease of fuel prices and exponential due to the effect of the discount rate. After each decade, a visible jump in prices appears - this corresponds to changing mission requirements within different epochs.

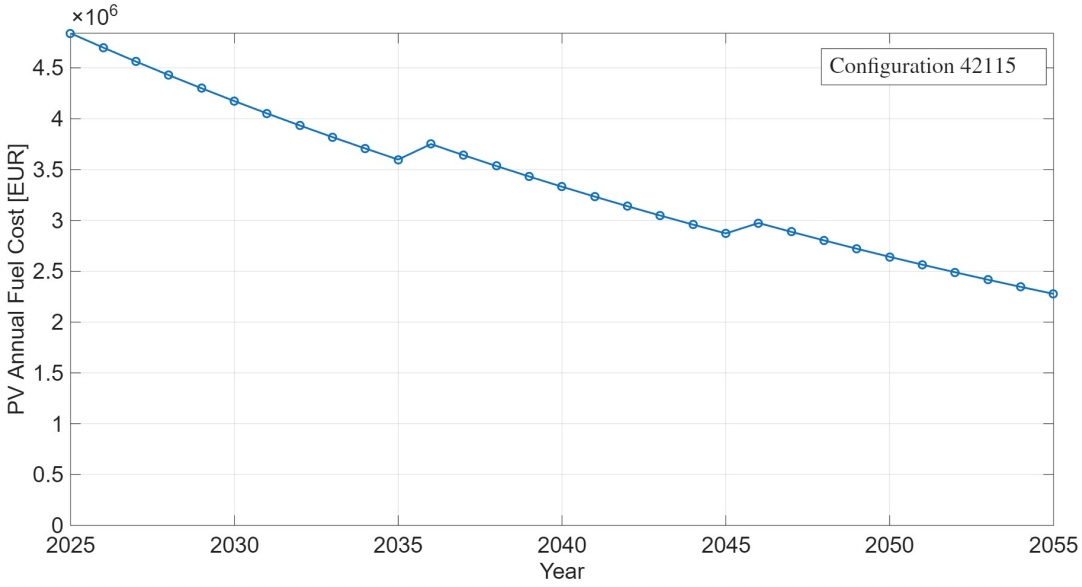

Figure 7.1: PV of Fuel Costs per Year Over the Years 2025 - 2055 for a Random Configuration.

These visual checks were used to check the model's internal consistency and the correct implementation of time-based economic effects and were repeated multiple times.

7. **Compute sample mean and variance**
   Simulation inputs generated from probability distributions should be checked whether they produce outputs with the expected statistical characteristics, such as mean and variance. While the model used in this thesis is deterministic for any given input combination, it is applied across a wide range of scenario inputs that reflect uncertainty in mission profiles, future pricing of carbon and fuel, and efficiencies of WASP, EHR, and FCs. The resulting output distributions, such as added hull length were analysed statistically using techniques like box plots and summary statistics. These distributions were visually evaluated to check for internal consistency.

8. **Usage of Commercial Simulation Package**
   Using dedicated commercial simulation software can reduce programming effort and decrease the likelihood of implementation errors. These platforms often include predefined logic blocks.

   In this thesis, the model was developed using MATLAB, a commercial but general-purpose numerical computing environment. MATLAB offers many built-in tools. For example, box plots and grouped scatter plots were used to examine output distributions across future scenarios, helping to detect trends, or - for verification - inconsistencies. The table-based structure allowed for easier organization and comparison of results.

In summary, the verification confirmed that the model was correctly implemented and logically consistent. While no external code review was possible, the combination of modular implementation, input variations, hand calculated checks, and visual inspection demonstrated that the computer model structure follows the mathematical model.

7.2. Validation

To assess the credibility and real-world applicability of the developed simulation model, several validation strategies were applied, as recommended by Law, 2015. These include comparisons with existing systems, expert opinion, and related modelling approaches.

1. **Comparison with an Existing System**
   The model should be compared to an existing system. If they are “similar”, the model can be seen as valid. In this case, no alternative-fuelled research vessel of comparable size could be identified in literature or operation. This absence of direct reference cases underlines the novelty and relevance of the research question.

   As a partial reference, the Maersk *Halifax* underwent a 15-metre hull extension during its methanol dual-fuel retrofit in 2024 (Maersk, 2024). While this vessel type differs significantly from research vessels and cannot be directly compared, the magnitude and purpose of the lengthening provide a useful reference point. It supports the conclusion that alternative fuels require more space.

   Partly, estimated values were compared to the original system. In Section 5.2, the endurance was calculated and found to align with the values provided by the operator of *RV Sonne*.

2. **Comparison with Expert Opinion**
   Furthermore, the model should be compared to expert opinions. In the case of this thesis, the output of the model was compared to existing literature.

   DNV GL, 2019, highlighted, that due to the low energy density of hydrogen, hydrogen may not be reasonably integrated into international shipping. This evaluation is consistent with the outcome of the model used, where hydrogen solutions were not technical possible for many configurations. In the same publication, it is stated, that methanol will be technical feasible for many applications, however, is more expensive than fossil fuels. The model similarly founds methanol configurations to be more expensive than MDO and LNG solutions.

   Also highlighted in DNV GL’s assessment, LNG, sustainable biofuels, and methanol, can be a viable option in deep-sea shipping. According DNV GL, LNG produces the least CO_2-emissions of all relevant fossil fuels, also the model developed shows this. Furthermore, it is stated, that LNG propulsed vessels can compete in terms of costs with MDO-fuelled vessels. However, the model developed in this thesis showed LNG expenses without carbon pricing higher than for MDO. Only, when carbon pricing is added, LNG is competitive to MDO. This divergence may be due to specific fuel cost pricing, or the particular adaption in research vessels, with higher energy consumption. Nonetheless, LNG was still found to be technically feasible and more robust than some alternative fuels like hydrogen.

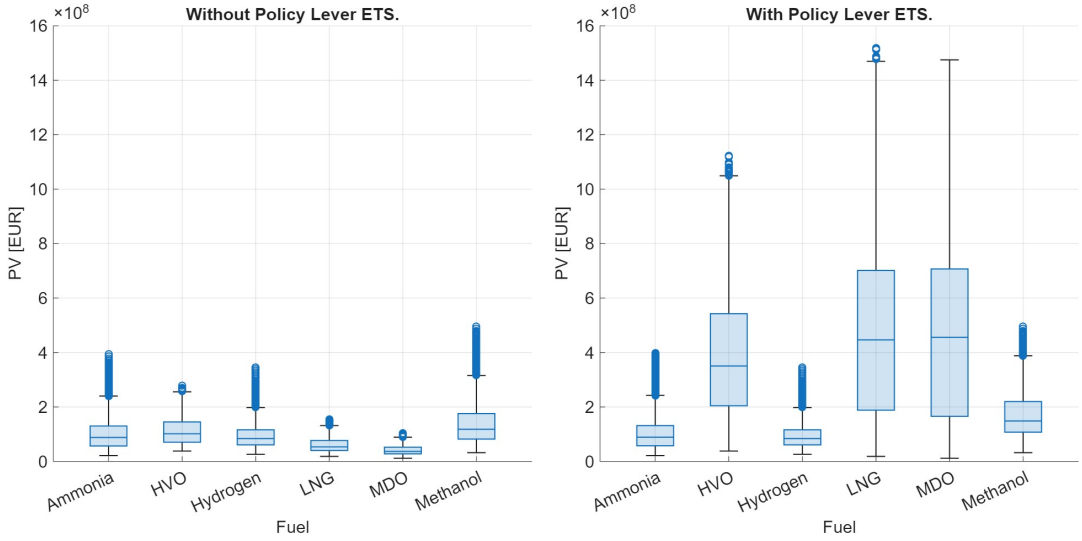

Figure 7.2: Present Value of Expenses With and Without Carbon Costs.

In DNV GL, 2019, ammonia was not further examined, instead it was stated, that the fuel will be discussed in follow-up literature. According to DNV, 2022a, ammonia will be introduced in larger quantities from 2030 ongoing. The model developed in this thesis, showed, that ammonia is technical feasible in many scenarios and competitive, underlining the opinion from DNV.

3. **Comparison with Another Model**
   Finally, Law, 2015, recommends comparing a simulation model with other independently developed models as a means of validation. However, in the context of this thesis, no publicly available model exists, that simulates decarbonisation strategies for research vessels under long-term uncertainty using multi-objective approaches. Nevertheless, MORDM has been applied in other maritime and energy-sector studies, e. g. Suy, 2022; Terün, 2020. Suy, 2022, came to the conclusion, that for zero-emission walk to work vessels, both ammonia and methanol are technically and economical feasible, which is somewhat consistent with the results of this model. Similarly, the poor performance of hydrogen aligns with findings from most decarbonisation studies focusing on deep-sea shipping.

Overall, the validation confirms that the simulation model behaves plausibly in line with existing technical systems, expert assessments, and comparable models. While direct validation through operational data or identical models was not possible, the strong consistency between model results and expert literature build confidence in its outcomes.

A notable deviation from expert trends was observed in the case of LNG, which DNV typically describes as cost-competitive. In the model developed, LNG configurations showed higher present-value expenses than MDO. This can be attributed to specific assumptions in the model. While this difference highlights the sensitivity of model outcomes to input assumptions, it does not diminish the model's validity. Instead, it underlines the value of the appliance of decarbonisation strategies for different kind of vessels.

7.3. Conclusion

The verification showed that the MATLAB implementation represents the conceptual model and is internally consistent. Through stepwise development, input variations, manual checks, and figure analysis of output trends and distributions, potential programming errors were minimized.

Validation further confirmed that the model outcomes are in line with available literature and expert assessments. The feasibility of methanol and ammonia and the limited applicability of hydrogen corresponds well with external evaluations. The observed deviation in LNG cost competitiveness illustrates the model's sensitivity to assumptions. After re-checking the underlying assumptions, it was decided to keep this deviation as it highlights the sensitivity of such results to technological progress and changing economic conditions, as the literature used is from DNV GL, 2019. At the same time, the limited availability of existing systems and similar models underscores the importance of this research.

Taken together, verification and validation provide confidence that the conceptual formulations of the model has been correctly translated into the simulation program and provides a sufficiently accurate representation of the real-world system for the purpose of this study.

This page is left blank intentionally.

8

Evaluation

Within the MORDM framework, steps 1 and 2 (decision framing and strategy evaluation) were carried out in Chapters 5 and 6. Chapter 8 continues with steps 3 to 5, assessing vulnerabilities, exploring trade-off's, and considering new futures and strategies under uncertainty. Building on the methodological foundation, the following chapter applies the model outputs to address Sub-questions 4 to 7.

- Section 8.1 assesses which configurations are technically viable and how robust they are under different assumptions. It directly addresses Sub-question 4 examining the role of operational profiles in the feasibility of alternative configurations, and Sub-question 5 assessing the efficiency of WASP and EHR and its contribution to decarbonisation potential.
- Section 8.2 analyses the economic impact of alternative fuels, WASP and EHR, thereby answering Item 6.
- Section 8.3 investigates the influence of decarbonisation strategies on emission reduction, answering Section 8.3.
- Section 8.4 combines the analysis of emission and costs and starts to answer the main research question.
- Two iterations are evaluated in Section 8.5. Iteration A introduces transitional blended fuels. In Iteration B, a fuller hull design is applied.

Together, these sections evaluate alternative propulsion strategies under uncertainty, beginning with feasibility and sensitivity, and progressing through economics, emissions, and combined trade-off analyses. This structure ensures that each sub-question is addressed systematically, while also building up toward the overall answer to the main research question.

8.1. Feasibility and Sensitivity

This section evaluates the technical feasibility of alternative fuel-converter configurations and tests how robust these results remain under different operational, technological, regulatory, and economic assumptions.

8.1.1. Feasibility

Feasibility is determined according to the geometric constraint introduced in Section 5.1, where a configuration is considered infeasible if the required hull extension leads to a length-to-beam ratio greater than 7. The overall feasibility of each configuration is quantified by the feasibility fraction F_i defined in Section 5.9. The assessment is conducted across all fuel-converter combinations, the three operational eras, and the optional technologies EHR and WASP. Figure 8.1 shows the distribution of the required added hull length ΔL across all fuel-converter combinations and eras. The dashed line indicates the threshold where L/B exceeds 7.

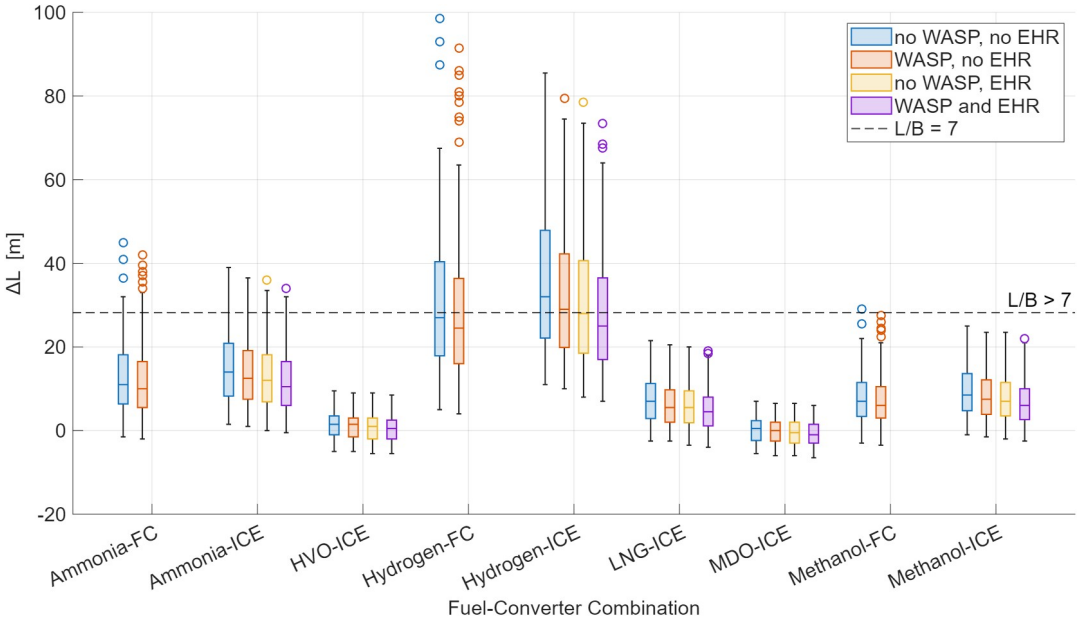

Figure 8.1: Technical Feasibility Visualised in Box Plot of ΔL by Configuration. The Area Above the Dashed Line has an L/B Ratio of More Than 7.

The results show three distinct groups of fuels:

- **Robust Fuels**
  HVO, LNG, MDO, and methanol in combination with an ICE are feasible in 100 % of the cases. Their high energy density and moderate converter space demand ensure compliance with the geometric constraint under all assumptions.
- **Borderline Fuels**
  Methanol FCs and ammonia systems are feasible in most, but not all cases. Methanol FC achieves feasibility fractions close to 100 %, while ammonia ICE and FC show lower feasibility, with fractions around 95 %.
- **Highly Infeasible Fuels**
  Hydrogen configurations reach feasibility in less than 60 % of the scenarios. These cases represent favourable assumptions, while in many scenarios hydrogen remains infeasible due to its very low volumetric energy density and the need for cryogenic tanks.

Table 8.1: Technical Feasibility by Fuel-Converter Combination.

Fuel	Converter	Feasibility
$conf$		F_{conf}
Ammonia	FC	94.8 %
Ammonia	ICE	94.7 %
HVO	ICE	100.0 %
Hydrogen	FC	58.3 %
Hydrogen	ICE	53.2 %
LNG	ICE	100.0 %
MDO	ICE	100.0 %
Methanol	FC	99.6 %
Methanol	ICE	100.0 %

To investigate whether borderline fuels and highly infeasible fuels can be made more robust, feasibility was further analysed across different WASP and EHR configurations. Percentages are presented in Table 8.2. Please note, that FCs don't produce heat, which is why EHR is not technically logical in those configurations.

For ammonia, feasibility improves with the integration of auxiliary systems from 95 % for both FC and ICE without EHR and WASP to 97 % for ICE configurations with both EHR and WASP. Robustness of configurations with methanol and FCs also benefits slightly, increasing feasibility from 99.6 % to 100 %, when WASP is installed. The results confirm that auxiliary systems, particularly EHR, can make borderline fuels more robust, and in the case of methanol-FCs fully feasible, by reducing energy demand and thereby mitigating tank volume constraints. Hydrogen, by contrast, reaches feasibility with auxiliary systems included in only about 60 % of the scenarios and therefore cannot be considered robust. It can

Table 8.2: Technical Feasibility by Fuel-Converter-Combination separated by WASP-EHR-Combination.

Fuel	Converter	no EHR, no WASP	no EHR, WASP	EHR, no WASP	EHR and WASP
Ammonia	FC	93.8 %	95.1 %	n/a	n/a
Ammonia	ICE	88.9 %	91.4 %	92.6 %	97.1 %
Hydrogen	FC	51.9 %	60.5 %	n/a	n/a
Hydrogen	ICE	44.4 %	48.1 %	51.9 %	56.4 %
Methanol	FC	98.8 %	100 %	n/a	n/a

be said, that WASP and EHR do not increase feasibility significantly. Although WASP increased feasibility to 100 % for methanol–FC configurations, this improvement originated from a baseline already close to full feasibility. In contrast, neither EHR nor WASP were able to raise the feasibility of ammonia- or hydrogen-based configurations to being fully feasible.

Technical feasibility is not only shaped by fuel and converter properties but also by the operational profile of the vessel. The role of missions in influencing robustness is therefore examined in Section 8.1.2, providing a direct follow-up to the baseline analysis presented here.

8.1.2. Role of Operational Profiles

Building on the baseline feasibility assessment in Section 8.1.1, this section examines how different operational profiles (eras) influence the feasibility and performance of propulsion strategies. The analysis directly addresses Sub-question 4:

How do operational profiles of research vessels impact the feasibility and performance of alternative fuels and WASP?

The operational profiles of global-class research vessels are represented by the three eras defined in Section 4.4.1. These eras, constructed of different epochs varying in combinations of mission range and share of precise research, represent distinct mission profiles: Era 1 represents shorter missions with lower research intensity, era 2 forms an intermediate case, and era 3 reflects long-range missions with higher fractions of precise research.

The added length of the configurations are shown in Figure 8.2, where the doted line marks the feasibility. Naturally, the additional hull length increases with higher operational requirements. In the lower-demand missions of era 1, the energy needed - and therefore the added length - remains modest, while both rises with higher requirements. This accounts for all fuels and converters. The box plot shows that - at least for non-carbon fuels with lower energy density - the interquartile range of era 1 ends approximately where the one of era 2 begins. In turn, era 2 ends, where era 3 begins. A distinct shift is visible towards larger ΔL with each era, underlining the strong influence of the operational profile on feasibility and robustness.

For some fuels, this influence insures complete robustness under less demanding conditions. Methanol-FC and ammonia configurations remain fully feasible in eras 1 and 2. This is not the case for hydrogen. In era 1, the feasibility fraction rises, suggesting that hydrogen can perform under favourable conditions for low-demanding vessel designs. However, even in this case feasibility does not reach 100 %, meaning that the design cannot be relied upon under the uncertainty presented. Overall, hydrogen remains infeasible as it fails to demonstrate robustness for lower-demanding eras. Given the high uncertainty in these profiles, hydrogen is excluded from further consideration.

Operational profiles also affect the lifecycle GHG emissions and costs of the vessel. Figure 8.3 shows the distribution of lifecycle GHG emissions for fossil fuels and HVO across the three eras.

A trend is visible: Era-1-vessels generally produce lower emissions, while era-3-vessels yield the highest values due to longer range and higher research intensity. However, the influence of the operational

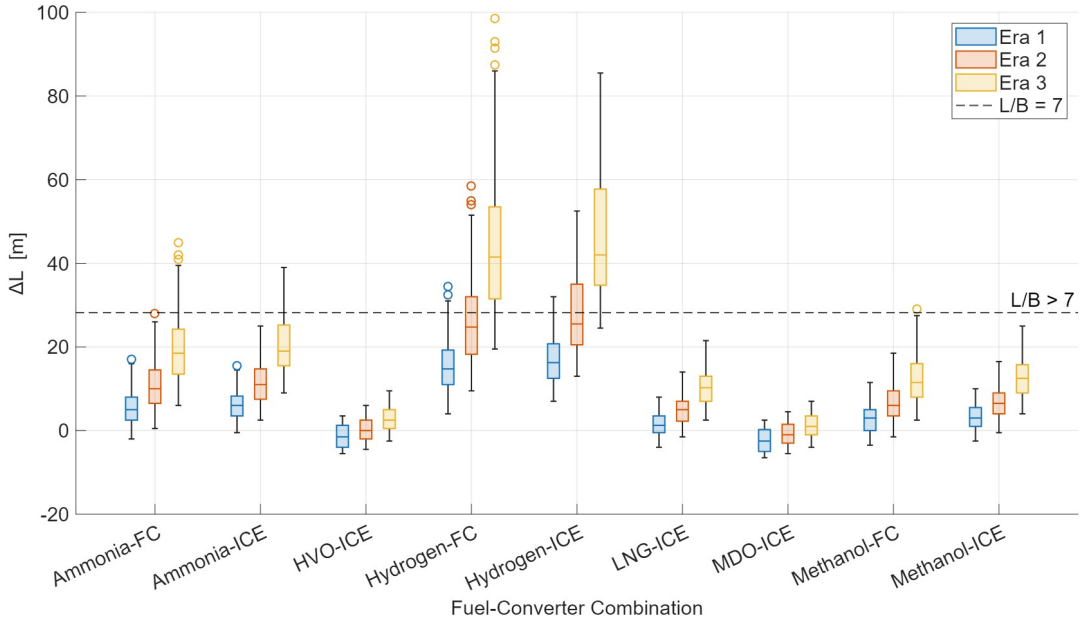

Figure 8.2: Technical Feasibility Visualised in Box Plot of ΔL by Fuel-Converter Combinations and Era. Area Above Dashed Line has a L/B-Ratio Higher Than 7.

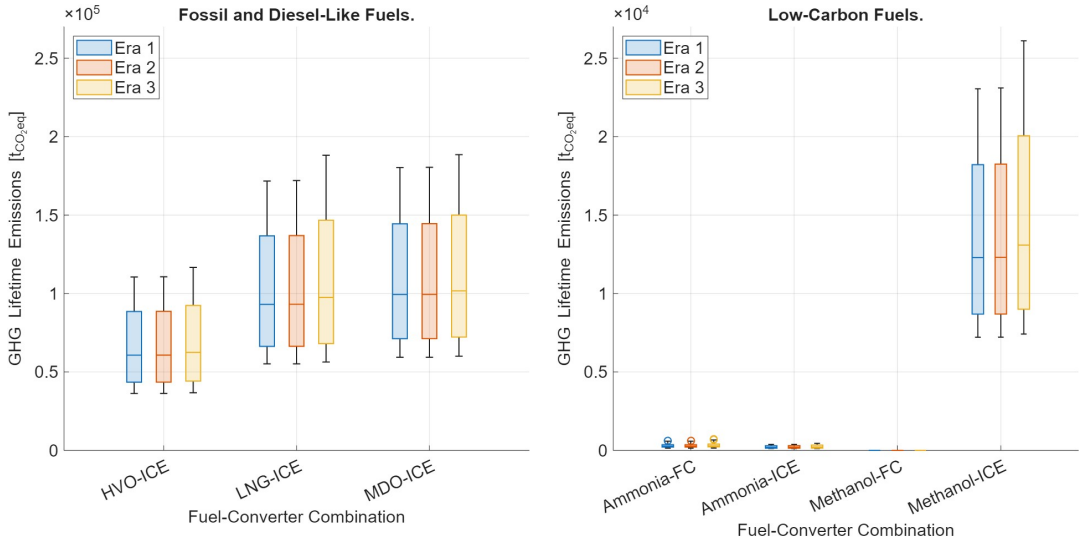

Figure 8.3: Lifecycle GHG Emissions, Visualised with Box Plot by Fuel-Converter Combinations and Eras (Colour-Coded). Left: Fossil/Diesel-Like Fuels, Right: Low-Carbon Fuels.

profile remains relatively small. Especially for era 1 and 2, the emissions are similar. In era 3, more emissions are produced, but the difference is of smaller magnitude than the difference between for example HVO and MDO. The increasing spread of emissions in era 3 is more pronounced. Both the interquartile range and the whiskers are larger than in era 1 and 2, indicating that the individual scenarios vary more widely. This can be explained by the overall higher energy demand in era 3: Minor differences in assumptions, such as auxiliary systems savings or efficiency of converters, lead to much larger absolute changes in total emissions, when the mission is long and energy-intensive. In contrast, era 1 and 2 show narrower distributions, as the lower baseline energy demand limits the impact of such uncertainties.

The same trends can be seen in ammonia and methanol configurations, with the exception of non-polluting methanol FCs. These low-carbon fuels have significantly lower emissions, yet they follow the same stepwise increase from era 1 to era 3 and display a wider spread under higher demands.

Inside the group of low-carbon fuels, methanol FCs, which were assumed to be carbon neutral archive the lowest, namely zero, lifecycle emissions. Ammonia configurations emit less than methanol-ICE configurations. Across all profiles, the ranking of fuels remain stable. For fossil and diesel-like fuels, HVO achieves the lowest emissions in every era, while MDO consistently shows the highest value and LNG falls in between. This underlines that although operational profiles affect the absolute level of emissions, they do not alter the relative positions of fuels.

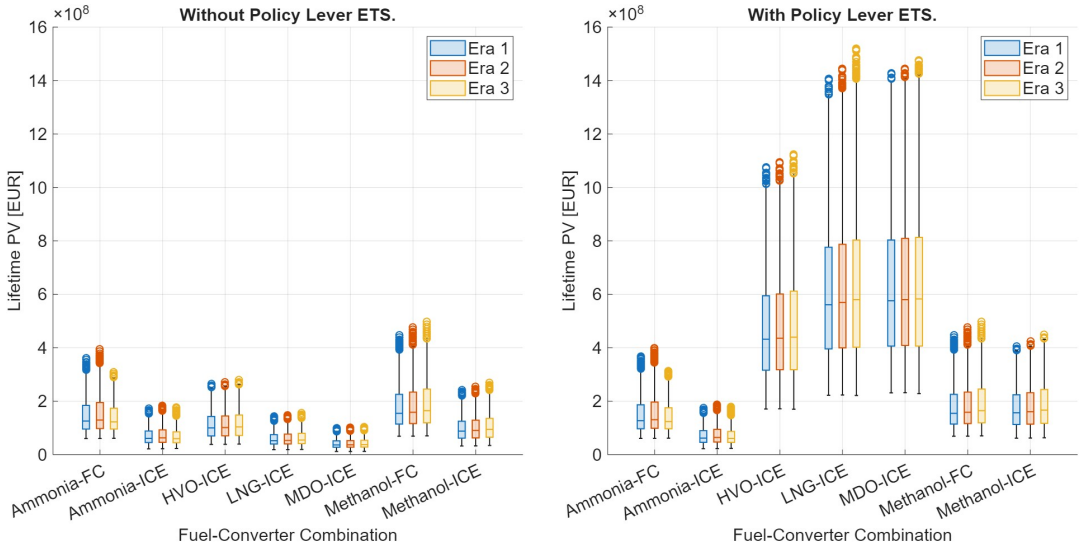

Figure 8.4: Lifecycle PV, Visualised with Box Plot by Fuel-Converter Combinations and Era (Colour-Coded). Left: Pure Market Prices, Right: Politically Influenced Prices.

The influence of operational profiles on lifecycle costs is illustrated in Figure 8.4. To allow for easier interpretation across different policy scenarios, the figure compares the results with and without an ETS. At this point, the ETS is used only as a scenario splitter to show how operating profiles behave under both conditions. The influence in terms of costs are presented and analysed in Section 8.1.4.

In case the ETS is not introduced, the costs of all three eras overlap strongly within the configurations, indicating that the mission profile itself has only a small effect compared to the fuel-converter choice. With carbon pricing included, the absolute cost level rises significantly for fossil fuels, while low- and zero-carbon options such as ammonia and methanol improve their relative competitiveness. Nevertheless, the variation between eras remains limited, confirming that the fuel choice is a more dominant driver of lifetime expenses, not the operational profile.

8.1.3. Efficiency of WASP and EHR

The influence of auxiliary technologies is further explored by varying their efficiency levels. This directly addresses Sub-question 5:

How does the efficiency of WASP and exhaust heat recovery systems influence the overall decarbonisation potential of research vessels?

In the model, both energy reducing technologies were parametrised as efficiency gains corresponding to a 5 %, 10 %, or 15 % reduction in propulsion or total energy demand. The efficiency of EHR constitutes primarily a technological uncertainty, as it reflect the design of the recovery system. In contrast, the efficiency of WASP combines technological and operational aspects. Next to technological uncertainties, the realised savings depend strongly on route-specific wind conditions.

Figures 8.5 and 8.6 show the effect of varying efficiencies of WASP and EHR, respectively, across all fuel-converter combinations. In all cases, higher efficiencies lead to a stepwise reduction in lifecycle GHG emissions. A stepwise downward trend is visible and was expected. Higher assumed efficiencies consistently lead to lower emissions, while the added weight was not sufficient to increase energy demands highly. This pattern holds for both WASP and EHR.

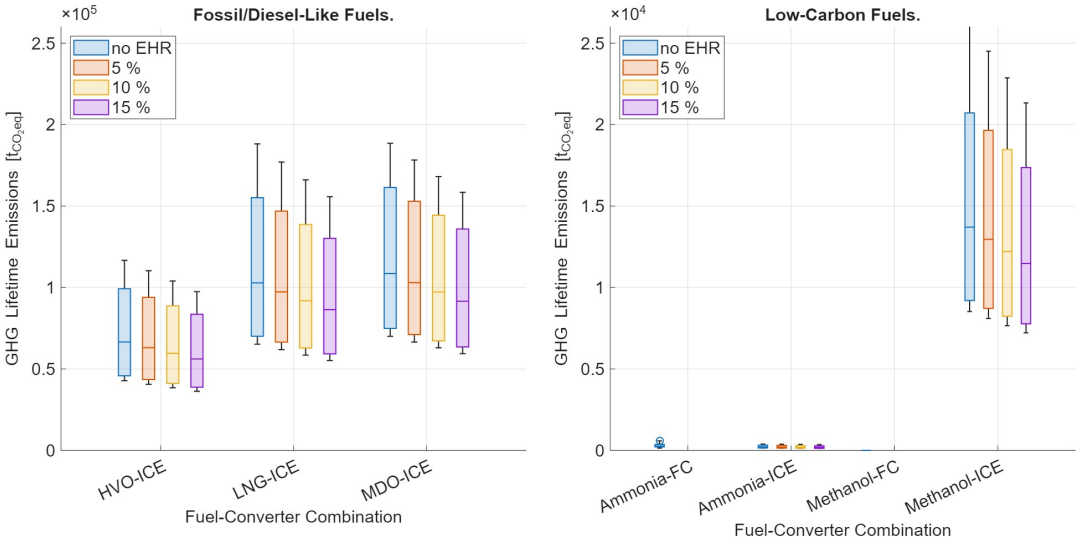

Figure 8.5: GHG Emissions, Visualised with Box Plot by Fuel-Converter Combinations and Efficiencies of EHR (Colour-Coded). Left: Fossil/Diesel-Like Fuels, Right: Low-Carbon Fuels.

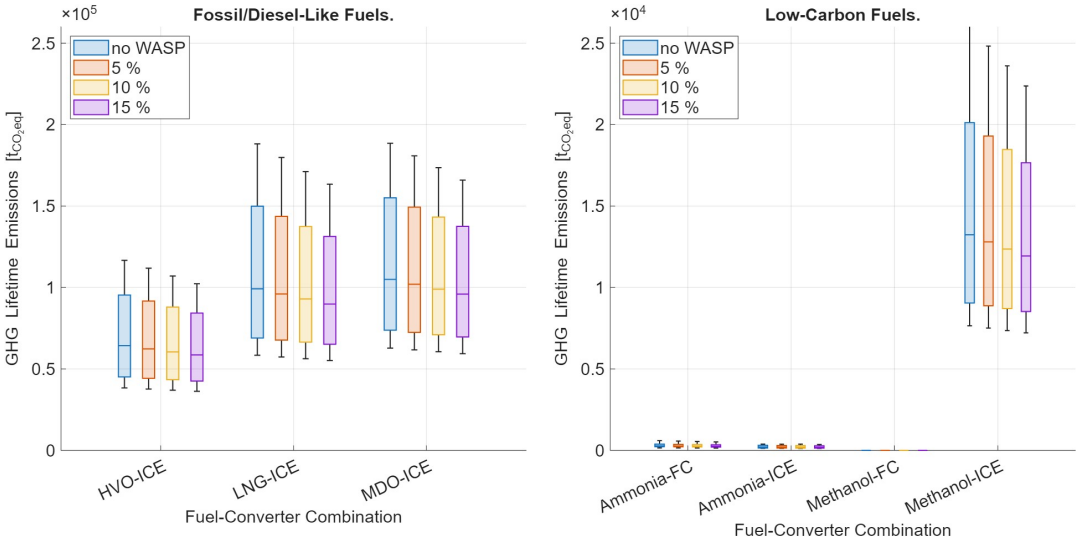

Figure 8.6: GHG Emissions, Visualised with Box Plot by Fuel-Converter Combinations and Efficiencies of WASP (Colour-Coded). Left: Fossil/Diesel-Like Fuels, Right: Low-Carbon Fuels.

The influence of WASP and EHR is clearly visible for fossil fuels, where higher efficiency levels reduce lifetime emissions. HVO also responds, though the absolute reductions are smaller due to its lower baseline intensity. For ammonia, the effect of WASP and EHR on GHG emissions is small in absolute terms due to the already low baseline, similarly the effect on methanol-FCs is zero as no emissions are produced. For methanol-ICEs, WASP and EHR also reduce lifecycle emissions by a similar relative share as for the other fuels.

As in Section 8.1.2, where the influence of operational profiles (eras) was found to be smaller than the differences between fuels, the same general trend holds true for auxiliary efficiencies. WASP and EHR reduce the absolute level of emissions, but the underlying fuel choice continues to dominate overall performance. Nevertheless, auxiliaries can influence the relative position of fuels with comparable baseline intensities as illustrated in Figure 8.5. For example, configurations with MDO and a highly efficient EHR may emit less over their lifetime than LNG without auxiliaries. Similarly, at an EHR efficiency of 15 %, the median and interquartile values for ammonia of ICE configurations equipped with EHR fall below those of FCs, where EHR do not work. The lower whiskers of the FC cases, however, remain below the ICE values, showing, that energy reduction measures can shift the “typical” perfor-

mance but do not eliminate the best-case advantage of FCs. These cases demonstrate that while those technologies do not close the gap to inherently low-emission fuels such as methanol or ammonia, they can significantly affect comparisons within the fossil fuel group and even blur the distinction between converters at certain efficiency levels.

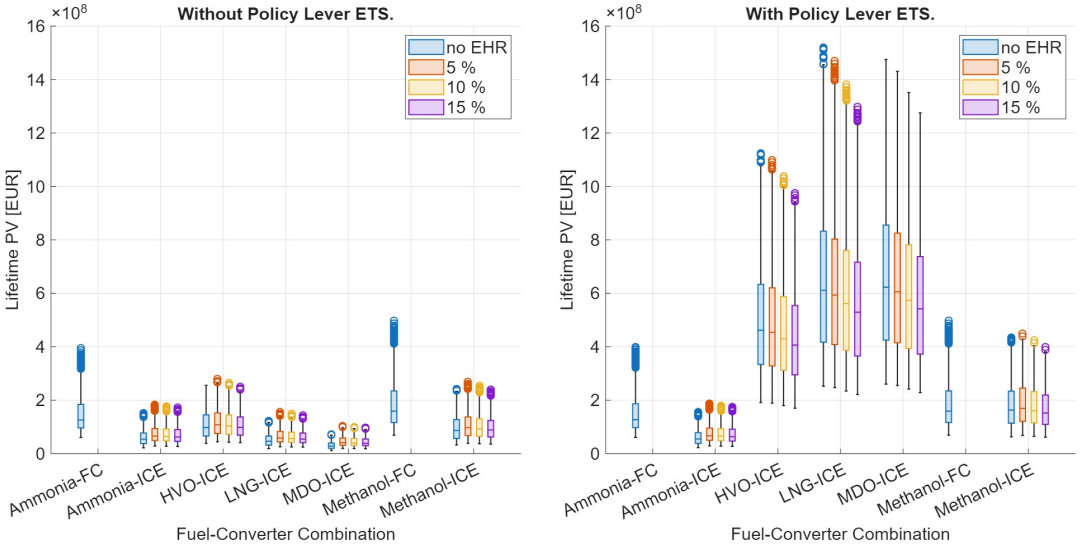

Figure 8.7: PV by Fuel-Converter Combination and Efficiencies of EHR (Colour-Coded). Left: Pure Market Prices, Right: Politically Influenced Prices.

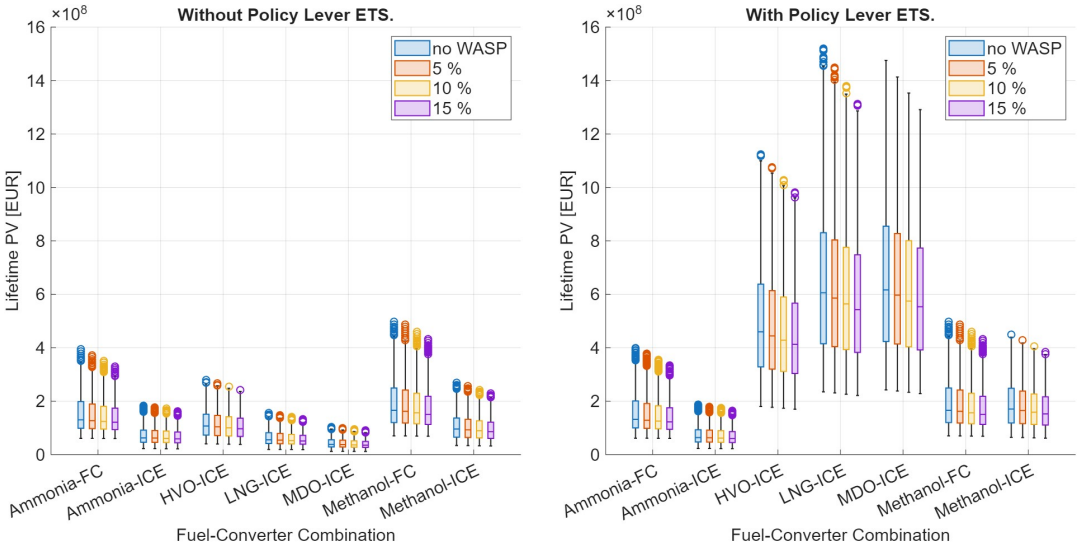

Figure 8.8: PV by Fuel-Converter Combination and Efficiencies of WASP (Colour-Coded). Left: Pure Market Prices, Right: Politically Influenced Prices.

Figures 8.7 and 8.8 show the influence of WASP and EHR efficiencies on lifecycle present value, both without (left column) and with (right column) the ETS. Without ETS, cost are only slightly affected by auxiliary efficiencies. For most fuels, the variation in costs between efficiencies of 5 %, 10 %, and 15 % are small relative to the overall spread of the results. The interquartile ranges of the different efficiency levels overlap strongly, showing that auxiliary efficiency assumptions have only a limited influence on lifecycle costs in the absence of carbon pricing. In some cases, notably for EHR, costs without auxiliaries appear slightly lower, since the additional capital investment is apparently not offset by fuel savings in the absence of carbon pricing.

With ETS, the picture changes for high-emission fuels as HVO, LNG, and MDO. Here, energy reducing technologies reduce both emissions and carbon costs, so higher efficiencies lead to systematically

lower lifetime PV. For the low-emission fuel ammonia, the influence of efficiencies on WASP and EHR remains small. FCs do not provide exhaust heat, so these cases were not analysed as stated in Section 4.4. For ammonia in particular, EHR does not deliver a positive economic case: the additional capital investment outweighs the marginal savings on fuel and carbon expenses, even at higher efficiencies. ICEs remain generally cheaper than FCs across ammonia and methanol, both with and without ETS.

8.1.4. Sensitivity of Economics

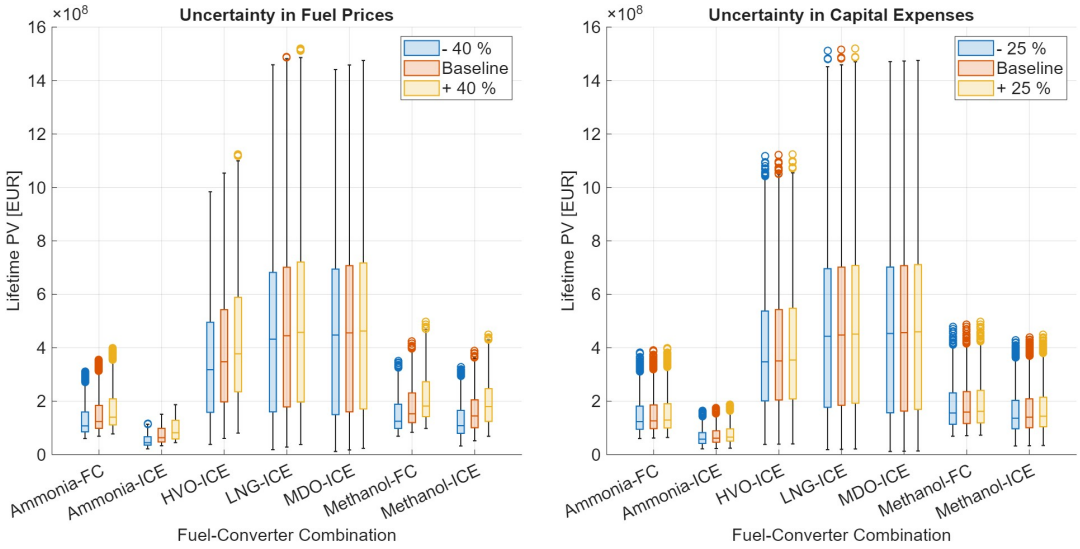

Figure 8.9: Present Value illustrated in Box Plots by Fuel-Converter Combination and Uncertainties of Expenses.

In order to assess the economic impact, it is necessary to understand the economic roles of uncertainties and policy levers. Figure 8.9 illustrates the influence of uncertainties in fuel prices (left) modelled as a $\pm$ 40 % variation and CapEx (right) modelled as a $\pm$ 25 % variation. Fuel price differences lead to visible shifts in lifetime costs, while the overall ranking of fuels remains unchanged. For CapEx variation the distributions almost overlap. First of all, this is because the deviation is smaller than the one of fuel prices. However, it also indicates that the level of CapEx is important for the structural differences between ICEs and FCs, but the uncertainty in CapEx itself is small compared to the influence of fuel prices. The influence of efficiencies of energy reduction technologies, discussed in Section 8.1.3, is also relatively minor.

In contrast to that, the introduction of a ETS exerts by far the strongest influence on economic outcomes. Figure 8.10 shows this impact. Unlike uncertainties, which mainly affect the spread of outcomes, ETS reshapes the economic order. Carbon-intensive fuels such as MDO, LNG, and HVO shift from being the cheapest solutions to the most expensive once emissions are priced. Conversely, ammonia and methanol ICEs improve their competitiveness and move into the lower cost range. FCs remain more expensive than ICEs, but the difference narrows when carbon costs are included.

8.2. Economic Impact

The sixth sub-question asks:

What is the economic impact of the introduction of alternative fuels and WASP for research vessels, taking into account investment costs, operating costs and market uncertainties?

With this section, the analysis enters step 3 of the framework, namely MORDM. In this and the following section, the two key performance measures - economic impact and emission reduction - are first examined individually before being combined into a full trade-off evaluation in later sections.

Figure 8.11 illustrates the effect of all possible propulsion configurations. Fuel-converter combinations are shown on the x-axes of both panels, while energy reduction technologies are colour-coded. The

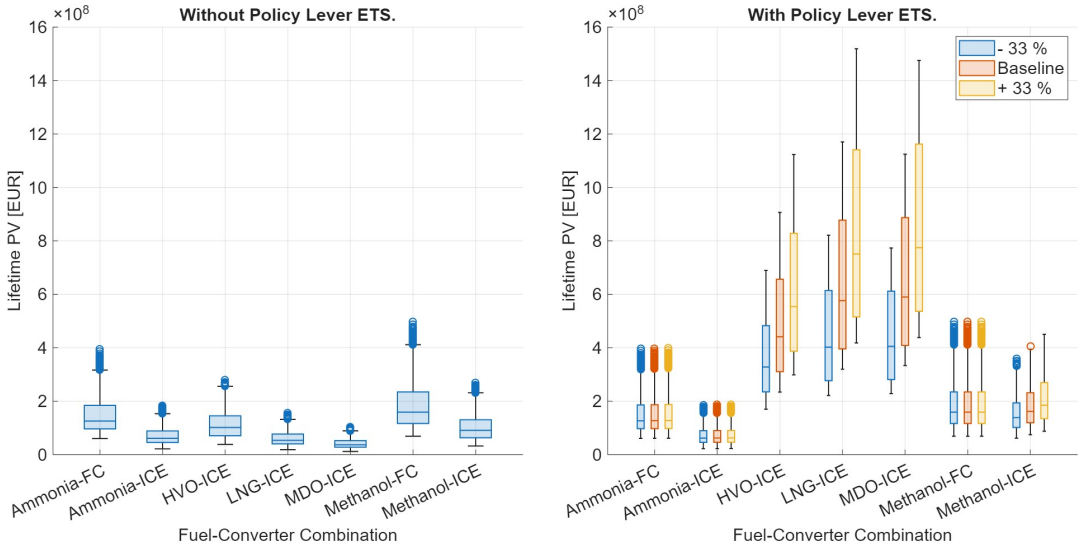

Figure 8.10: Lifecycle Present Value, Visualised with Box Plot by Fuel-Converter Combinations and Uncertainty of Policy Lever ETS (Colour-Coded). Left: Pure Market Prices, Right: Politically Influenced Prices.

panels distinguish between the introduction of an ETS, which is the most influential uncertainty parameter. Without ETS (left panel), the fundamental cost hierarchy is clear: fossil and diesel-like fuels remain in the lowest cost range, while ammonia and methanol occupy systematically higher cost levels. Within each fuel the spread between configurations with and without WASP or EHR is narrow, and in several cases EHR slightly increases costs, as savings do not fully offset the additional investment, as also shown in the previous section. With ETS (right panel), the ordering is reshaped: fossil and diesel-like fuels shift upwards on the cost axis, while ammonia and methanol become absolutely cost-competitive. Under this circumstances, energy reducing technologies gain economic importance for fossil and diesel-like fuels. WASP and EHR systematically lower PV for this group by reducing fuel consumption and therefore the carbon-cost component. For ammonia, EHR still lacks a positive business case.

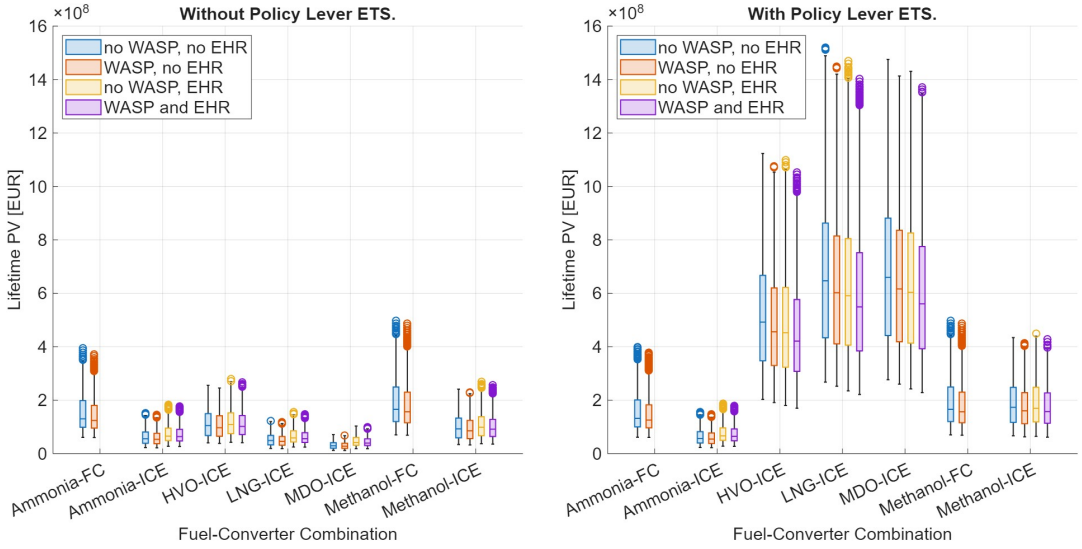

Figure 8.11: Lifecycle PV, Visualised with Box Plot by Fuel-Converter Combinations and Energy Reducing Technologies (Colour-Coded). Left: Pure Market Prices, Right: Politically Influenced Prices.

In summary, the results and figures allow a direct answer to Sub-question 6: Without an ETS, the baseline fuel MDO is the cheapest option, followed by LNG and then HVO. Ammonia and methanol appear more expensive. ICE configurations are consistently less costly than their FC counterparts.

When ETS is introduced, however, the order changes fundamentally: carbon-intensive fuels (MDO, LNG, and HVO) become the most expensive options, while ammonia and methanol ICEs shift into the competitive range and achieve the lowest cost levels. The figure also shows that the spread in the left panel (without ETS) is much more narrow for fossil- and diesel-like fuels, meaning they are not only cheaper but also less sensitive to uncertainties. Once ETS is introduced, their distributions shift upwards and become wider, which indicates that these fuels are not only more expensive but also riskier in economic terms. This effect is mainly driven by the highly uncertain future carbon price. FCs remain more costly than ICEs for ammonia. For methanol emitting more CO_2-equivalents, FCs can be the cheaper option for certain futures. For ammonia, the figure also illustrates again, that EHR does not provide a positive business case, as the additional investment offsets the expected savings. The overall economic impact is therefore strongly shaped by policy conditions, with carbon pricing able to reverse the hierarchy between fossil and diesel-like renewables on one side and alternative low-carbon fuels on the other side.

8.3. Emission Reduction Potential

After considering the economic outcomes in Section 8.2, the focus now shifts to the environmental perspective. This is expressed in the seventh sub-question:

What are the emission reduction potentials of combined decarbonisation strategies?

To address this, the following section evaluates the lifecycle GHG emissions of different fuel-converter combinations and energy reducing systems. Figure 8.12 presents the distribution of lifecycle emissions

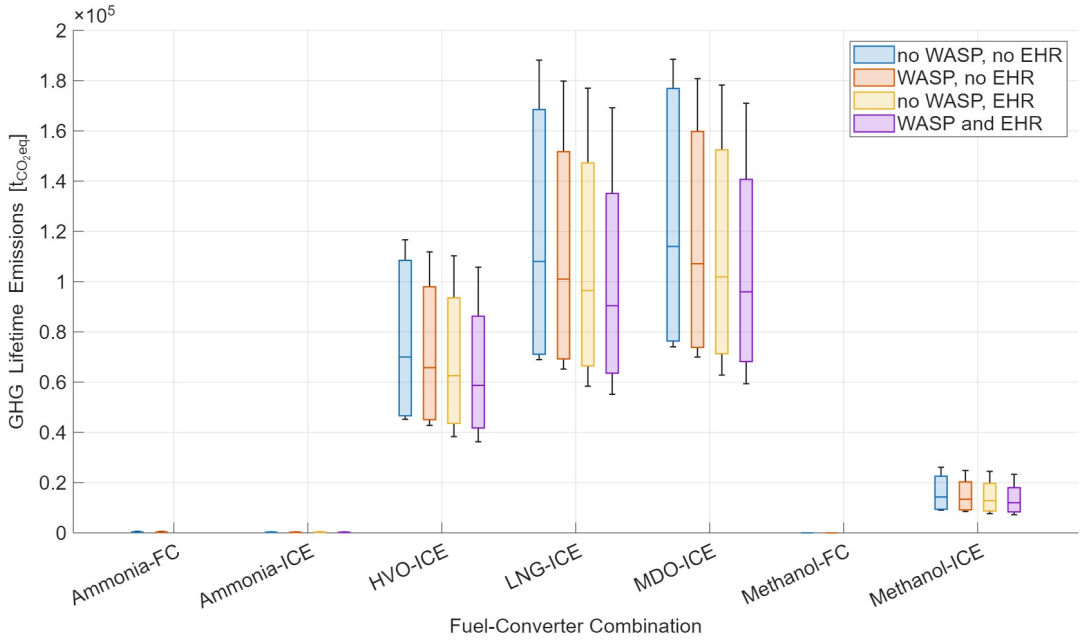

Figure 8.12: GHG Lifecycle Emissions, Visualised with Box Plot by Fuel-Converter Combinations and Energy Reducing Technologies (Colour-Coded).

across all scenarios. The baseline fuel MDO shows the highest emissions, reaching values in the order of 10^5 tonnes of $CO_{2\,eq}$ over the vessels lifetime. Compared to that, the interquartile ranges and medians of LNG and HVO are shifted downwards, indicating systematically lower emissions in typical scenarios. Within this group, HVO achieves the largest reduction relative to MDO. Nevertheless, these relative differences remain modest compared to the difference that results from switching to low-carbon fuels. Relative to the fossil/diesel-like group, ammonia and methanol exhibit substantially lower WtW emissions. Ammonia shows the lowest distribution, laying two orders of magnitude below the fossil/diesel-like fuels. Methanol obtains lifecycle emissions about one order of magnitude below the fossil/diesel-like cases.

The comparison between ICE and FC configurations shows that FCs tend to achieve lower median emissions. However, the interquartile ranges and whiskers overlap strongly, indicating that under favourable assumptions some ICE cases can perform similarly to FCs. This pattern suggests that while FCs provide a systematic advantage in typical scenarios, the overall range of outcomes is dominated by technological uncertainties.

The effect of auxiliary systems is illustrated by the colour-coded distributions in the same Figure 8.12. For fossil and diesel-like fuels, both WASP and EHR reduce lifetime emissions, naturally with the strongest effect visible when both are applied together. While the relative reduction is modest compared to the effect of a fuel change, the shift is still noticeable. Interquartiles move downward by tens of thousand of tonnes $CO_{2\,eq}$, particularly for MDO and LNG. For ammonia and methanol, those technologies also lower emissions, though the effect is less pronounced given the already low baseline.

In summary, sub-question 7 can clearly be answered. Compared to the baseline fuel MDO, all other fuels achieve lower lifecycle GHG emissions in typical scenarios. Within the fossil and diesel-like group, HVO shows the strongest relative reduction, followed by LNG. A decisive improvement, however, requires a switch to alternative fuels: ammonia reduces emissions by more than 99 % relative to MDO, while green methanol in combination with FCs effectively eliminates lifecycle emissions altogether. FCs tend to improve typical performance further, but ICEs remain close in best-case cases.

8.4. Multi Objective Trade-off Analysis

With the previous sections addressing economic impact (Section 8.2) and emission reduction potential (Section 8.3) individually, the analysis brings both perspectives together now. As part of step 4 of the framework (Marchau et al., 2019), this section further contributes to answering the main research question by identifying configurations that perform robustly across multiple objectives and by clarifying where synergies exists and where trade-off's must be accepted.

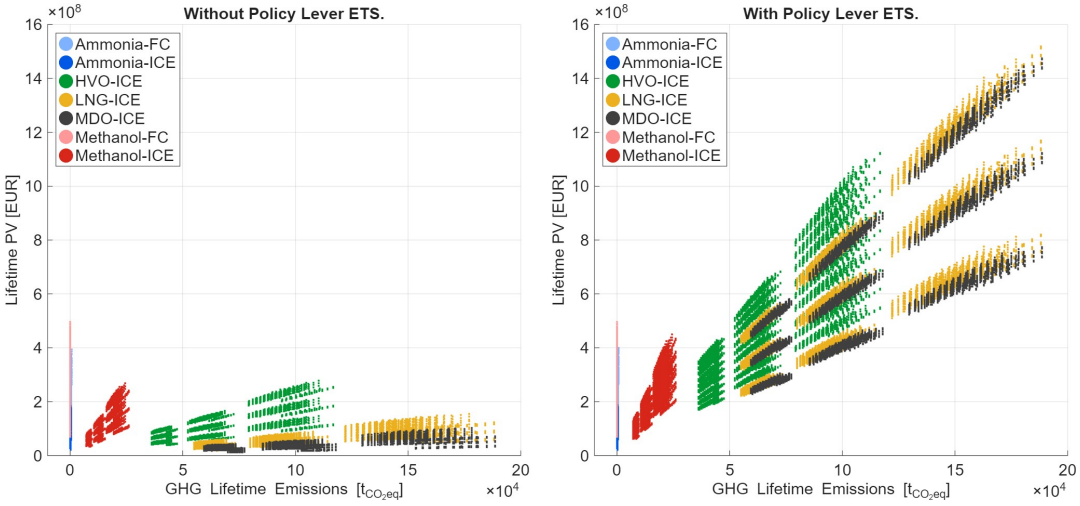

Figure 8.13: Lifecycle PV against GHG emissions, Visualised with Scatter Plot by Fuel-Converter Combinations (Colour-Coded). Left: Pure Market Prices, Right: Politically Influenced Prices.

Figure 8.13 presents the trade-off between lifetime PV of the expenses related to the propulsion system and lifecycle GHG emissions across all fuel-converter configurations, separated into scenarios without (left) and with (right) ETS. Each point represents one scenario outcome. Since Section 8.2 demonstrated that the ETS is by far the most influential uncertainty for economic outcomes, the trade-off analysis is shown in two separate panels. The left panel reflects purely market driven scenarios, while the right one shows the reshaping under policy levers.

Without ETS, the trade-off space is characterised by a opposition between economic and environmental performance. Fossil fuels in combination with ICEs dominate the low cost, high emission corner, with LNG emitting less than MDO but both setting the cost frontier in the absence of carbon pricing. HVO attains the lowest emission within the fossil/diesel-like set, yet is systematically more expensive than

MDO and LNG. The group shows noticeable variation in both dimensions due to differences in technical properties, market assumptions, and operational requirements, but compared to ammonia and methanol they remain consistently emission-intensive. Low-carbon fuels cluster in the low-emission region at higher present values. Ammonia attains the lowest GHG levels, and is not excessively expensive. However, as shown in Section 8.1.2 its technical feasibility is not fully robust, especially for higher operational requirements. Methanol-ICE combinations exhibit lower, but non-zero emissions than MDO, LNG, and HVO. Both ammonia and methanol FCs show very low emissions, but at systematically higher costs than ICE combinations.

With ETS, the order on the cost axis is restructured. Fossil (LNG and MDO) and diesel-like (HVO) fuels shift sharply upward in PV of their costs. Methanol with FC combinations become cost-competitive to the ICE configuration, however, both methanol and ammonia move into the cost competitive range compared to fossil and diesel-like fuels. Overall, ETS reduces the tension between economic and environmental objectives by eliminating the fossil/diesel-like cost advantage and pushing low-carbon fuels to the low-cost, low-emission domain. Ammonia enters a competitive region, offering both low emissions and costs that are not higher than fossil and diesel-like fuels penalised by carbon pricing. Methanol remains systematically more expensive than ammonia, but is close to being fully technical robust. Thus, ETS reduces the conflict between economic and environmental objectives.

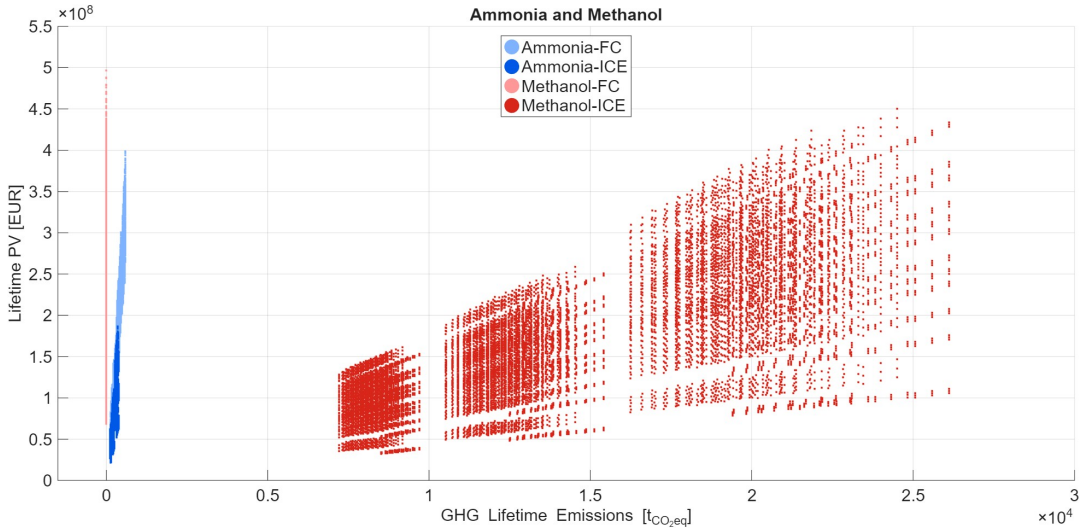

Figure 8.14: Lifecycle PV against GHG emissions for Low-Carbon Configurations, Visualised with Scatter Plot by Fuel-Converter Combinations (Colour-Coded).

A closer look at the role of converter choice shows that, for ammonia, ICE and FC configurations overlap strongly in both cost and emissions. As illustrated in Figure 8.14, FCs achieve lower emissions in some cases, but there are also many scenarios, where they perform worse than ICEs. At the same time, ICEs are systematically cheaper. This means that FCs do not provide a robust advantage and cannot be considered a clearly superior option.

Another observation concerns the robustness of outcomes under uncertainty. Fossil fuels show the widest spread in lifetime costs, driven by the possibility of carbon pricing for research vessels, as well for GHG emissions. Ammonia and methanol exhibit much more compact distributions in both costs and emissions. This indicates that, beyond their environmental advantages, alternative fuels also provide more predictable outcomes under uncertainty, which increases their attractiveness in long-term planning.

The trade-off analysis demonstrates that no single propulsion configuration provides a universally superior solution under all conditions of cost and emissions. Ammonia and methanol consistently occupy the low-emission region but differ in economic and technical robustness: Ammonia is relatively cost-competitive but only around 95 % technically feasible, while methanol consistently achieves carbon neutrality but at systematically higher cost levels. Once ETS is introduced, however, both fuels are definitely cost-competitive, with ammonia in the lowest cost range, which increases their robustness.

Converter choice does not completely overturn these findings. In general, FCs do not provide a robust advantage, as they are more expensive and not reliably cleaner than ICEs, with one exception: For methanol configurations under an ETS, FCs can be cost competitive to ICEs.

8.5. Iterations within the MORDM Framework

The purpose of step 5 of the MORDM is to find new strategies or future scenarios based on the findings from the first four steps. In Section 8.4, a clear trade-off between emissions and costs was identified, at least prior to the introduction of ETS.

8.5.1. A: Blended low-carbon fuels

This iteration reflects a practical approach: configurations for methanol or ammonia, where the fuel consists of grey and green methanol and, with the introduction of an ETS, can be switched to green fuel. In this iteration, ammonia and methanol are tested with a supply of 80 % grey and 20 % green fuels. All technical assumptions remain unchanged, as the fuels properties are the same for green and grey fuel. Only fuel prices and emissions are mixed according to the 80/20 split. The results are evaluated with and without ETS using the same scatter plots.

Equations 8.1 and 8.2 are applied to compute WtT and TtW emissions. For the 80/20 blended fuel, the factors are obtained by linear mixing of the grey and green pathways.

$$GHG_{WtT,\,blend} = 0.8 \cdot GHG_{WtT,\,grey} + 0.2 \cdot GHG_{WtT,\,green} \tag{8.1}$$

$$GHG_{TtW,\,blend} = 0.8 \cdot GHG_{TtW,\,grey} + 0.2 \cdot GHG_{TtW,\,green} \tag{8.2}$$

Where

- $GHG_{WtT,\,blend}$ and $GHG_{TtW,\,blend}$ are the WtT and TtW GHG emissions for blended fuel.
- $GHG_{WtT,\,grey}$ and $GHG_{TtW,\,grey}$ are the WtT and TtW GHG emissions for grey fuel.
- $GHG_{WtT,\,green}$ and $GHG_{TtW,\,green}$ are the WtT and TtW GHG emissions for green fuel.

Fuel costs are treated similarly:

$$C_{fuel} = 0.8 \cdot C_{fuel,\,grey} + 0.2 \cdot C_{fuel,\,green} \tag{8.3}$$

Where

- C_{fuel} is the price per kg of the blended fuel.
- $C_{fuel,\,grey}$ is the price per kg of grey fuel.
- $C_{fuel,\,green}$ is the price per kg of green fuel.

The blended factors and prices are then used exactly as in the first iteration, in particular, fuel costs enter the model via Equation 6.11, and results are reported with and without ETS using the same scatter plots.

Figure 8.15 shows the distribution of lifetime costs, after applying Equations 8.1 to 8.3. Without ETS, medians are lowest for MDO, already followed by ammonia in combination with ICEs, and LNG. Methanol-ICE combinations are more expensive, while the upper bound is formed by HVO and less expensive combinations with FCs. FC variants also show the widest interquartile ranges and frequent high-cost outliers, indicating limited cost robustness. Introducing an ETS, reverses this ordering. In this case, HVO-options are the cheapest option, with LNG and MDO close by and overlapping ranges. The 80/20 blends exhibit higher medians, but the difference is moderate. However, the interquartile range is - particularly for ammonia - greater than for MDO, HVO, and LNG. FC variants have medians similar to their ICE counterparts, while their interquartile ranges and outliers are wider spread. Figure 8.16 shows the WtW lifetime emissions by fuel-converter under four different energy reducing technology settings, when ammonia and methanol consists of 80 % grey and 20 % green fuels. Lowest emissions are now archived by Methanol-FC combinations, followed by HVO and LNG. MDO and methanol-ICE configurations have very similar lifetime GHG emissions, while ammonia achieves the highest emissions.

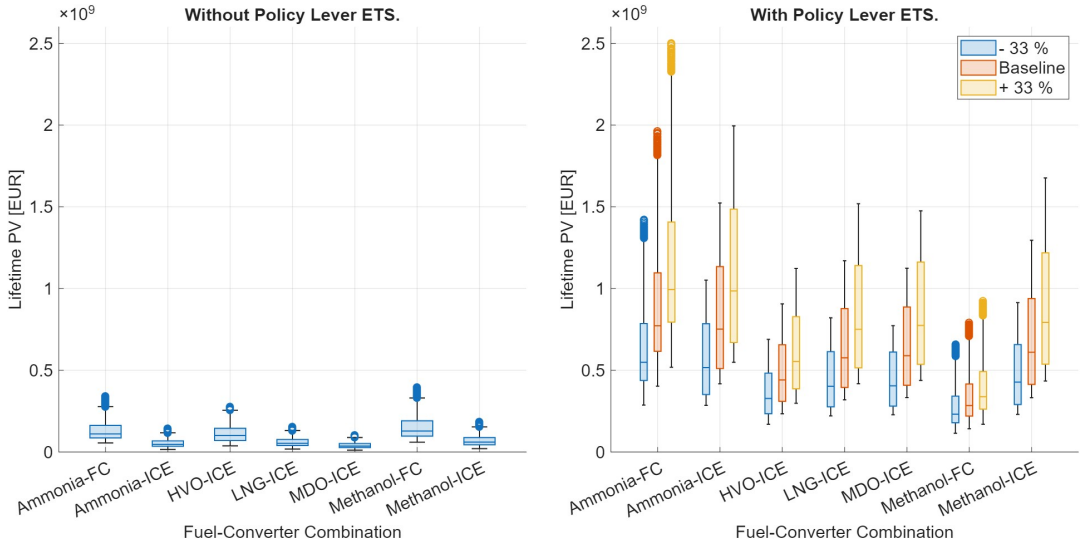

Figure 8.15: Lifecycle PV, Visualised with Box Plot by Fuel-Converter Combinations and Uncertainty of Policy Lever ETS (Colour-Coded). Left: Pure Market Prices, Right: Politically Influenced Prices. Ammonia and Methanol as Blended Fuel with 80 % Grey and 20 % Green Composition.

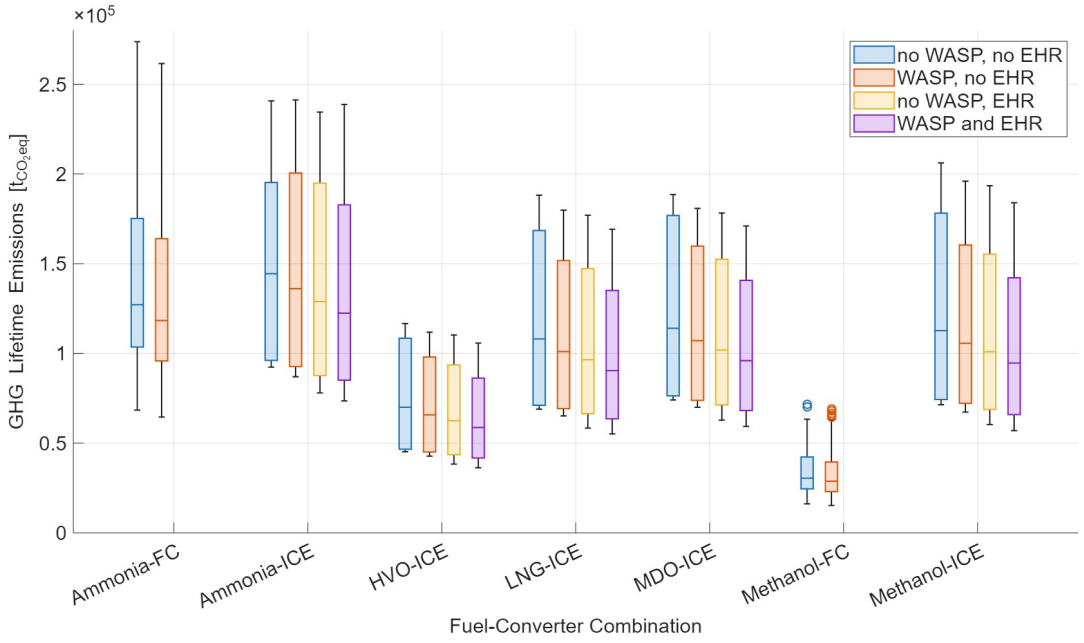

Figure 8.16: GHG Lifecycle Emissions, Visualised with Box Plot by Fuel-Converter Combinations and Energy Reducing Technologies (Colour-Coded). Ammonia and Methanol as Blended Fuel with 80 % Grey and 20 % Green Composition.

Figure 8.17 presents now the combined distribution of lifetime costs and GHG emissions, ammonia and methanol are again blended by 80 % grey and 20 % green fuel. Each point is one scenario, while the left panel shows the distribution if no regulatory lever is applied. The right panel shows all scenarios with an ETS applied. On the left panel, the clusters appear as clouds distinguishable by fuels. Compared to Figure 8.13, the left panel of Figure 8.17 does not show a clear trade-off between expenses and emissions anymore. Rather, the fuels are more clustered. However, HVO is still the most expensive option with lowest emissions. Ammonia-ICE combinations show similar attributes as MDO: This clusters more in the medium to high emission area at low costs. Methanol has lower emissions, but is also a bit more expensive. ICEs span again the economically more relevant frontier, while emissions are similar, if not higher.

With ETS (right panel), the form of the clouds change to bands, with positive slopes, indicating that the

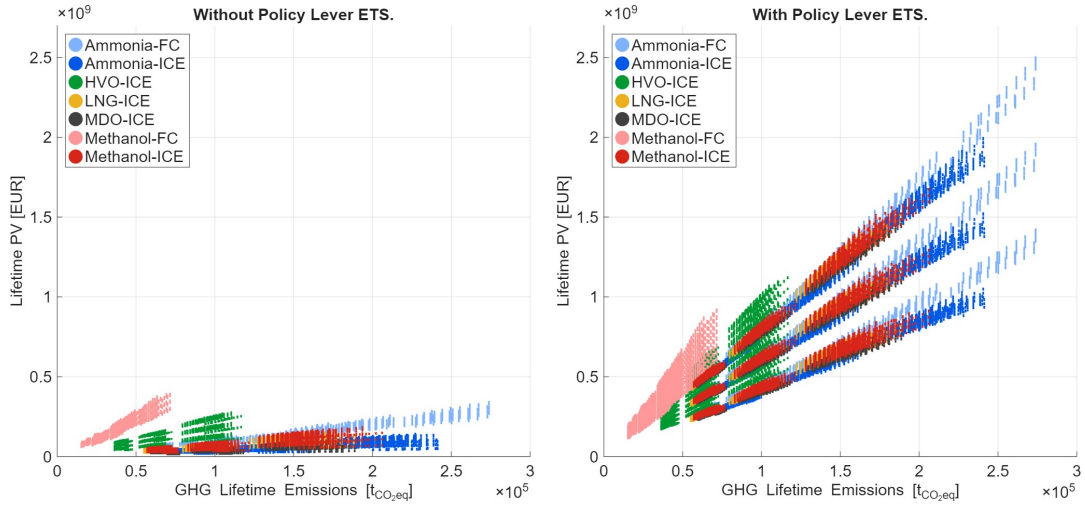

Figure 8.17: Lifecycle PV against GHG emissions, Visualised with Scatter Plot by Fuel-Converter Combinations (Colour-Coded). Left: Pure Market Prices, Right: Politically Influenced Prices. Ammonia and Methanol as Blended Fuels with 80% Grey and 20% Green Composition.

higher the emissions are, the higher the costs are. Under this regime, the blended fuels also lie in the group of the other fuels, while HVO has the lowest spread in emission direction and methanol is less costly than ammonia.

In summary, the 80/20 blends can increase the cost-robustness for ammonia and methanol relative to fully green supply. 80/20 blends place ammonia and methanol in a middle-cost area, where they are not prohibitively more expensive than MDO, in the case of ammonia even cheaper than LNG, but definitely less expensive than HVO. Emissions are slightly higher than for other fuels, for HVO the interquartiles are hardly overlapping. This makes the blended supply a practical transitional choice when green availability or price is constraining. With ETS in place, the step from 80/20 to fully green fuel is small, only the fuel type needs to be changed when bunkering.

8.5.2. B: Increase of c_B

In this iteration c_B is increased from the baseline value $c_B = 0.69$ to a scenario value of $c_B = 0.80$. In this design variant, the hull volume is increased to reduce space constraints and enable larger tank capacities. It is introduced here not because it would be a conventional design choice, but to investigate whether a fuller hull form can improve the feasibility and the cost–emission trade-off of alternative propulsion concepts by providing additional volume.

The increase of c_B directly influences the c_M, which is recalculated using the same relation as in Equation 5.3. All subsequent formulas remain unchanged, with the exception of those explicitly adapted below for the fuller hull form. The transit power is recalculated via the constant c from the base case.

$$P_{transit} = c \cdot v_s^3 \cdot S' \tag{8.4}$$

This represents a very simplified approach, as c contains resistance effects that would most likely increase for a fuller form. However, to the knowledge of the author, no empirical correlation is available to adjust this factor directly. In the present equations, the effect of a higher block coefficient is therefore approximated by recalculating the wetted surface area, such that the resulting power demand still reflects the increased hull-water interaction, even if the change in resistance coefficient itself cannot be modelled here.

The initial additional enclosed volume created by the fuller form is expressed in Equation 8.5 and converted into an usable length below the waterline in Equation 8.6.

$$V_{c_B add} = (c'_B - c_B) \cdot L_{pp} \cdot B \cdot D \tag{8.5}$$

$$L_{c_B add} = \frac{V_{c_B add}}{A'_M} \cdot \eta_{relocation} \tag{8.6}$$

This conversion is required because the additional volume does not occur as a block at midship, but is mainly distributed in the fuller fore- and aftbody sections of the hull. To use this volume effectively for tanks or converters, internal arrangements must be relocated and adapted. The same relocation factor $\eta_{relocation}$ that was introduced for shifting spaces from above to below the waterline is therefore applied here.

The below-water length demand is reduced accordingly:

$$\Delta L'_u = \frac{\Delta V_{fuel}}{A_{M,\,t}} + \frac{\Delta V_c}{A_M} - \frac{V_{free}}{A_M} \cdot \eta_{relocation} - L_{c_B add} \tag{8.7}$$

All other steps of the framework including the iterative loop remain unchanged.

Table 8.3 shows that the design change to a fuller hull increases technical feasibility for borderline and infeasible fuels. All non-hydrogen solutions are now feasible in 97 % or more, while hydrogen remains limited but definitely more robust. The improvement is consistent with the mechanisms shown before: a higher c_B increases the usable midship areas and the additional enclosed volume $V_{c_B add}$, reducing the required added length. As more configurations satisfy the L/B constraint, feasibility rises.

Table 8.3: Technical Feasibility by Fuel-Converter Combination with increased c_B.

Fuel	Converter	Feasibility
Ammonia	FC	97.5 %
Ammonia	ICE	99.1 %
HVO	ICE	100 %
Hydrogen	FC	70.4 %
Hydrogen	ICE	66.7 %
LNG	ICE	100 %
MDO	ICE	100 %
Methanol	FC	100 %
Methanol	ICE	100 %

These findings should be interpreted with care. The hydrodynamic constant c is held from the base case, for a fuller form the underlying resistance coefficient would likely increase. Currently, this is approximated only through the larger wetted surface S, so the additional power may be underestimated. A more detailed recalculation would in principle be possible using empirical methods such as Holtrop and Mennen, 1982, but this would require further assumptions, which would also introduce uncertainty and limit the precision of the results. Alternatively, resistance could be determined through CFD analyses or ultimately by conducting physical model tests, requiring substantially greater modelling effort and resources. Likewise, in the structural weight estimation, the increase in c_B does not trigger any extra weight, as the used Equation 5.34 is a function of only ΔL and B. Changing the fullness at constant B and H does not change the steel weight beyond what comes from the lengthening itself, neglecting effects as possible local reinforcements.

Figure 8.18 compares lifetime PV and emissions for the fuller hull design with and without the introduction of an ETS. The plot closely resembles the baseline figure: fuel-converter clusters occupy almost identical regions in the cost-emission plane, and the relative ordering does not change. Apparently, the fuller hull may increase feasibility by providing more usable space, while costs and emissions are only very slightly affected. These results must again be treated with caution. As already explained, c is retained from the base case, meaning that additional resistance is likely to be underestimated. If so, required energy and fuel costs are also underestimated. Likewise, steel weight and capital costs for energy converters may be too low. In addition, seagoing properties such as sea-keeping, manoeuvrability, and passenger comfort can be influenced by a fuller hull form, but are not reflected in the present framework. A reliable assessment of a fuller hull form would therefore require a dedicated design process, including hydrodynamic evaluation through CFD or model-scale testing.

Within these limitations, the results are still interesting: They show that increasing the block coefficient can improve feasibility without visibly worsening cost and emissions. This suggests that hull-form adjustments may open new options for integrating high-volume fuels, but the present outcomes should be seen as indicative signals rather than quantitative predictions, highlighting where more detailed design investigations could be worthwhile.

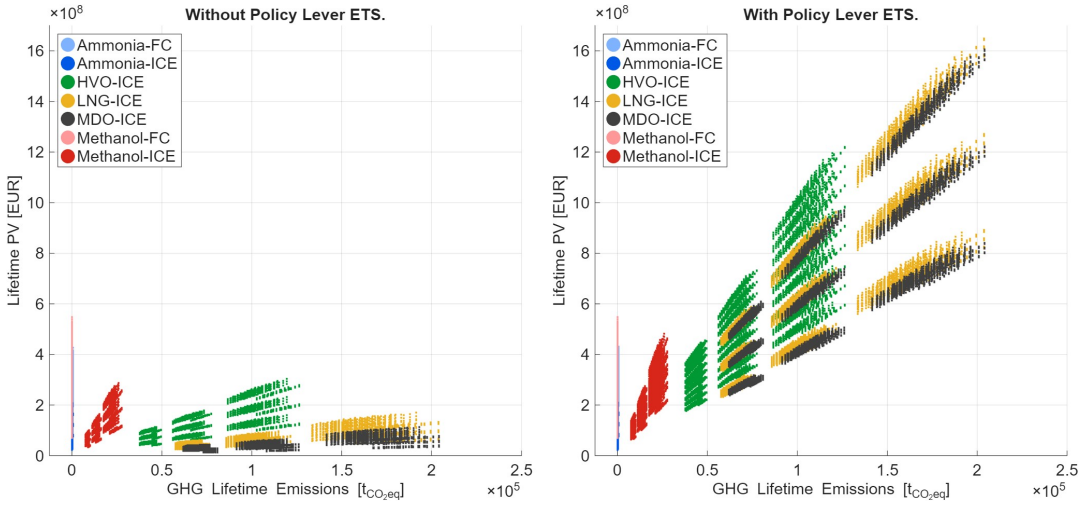

Figure 8.18: Lifecycle PV against GHG Emissions for Fuller Hull, Visualised with Scatter Plot by Fuel-Converter Combinations (Colour-Coded). Left: Pure Market Prices, Right: Politically Influenced Prices.

8.6. Conclusion

Chapter 8 evaluated the technical, environmental, and economic performance of alternative strategies under deep uncertainty. This resulted in three levels of feasibility:

- Robust options are technically feasible in 100 % of the scenarios. These are propulsion systems with HVO, LNG, MDO and methanol-ICEs.
- Borderline options achieve a feasibility of $\sim$ 90 % (ammonia) to 99 % (methanol-FCs).
- Infeasible fuels are feasible in only about 10 % of the scenarios. This is the case for hydrogen configurations, which are no longer being considered.

Additional energy reducing technologies can improve borderline cases (e.g. the feasibility of ammonia ICEs with EHR and WASP increases to 97 %), but none of them achieve complete robustness. However, technical feasibility is era-sensitive. Operating profiles (eras) shift the energy demand and thus ΔL, leading to fully feasible configurations in era 1 and 2 for ammonia and methanol-FC configurations, whereas the higher eras stay below 100 % for these configurations.

On emissions, all alternatives outperform MDO, which forms the high-emission benchmark. Within fossil and diesel-like fuels, HVO achieves the lowest WtW emissions, followed by LNG. FCs offer lower emissions than their ICE counterpart for methanol configurations. Energy-saving technologies consistently reduce emissions across fuels, with the largest absolute effects for fossil/diesel-like options. The relative ordering by fuel remains dominated by fuel choice rather than auxiliary efficiencies, as - at least WASP - has the same relative effect on all fuels. Nevertheless, the efficiencies of EHR are not large enough to outweigh the emission-related advantages of FCs in methanol configurations.

The sensitivity analysis on the economics showed that fuel price uncertainty dominates CapEx uncertainty. Still, CapEx differences explain the structural cost hierarchy between converters: across all fuels, FCs are systematically more expensive than ICEs, due to higher capital expenses, with only a few exemptions. A clear fuel-based cost hierarchy also emerges: without ETS, fossil and diesel-like fuels (MDO, LNG and HVO) cluster in the lowest cost range, while low-carbon fuels (ammonia and methanol) are more expensive. However, as the most influential uncertainty factor on the lifecycle costs is the policy lever ETS, fossil/diesel-like options shift sharply upward on the cost axis, when introduced. Low-carbon fuels move into the cost-competitive region. In this regime, ammonia-ICE configurations belong to the most economical solutions, and, methanol FCs are cost-competitive to methanol ICEs. This demonstrates, that policy design can outweigh converter and fuel choice.

The trade-off analysis confirms the structural opposition between cost and emissions. Without ETS, fossil and diesel-like fuels dominate the low-cost/high-emission corner, while ammonia and methanol occupy the low-emission/high cost region. Converter choice does not overturn this pattern: FCs are

systematically more expensive and only marginally cleaner than ICEs. For methanol, only FCs achieve full carbon neutrality, whereas ICEs still produce non-negligible emissions. This outcome is closely linked to the assumptions applied in this thesis, particularly the treatment of methanol pathways. With more detailed or updated data, especially from European regulatory sources, these results may shift. Once ETS is introduced, the trade-off space is reshaped: fossil and diesel-like fuels shift sharply upward on the cost axis, while ammonia and methanol are both more clean and less expensive. Under these circumstances, the tension between economic and environmental performance is strongly reduced, and low-carbon fuels emerge as attractive solutions. However, technical robustness limits these results: methanol-ICE remains fully feasible in all scenarios, while ammonia configurations achieve a feasibility of around 95 %. Although ammonia appears to be very competitive in economic and emission-related trade-off, its limited robustness must be taken into account.

A fuel-oriented iteration with blended fuels consisting of 80 % grey ammonia or methanol and 20 % green fuel shows how transitional strategies can enhance economic robustness. These blends improve costs and shift ammonia and methanol in lower cost-regions. However, their emissions remain significantly higher than fully green variants and, on average, even higher than MDO cases. With ETS in place, the transition to fully green fuels is very easy, with significantly lower costs.

A design-oriented iteration evaluated the effect of increasing c_B. The results show that this change improved technical feasibility. The underlying mechanism is the additional enclosed volume, which reduces required added length. The cost-emission trade-off remains essentially unchanged. These results must be treated with caution, as resistance effects are only approximated through the wetted surface, and seagoing properties such as sea-keeping and manoeuvrability are not reflected. Nevertheless, Iteration B provides an interesting indication that hull-form adjustments could be a viable lever in a newbuilt context including design steps, improving feasibility without fundamentally worsening costs and emissions. Taken together, Iterations A and B demonstrate that the MORDM framework can be applied not only to explore alternative fuel mixes but also assess design changes. This highlights its flexibility as a tool guiding both operational and design-oriented pathways towards the decarbonisation of research vessels.

9 Conclusion

This chapter discusses the results obtained with the developed model in relation to the research questions. It first reviews how the research questions have been addressed in Section 9.1, before reflecting on the limitations of the thesis (Section 9.2). Scientific contribution is then outlined in Section 9.3 together with an outlook (Section 9.4). In this way, the chapter brings together the findings of the thesis and positions them within the wider context of research vessel decarbonisation.

9.1. Research Questions

The literature review has established a theoretical and methodological foundation for evaluating decarbonisation strategies for research vessels. As outlined in Chapter 1, the motivation for this research is the increasing need to reduce GHG emissions from maritime transport. The research gap identified in the introduction - namely the lack of studies addressing the integration of decarbonisation strategies onboard of research vessels - has framed the literature analysis in the preceding chapters.

The central research question,

> *Which alternative fuels and WASP achieve the highest technical and economic viability for research vessels under market uncertainties and different operating profiles?*

has been divided into eight subquestions. The literature review, covering Chapter 2 through Chapter 4, has provided detailed answers to the first three of them:

1. *What is the current state-of-the-art in the design of research vessels, considering regulatory requirements, operational profiles, and fuel consumption patterns?*

Chapter 2 characterised research vessels by operational class (coastal, regional, ocean, global). For the German research vessel *RV Sonne*, the power demand, and for her and the *Maria S. Merian* the fraction of transit and port operation were shown. Chapter 2 also mapped the fragmented regulatory environment, confirming that emission constraints are limited or absent. These findings underscore the necessity of self-directed sustainability efforts and context-specific decarbonisation solutions.

2. *What energy reduction methods and alternative energy options are technically feasible, including alternative fuels and WASP?*

Chapter 3 offered a comparative assessment of low- and zero-emission fuel options. Examined were low-emission fossil fuels as LNG and LPG, the renewable fuel HVO, hydrogen carriers like ammonia, hydrogen, and sodium borohydride, alcohol fuels as methanol, as well as metal-based fuels like iron powder, and energy carriers as batteries. Each option was evaluated across criteria including physical and chemical properties, emissions, technological readiness and fuel availability, safety and costs. The fuels were analysed alongside energy converters and auxiliary technologies. While no single configuration emerged as universally superior, several combinations were identified. Notably, WASP and EHR show potential for emission reduction.

3. *Which research methods, concerning parametric modelling, uncertainty analysis, and economic evaluation, are best suited to assess the feasibility of alternative fuels and WASP for research vessels?*

In Chapter 4, the literature review dealt with various decision-making frameworks and uncertainty typologies. It concluded, that the MORDM framework in combination with an EEA is best suited for this context, given the level three to four uncertainties across technological, economic, and regulatory dimensions. MORDM supports the identification of robust, non-dominated solutions across two performance metrics - emissions and expenses. The approach differs from classical optimisation by shifting focus from an ideal outcome to the identification of strategies that perform acceptably well across a wide range of uncertain future scenarios. To be able to implement this approach, a parametric model was implemented within the XLRM matrix. The model integrates uncertainty factors directly into its structure and evaluates vessel configurations to simulate ship performance over the defined eras.

The remaining sub-questions, which deal with operational and technical sensitivity, economic impacts, emission reductions, and validation, are addressed in the research section, which comprises Chapters 5 to 8.

4. *How do operational profiles of research vessels impact the feasibility and performance of alternative fuels and WASP?*

Operational variability was formalised with an EEA implemented in the MORDM framework to span plausible mission patterns over a 30-year vessel life. The analysis shows that operational profiles are a decisive factor for feasibility. Operational profiles (the defined eras) shift energy demand and the required added hull length, which in turn governs technical feasibility via the L/B constraint. Less demanding profiles keep added length modest, while more demanding profiles push low-density options toward infeasibility. Within this pattern, methanol-FC and ammonia configurations remain fully feasible in the lower-demand eras. The profiles also shift lifecycle emissions and costs, but these affects smaller than the influence of fuel choice, and the relative ranking of fuels remains stable across eras.

5. *How does the efficiency of WASP and exhaust heat recovery systems influence the overall decarbonisation potential of research vessels?*

The efficiency of WASP and EHR systems is characterised by uncertainties that depend on external conditions of technical and operational nature. EHR and WASP reduce emissions across all efficiency levels. On the cost side, WASP can reduce expenses in all cases. EHR, on the other hand, only reduces costs slightly due to its high capital investment, and in some cases it cannot reduce costs at all. With an ETS, efficiency improvements also avoid CO_2 costs, which means that EHR can significantly reduce the cost of carbon fuels.

6. *What is the economic impact of the introduction of alternative fuels and WASP for research vessels, taking into account investment costs, operating costs and market uncertainties?*

The economic outcomes are primarily driven by fuel choice and policy, rather than by technical, operational, or economic uncertainties. Without ETS, MDO, LNG, and HVO cluster in the high emissions/low costs region, while HVO has the lowest emissions and the highest costs in this group. Methanol-ICEs have medium emissions and medium costs in the range of HVO, while ammonia and methanol-FCs have the lowest emissions, with costs close to them of HVO and methanol. The ETS reverses the cost hierarchy and pushes fossil and diesel-like fuels from the cheapest to the most expensive options once emissions are priced. Also methanol shows increased expenses, while ammonia and methanol-FCs are highly untouched. WASP and EHR have little effect on costs without ETS. EHR in particular lacks a positive business case for all ammonia-configurations due to the initial investment required. However, it becomes more important under ETS reducing the CO_2 costs of fossil/diesel-like fuels. ICEs are structurally cheaper than FCs. Blended fuels with 20 % green content improve the cost position of methanol and ammonia, under the absence of ETS.

7. *What are the emission reduction potentials of combined decarbonisation strategies?*

Combined strategies show that fuels and converters drive most of the decarbonisation potential, while WASP and EHR only shift results slightly. Green methanol and ammonia provide the largest reduc-

tions, while HVO and LNG remain emission-intensive. Blended fuels (with 20 % green and 80 % grey composition) leave emissions close to or even higher than MDO. FCs can lower emission in specific cases though their benefit is small.

8. *How can the model and results be verified and validated to ensure their reliability for real-world application in research vessel decarbonisation?*

Verification was ensured through modular implementation with visual analysation. Systematic input variations confirmed stable behaviour and plausible monotonic responses. Hand-calculations were done to trace parts of the model. Simplified assumptions are used to trace interims wise, but also simplified structures are kept to ensure transparency. Visualised samples showed internal consistency and correct implementation of time-based economic effects, while resulting outputs are visually evaluated regarding means and variances. Furthermore, a commercial but general purpose computing environment, namely MATLAB, was used, reducing the likelihood of implementation errors. The validation is based on available literature, models and expert opinions, which confirm that the relative ranking of fuels and converters is consistent with published data. While these steps strengthen confidence in the results, real-world data for alternative fuels, FCs, WASP and EHR systems remain limited, meaning that external validation is constrained.

Finally, an answer on the main research question can be found.

How do alternative fuels and energy reduction technologies influence the technical and economic viability of research vessels under market uncertainties and different operating profiles?

To answer that question, results from the technical robustness assessment, and the cost and emissions evaluations are combined. Table 9.1 summarises these results of all fuel-converter combinations. WASP and EHR are not included in the table, as Chapter 8 showed that they do not have decisive influence.

The results across all scenarios show that no single propulsion configuration provides a universally superior solution. LNG and HVO are technically fully feasible. Methanol-ICE configurations are the only low-carbon configuration that is fully feasible across all operational profiles and uncertainties. Ammonia-ICE performs well, and is fully feasible when lower requirements are given. FCs are generally less robust, while hydrogen is not robustly feasible.

LNG and HVO remain consistently emission-intensive and therefore cannot contribute sufficiently to long-term decarbonisation. Methanol and ammonia provide substantial emission reductions, with ammonia reaching near carbon-neutrality if produced from sustainable feedstocks. Both, however, are more expensive without carbon trading, while fossil and diesel-like fuels occupy the low-cost high-emission corner. The introduction of an ETS reverses this hierarchy, aligning methanol and ammonia with competitive costs. FCs offer additional emission reductions, but remain structurally more expensive than ICEs. Blended fuels can play an important transitional role in this context. By equipping vessels already with methanol- or ammonia based ICEs and initially operating them on blends of grey and green methanol, owners can ensure technical feasibility and prepare for future green fuel availability. This approach reduces exposure to high fuel prices and creates a pathway for future-proof research vessels. In this way, blended fuels enhance the robustness of methanol and ammonia by making them cheaper now, but enabling the switch to green fuels, when availability increases or an ETS is applied. Iteration B further provided an indication of how design changes could influence feasibility. By testing a fuller hull form, it became apparent that space constraints can be softened without fundamentally shifting the cost-emissions trade-off. These results must be treated carefully, but they suggest directions in which a full design process - supported by hydrodynamic testing and detailed structural assessment - could be explored in the future.

Taken together, these findings underline that future-proof research vessels must be based on fuels that are both technically feasible and robust under uncertainty, while also enabling compliance with long-term climate targets. Methanol - and to slightly lesser extent ammonia - meet these requirements, while fossil and diesel-like fuels do not.

The results show that fuel and converter choice are the decisive factor for decarbonising research vessels. Methanol in ICE configurations emerge as the only low-carbon option being fully robust across all

Table 9.1: Possible Propulsion Configurations. Red: Technically Not Plausible or Infeasible. Green: Robust in This Criterion.

Fuel	Converter	Technical Feasibility	Economic Viability	Emission Performance
Ammonia	**ICE**	95 % feasible, fully feasible in era 1 and 2	more expensive without ETS, competitive with ETS	nearly carbon neutral, if green
HVO		fully feasible	more expensive than fossil fuels	more emissions than low-carbon fuels
LH_2		rarely feasible, therefore excluded	not assessed	not assessed
LNG		fully feasible	competitive with MDO with ETS, slightly more expensive without	slightly less
Methanol		fully feasible	more expensive with ETS without ETS, competitive with ETS	low emission, if green
Ammonia	**FC**	95 % feasible, fully feasible in era 1 and 2	more expensive than ICE configuration	nearly carbon neutral, if green
HVO		technically not possible	not assessed	not assessed
LH_2		rarely feasible, therefore excluded		
LNG		technically not possible		
Methanol		99 % feasible, fully feasible in era 1 and 2	more expensive than ICE configuration	zero emissions

uncertainties, while ammonia represents a strong alternative for lower-demand vessels. LNG and HVO remain technically feasible but offer only slight carbon savings. LNG is slightly more expensive than MDO, while HVO doubles costs. In case an ETS is applied, both fossil and diesel-like fuels are highly expensive. FCs are constrained by cost and feasibility: for methanol they offer additional carbon savings, while for ammonia emissions can even rise as only WtT emissions are present. Complementary measures such as WASP and EHR support emission reduction and can improve in most cases, but they do not change the overall ranking. Blended fuels support viable pathways to future-proof research vessels by offering a short-term pathway until green fuel availability is higher leading to reduced costs or ETS is applied.

9.2. Limitations and Future Work

While this thesis identifies robust pathways for the decarbonisation of research vessels, several limitations should be noted. Safety concerns associated with alternative fuels such as ammonia (toxicity, low temperature), methanol (low flammability), and LNG (low flammability, low temperature) were already addressed in Section 3.2 but could not be addressed in the modelling framework. Similarly, the study relied on several simplifications to manage deep uncertainty: operational profiles were generalised into eras, complex tank and hull integrations were simplified to added length, and cost modelling relied on assumed ranges excluding factors such as crew training. The effect of a fuller hull form was approximated, but additional resistance, and sea-keeping behaviour were neglected. Furthermore, validation was limited by the absence of real world data for alternative fuels and EHR. These simplifications limit the precision of individual results but do not undermine the robustness of the overall findings. The model developed in this thesis is therefore not sufficient to directly derive an individual vessel design, but it can serve as a valuable indication and starting point for the design process, helping to narrow down feasible and robust fuel-converter pathways before more detailed naval architecture is undertaken.

Building on these limitations, several directions for future work emerge. The most immediate step would be to sample and incorporate high-resolution operational data into the modelling framework, in order to capture realistic load profiles, seasonal variations, and peak conditions more accurately. Further improvements should focus on a more detailed representation of cost structures, fuel availability, and safety measures. Finally, the framework can be developed towards a design tool by integrating naval architectural aspects more explicitly, for instance through detailed tank and hull modelling, while also applying CFD calculations in a further step. Together, these extensions would increase the precision of the model while preserving its strength as a tool for decision-making under deep uncertainty.

9.3. Scientific Contribution

The scientific contributions of this thesis can be summarised in three main aspects, which build directly on the identified research gap and research questions: addressing the gap itself, developing a methodological innovation, and generating insights with practical relevance.

- **Research Gap**
  As outlined in Section 1.2, existing studies on maritime decarbonisation primarily focus solely on specific technological measures, or commercial vessels and therefore neglect the particular challenges of research vessels. This thesis addresses that gap by systematically analysing research vessels as a distinct case, characterised by regulatory exemptions, high auxiliary loads, and highly variable operational profiles. By incorporating an era-based sensitivity analysis, reflecting operational profiles from low demand (era 1) to high demand (era 3) vessels, the thesis shows that fuel choices are not universally applicable but shift with operational intensity. The results highlight that ammonia can be a robust, competitive, and more emission-free variant for lower-demand vessels, whereas methanol remains the only fully robust low-carbon fuel for high-demand vessels. In doing so, the thesis not only closes the research gap identified in Section 1.2 but also introduces a dynamic perspective on how operational diversity reshapes decarbonisation strategies for research vessels.

- **Methodological Innovation**
  Building on this research gap, a second scientific contribution of this thesis lies in the development of what is, to the knowledge of the author, a novel methodological framework for evaluating

decarbonisation strategies under deep uncertainty. This integration was done specifically to address the uncertainties arising from diverse operational profiles of research vessels, ensuring that both feasibility and robustness across varying demand levels could be evaluated. The framework enabled the exploration of thousands of propulsion configurations under changing assumptions of fuel prices, energy demand, and technological performance. By structuring the analysis into eras of increasing vessel requirements, the methodology not only captures average performance but also reveals how the competitiveness of fuels shifts with operational intensity. In this way, the methodological innovation directly arises from the identified research gap and offers a richer and more realistic perspective than conventional scenario-based approaches, which typically assume static operating conditions.

- **Empirical Insights**
  Finally, and very much as a necessary outcome of the research gap and questions defined in the introduction, this thesis provides a third scientific contribution in the form of new empirical insights into the decarbonisation of research vessels. By systematically applying the developed methodological framework, it was possible to uncover how fuel feasibility shifts across different operational demand levels. The results show that ammonia can be a robust and competitive option for lower-demand vessels, while methanol remains the only consistently robust low-carbon solution across all operational requirement levels. In contrast, LNG and HVO, though technically feasible, provide only marginal emission reductions and lose competitiveness under applied regularities. Furthermore, the analysis showed, that hydrogen is highly infeasible even under era 1 requirements. The analysis moreover indicates that auxiliary systems such as WASP and EHR improve efficiency, yet their overall impact on feasibility and measures remains limited and not decisive. The method further demonstrates in an iterative step how blended fuels can serve as transitional pathways, improving cost robustness in early adoption phases while enabling a smooth shift to carbon neutrality or at least high carbon savings once supply chains and regulations mature. These findings not only represent a contribution that directly follows from the identified research gap and question, but also carry practical relevance: they provide actionable guidance for ship designer in the early stages of concept development, and for operators in planning long-term fuel strategies.

Taken together, these contributions address the research gap, advance methodology, and provide new and useful insights for creating a future-proof pathway to the decarbonisation of research vessels.

9.4. Outlook

The findings of this thesis highlight that fuel and converter choice is the decisive factor in decarbonising research vessels, with methanol emerging as the only fully robust low-carbon option and ammonia as a strong alternative for vessels with lower energy demand. These insights, however, will evolve as external developments reshape the option space.

Shifts are expected from the scale-up of green methanol and ammonia production. At present, their competitiveness is constrained by limited availability and high costs. This aspect was already explored in the thesis through varying fuel price assumptions across the years, yet future developments may exceed the considered ranges. Large-scale production facilities and new bunkering infrastructure could lower costs more rapidly than anticipated, while geopolitical or supply-chain shocks could equally push them higher. On the contrary, as better data is available, models like the one developed can be refined to deliver more precise insights.

Technological progress will also influence the option space. In this thesis, ICEs proved being more robust than FCs, primarily due to cost and maturity constraints. However, continued development of high-power methanol or ammonia FCs may alter this balance by combining higher efficiency with near-zero emissions. If cost reductions and reliability gains are achieved, FCs could become a stronger alternative for certain vessel classes. Beyond the fuels analysed in depth, novel energy carriers such as iron fuel or sodium borohydride, excluded during the literature review due to low technological readiness, may become relevant in the longer term. In deep sea vessels, batteries are today limited to auxiliary applications such as peak shaving. However, with ongoing improvements in storage capacity, batteries may in the longer term evolve into a viable option for a wider range of missions.

Regulatory change is another factor. Although research vessels are currently exempt from many international and European instruments, initiatives such as the IMOs Net Zero Framework suggest that exemptions may not last. If research fleets were to fall under carbon pricing, the competitiveness of fossil fuels would decline sharply, strengthening the case for methanol and ammonia.

Taken together, these developments suggest that the model presented in this thesis should be understood as a model in progress. It can and should be adapted as new data on fuels, technologies, and regulations becomes available, ensuring that the insights remain relevant and continue to support the transition towards truly climate-neutral, future-proof research vessels.

9.5. Reflection

The aim of this work was to develop and evaluate strategies for decarbonising research vessels under conditions of high uncertainty. After introduction of motivation, background, and research questions, the state-of-the-art technologies, regularities, and methods were presented in the research review. Based on these findings, a parametric model was developed, verified and validated to represent fuel pathways, converter technologies, and integration into ships under different scenarios. This model was then applied to identify robust and unfeasible options, evaluate emissions and costs, and test extensions trough iterations A and B. In this way, the sub- and central research questions were answered. The analysis shows which fuel pathways and configurations remain feasible in a wide range of future scenarios. Finally, the necessary simplifications are highlighted, and directions for further research are indicated.

Conducting this research has been both challenging and rewarding, and I hope it can serve as a useful step towards designing cleaner, more sustainable vessels in the years ahead.

This page is left blank intentionally.

References

airseas. (n.d.). Seawing. Retrieved March 26, 2025, from https://airseas.com/en/seawing-system/

airseas. (2021, December). Product installations. Retrieved March 26, 2025, from https://airseas.com/en/product-installations/

Al-Aboosi, F. Y., El-Halwagi, M. M., Moore, M., & Nielsen, R. B. (2021). Renewable ammonia as an alternative fuel for the shipping industry. *Current Opinion in Chemical Engineering*, *31*, 100670. https://doi.org/https://doi.org/10.1016/j.coche.2021.100670

Argus O.M.R. (2024, October). LPG bunker demand lags despite competitive pricing | Latest Market News. Retrieved April 9, 2025, from https://www.argusmedia.com/en/news-and-insights/latest-market-news/2623153-lpg-bunker-demand-lags-despite-competitive-pricing

Argus O.M.R. (2025, April). Diesel & HVO monthly averages. Retrieved April 6, 2025, from https://omr.de/en/products/diesel-hvo-monthly-averages

arianeGroup. (2023, September). Ariane 6 Cargo Ship Canopée spreads its wings. Retrieved May 8, 2025, from https://ariane.group/en/news/ariane-6-cargo-ship-canopee-spreads-its-wings/

Atilhan, S., Park, S., El-Halwagi, M. M., Atilhan, M., Moore, M., & Nielsen, R. B. (2021). Green hydrogen as an alternative fuel for the shipping industry. *Current Opinion in Chemical Engineering*, *31*, 100668. https://doi.org/https://doi.org/10.1016/j.coche.2020.100668

AWI. (n.d.). Uthörn. Retrieved February 20, 2025, from https://www.awi.de/en/fleet-stations/research-vessel-and-cutter/uthoern.html

Baltic Shipping. (n.d.). CRV LEONARDO, Research vessel, IMO 9251303 | Vessel details | BalticShipping.com. Retrieved June 2, 2025, from https://www.balticshipping.com/vessel/imo/9251303

Barbu, F., Ungureanu, C., & Rusu, E. (2024). Harnesing wind power in maritime shipping: A comparative analysis of innovative hull design and retrofitted solutions for decarbonisation [Section: Articles]. *Annals of "Dunarea de Jos" University of Galati. Fascicle XI Shipbuilding*, *47*(0), 10. Retrieved April 7, 2025, from https://gup.ugal.ro/ugaljournals/index.php/fanship/article/view/7236

Barrass, C. B., & Derrett, D. R. (2012). *Ship Stability for Masters and Mates (Seventh Edition)* (C. B. Barrass & D. R. Derrett, Eds.; Seventh Edition). Butterworth-Heinemann. https://doi.org/https://doi.org/10.1016/B978-0-08-097093-6.00005-0

BBC. (2008). Kite to pull ship across Atlantic. *BBC News*. Retrieved May 6, 2025, from http://news.bbc.co.uk/2/hi/europe/7201887.stm

Berger, J. (2025, February). How the Green Deal Makes Maritime Shipping More Sustainable. Retrieved April 14, 2025, from https://www.bergermaritiem.nl/en/green-deal-maritime-shipping-sustainable

Bergeson, L., & Greenwald, C. K. (1985). Sail assist developments 1979–1985. *Journal of Wind Engineering and Industrial Aerodynamics*, *19*(1), 45–114. https://doi.org/https://doi.org/10.1016/0167-6105(85)90056-X

Bergthorson, J. M., Goroshin, S., Soo, M. J., Julien, P., Palecka, J., Frost, D. L., & Jarvis, D. J. (2015). Direct combustion of recyclable metal fuels for zero-carbon heat and power. *Applied Energy*, *160*, 368–382. https://doi.org/https://doi.org/10.1016/j.apenergy.2015.09.037

Bernatik, A., Senovsky, P., & Pitt, M. (2011). LNG as a potential alternative fuel – Safety and security of storage facilities. *Journal of Loss Prevention in the Process Industries*, *24*(1), 19–24. https://doi.org/https://doi.org/10.1016/j.jlp.2010.08.003

BloombergNEF. (2025, March). Europe's New Emissions Trading System Expected to Have World's Highest Carbon Price in 2030 at €149, BloombergNEF Forecast Reveals [Section: Press Release]. Retrieved May 20, 2025, from https://about.bnef.com/blog/europes-new-emissions-trading-system-expected-to-have-worlds-highest-carbon-price-in-2030-at-e149-bloombergnef-forecast-reveals/

Blue World Technologies. (2024, June). Blue World completes successful testing of 200 kW maritime fuel cell system to run on green methanol. Retrieved April 7, 2025, from https://www.blue.

world/blue-world-completes-successful-testing-of-200-kw-maritime-fuel-cell-system-to-run-on-green-methanol/

Bøckmann, E., & Steen, S. (2011). Wind Turbine Propulsion of Ships, 10. Retrieved March 27, 2025, from https://www.marinepropulsors.com/smp/files/downloads/smp11/Paper/FA1-2_Bockmann.pdf

Bora, N., Singh, A. K., Pal, P., Sahoo, U. K., Seth, D., Rathore, D., Bhadra, S., Sevda, S., Venkatramanan, V., Prasad, S., Singh, A., Kataki, R., & Sarangi, P. K. (2024). Green ammonia production: Process technologies and challenges. *Fuel*, *369*, 131808. https://doi.org/https://doi.org/10.1016/j.fuel.2024.131808

Briese Research. (n.d.). BRIESE - RV SONNE. Retrieved May 14, 2025, from https://briese-research.de//research-department/research-vessels/rv-sonne

British Antarctic Survey. (2023, July). Trial of lower carbon alternative fuel begins on RRS Sir David Attenborough. Retrieved March 31, 2025, from https://www.bas.ac.uk/media-post/trial-of-hvo-fuel-sda/

BSH. (n.d.). The New ATAIR. Retrieved February 20, 2025, from https://www.bsh.de/EN/The_BSH/Our_ships/New_Atair/new_atair_node.html

Carl Roth. (2024a, September). Safety Data Sheet Methanol. Retrieved April 4, 2025, from https://www.carlroth.com/medias/SDB-AE01-AU-EN.pdf?context=bWFzdGVyfHNlY3VyaXR5RGF0YXNoZWV0c3wzNTY5MDN8YXBwbGljYXRpb24vcGRmfGFEWTJMMmhpWWk4NU1UYzNORFEwTXpnME56azRMMU5FUWw5QlJUQXhYMEZWWDBWT0xuQmtaZ3w2YjY0MzYyM2U4MzRkNTZkMWMzZGU4MzFhMTczMzIyNWJhYTdmZGVkZmZjNDUxNmU0NmNiZmFkNTNkMDM0ZWM2

Carl Roth. (2024b, September). Voluntary safety information following the Safety Data Sheet format according to regulation (EC) No. 1907/2006 (Reach). Retrieved April 7, 2025, from https://www.carlroth.com/medias/SDB-9454-MT-EN.pdf?context=bWFzdGVyfHNlY3VyaXR5RGF0YXNoZWV0c3wyMjE4NDl8YXBwbGljYXRpb24vcGRmfGFEa3pMMmd6WkM4NU1UYzRORFF6TkRneE1URTRMMU5FUWw4NU5EVTBYMDFVWDBWT0xuQmtaZ3xmMzM4Y2U5YjE5YWYwNWFiNTU2NTE0MWY2NGE2MGVlOWIzMmVjMzI0Mzk2NTk5MGYyYzFjNTA2ZjMwZjUzYWJh

Center for Sustainable Systems, University of Michigan. (2024, October). Hydrogen Factsheet [Pub.No. CSS23-07]. Retrieved March 18, 2025, from https://css.umich.edu/sites/default/files/2024-10/Hydrogen_CSS23-07.pdf

Chai, W. S., Bao, Y., Jin, P., Tang, G., & Zhou, L. (2021). A review on ammonia, ammonia-hydrogen and ammonia-methane fuels. *Renewable and Sustainable Energy Reviews*, *147*, 111254. https://doi.org/https://doi.org/10.1016/j.rser.2021.111254

Charrier, B., Constans, J., Cousteau, J.-Y., Daïf, A., Malavard, L., & Quinio, J.-L. (1985). Fondation Cousteau and windship propulsion 1980 – 1985 system Cousteau - Pechiney. *Journal of Wind Engineering and Industrial Aerodynamics*, *20*(1), 39–60. https://doi.org/https://doi.org/10.1016/0167-6105(85)90011-X

Chatterjee, S., Parsapur, R. K., & Huang, K.-W. (2021). Limitations of Ammonia as a Hydrogen Energy Carrier for the Transportation Sector [Publisher: American Chemical Society]. *ACS Energy Letters*, *6*(12), 4390–4394. https://doi.org/10.1021/acsenergylett.1c02189

Cheliotis, M., Boulougouris, E., Trivyza, N. L., Theotokatos, G., Livanos, G., Mantalos, G., Stubos, A., Stamatakis, E., & Venetsanos, A. (2021). Review on the Safe Use of Ammonia Fuel Cells in the Maritime Industry [Number: 11 Publisher: Multidisciplinary Digital Publishing Institute]. *Energies*, *14*(11), 3023. https://doi.org/10.3390/en14113023

Chica, M., Hermann, R. R., & Lin, N. (2023). Adopting different wind-assisted ship propulsion technologies as fleet retrofit: An agent-based modeling approach. *Technological Forecasting and Social Change*, *192*, 122559. https://doi.org/https://doi.org/10.1016/j.techfore.2023.122559

Climate Change Connection. (2020, June). CO2 equivalents. Retrieved May 21, 2025, from https://climatechangeconnection.org/emissions/co2-equivalents/

Conoship International. (n.d.). eConowind unit - Conoship International Ship Design. Retrieved May 6, 2025, from https://www.conoship.com/portfolio-item/e-conowind-unit/

De Kwant, J. (2021, August). *Design implication and performance assessment of iron fuelled ships* [Master's thesis, Delft University of Technology]. Retrieved March 24, 2025, from https://resolver.tudelft.nl/uuid:966ab159-1fae-463f-a53c-b7b2d42d3690

Deutsche Forschungsgemeinschaft e. V. (n.d.). Research Vessels | SONNE. Retrieved April 10, 2025, from https://www.portal-forschungsschiffe.de/en/vessels-sonne.html

Diab, F., Lan, H., & Ali, S. (2016). Novel comparison study between the hybrid renewable energy systems on land and on ship. *Renewable and Sustainable Energy Reviews*, *63*, 452–463. https://doi.org/https://doi.org/10.1016/j.rser.2016.05.053

DLR. (2025, February). DLR awards contract for new research ship to Lloyd Werft. Retrieved April 16, 2025, from https://www.dlr.de/en/latest/news/2025/dlr-awards-contract-for-new-research-ship-to-lloyd-werft

DNV. (2022a). *Alternative Fuels for Containerships - LNG, Methanol Extended, Ammonia* (tech. rep.). Retrieved February 28, 2025, from https://www.dnv.com/maritime/publications/alternative-fuels-for-containerships-methanol-and-ammonia-download/

DNV. (2022b). *Hydrogen Forecast to 2050: Energy Transition Outlook 2022* (tech. rep.). DNV. Høvik, Norway. Retrieved May 19, 2025, from https://aben.com.br/wp-content/uploads/2022/06/DNV_Hydrogen_Report_2022_Highres_single1.pdf

DNV. (2023, April). Methanol as fuel heads for the mainstream in shipping. Retrieved February 27, 2025, from https://www.dnv.com/expert-story/maritime-impact/Methanol-as-fuel-heads-for-the-mainstream-in-shipping/

DNV. (2024). Rules for Classification of Ships. Retrieved April 14, 2025, from https://standards.dnv.com/explorer/documents

DNV. (2025a, February). Rising LNG demand: Overcoming bunkering challenges. Retrieved March 21, 2025, from https://www.dnv.com/expert-story/maritime-impact/rising-lng-demand-overcoming-bunkering-challenges/

DNV. (2025b, April). IMO MEPC 83: New GHG requirements approved. Retrieved May 23, 2025, from https://www.dnv.com/news/imo-mepc-83-ghg-requirements-approved-taking-effect-from-2028/

DNV GL. (2019, June). *Assessment of Selected Alternative Fuels and Technologies* (tech. rep.).

Duckworth, R. (1985). The application of elevated sails (kites) for fuel saving auxiliary propulsion of commercial vessels. *Journal of Wind Engineering and Industrial Aerodynamics*, *20*(1), 297–315. https://doi.org/https://doi.org/10.1016/0167-6105(85)90023-6

Duran, K. (2025, January). Shipyard Selection Begins for Hydrogen-Hybrid Coastal Class Research Vessel | Scripps Institution of Oceanography. Retrieved February 19, 2025, from https://scripps.ucsd.edu/news/shipyard-selection-begins-hydrogen-hybrid-coastal-class-research-vessel

Econowind. (n.d.-a). Chemship | Client story. Retrieved March 27, 2025, from https://econowind.nl/client-stories/chemship/

Econowind. (n.d.-b). Econowind. Retrieved March 27, 2025, from https://econowind.nl/

Econowind. (n.d.-c). Why wind? Retrieved March 27, 2025, from https://econowind.nl/why-wind/

Ellis, J., & Tanneberger, K. (2015, December). *Study on the use of ethyl and methyl alcohol as alternative fuels in shipping* (tech. rep.). European Maritime Safety Agency. Retrieved February 27, 2025, from https://eibip.eu/wp-content/uploads/2018/01/Study-on-the-use-of-ethyl-and-methyl-alcohol-as-alternative-fuels.pdf

EMSA. (2023, November). *Guidance on the Safety of Battery Energy Storage Systems on board ships* (tech. rep.). European Maritime Safety Agency. Retrieved April 7, 2025, from https://www.emsa.europa.eu/electrification/bess.html

Eurofleets. (n.d.). RV AEGAEO. Retrieved September 22, 2025, from https://www.eurofleets.eu/vessel/rv-aegaeo/

European Central Bank. (2025a). Euro exchange rates charts - US Dollar. Retrieved April 9, 2025, from https://www.ecb.europa.eu/stats/policy_and_exchange_rates/euro_reference_exchange_rates/html/eurofxref-graph-usd.en.html

European Central Bank. (2025b, July). Long-term interest rate for convergence purposes - 10 years maturity, denominated in Euro - Euro area 20 (fixed composition) as of 1 January 2023, Euro area 20 (fixed composition), Monthly. Retrieved July 18, 2025, from https://data.ecb.europa.eu/data/datasets/IRS/IRS.M.I9.L.L40.CI.0000.EUR.N.Z

European Comission. (n.d.-a). About the EU ETS. Retrieved March 6, 2025, from https://climate.ec.europa.eu/eu-action/eu-emissions-trading-system-eu-ets/about-eu-ets_en

European Comission. (n.d.-b). Decarbonising maritime transport – FuelEU Maritime. Retrieved March 20, 2025, from https://transport.ec.europa.eu/transport-modes/maritime/decarbonising-maritime-transport-fueleu-maritime_en

European Comission. (n.d.-c). ETS2: Buildings, road transport and additional sectors. Retrieved May 20, 2025, from https://climate.ec.europa.eu/eu-action/eu-emissions-trading-system-eu-ets/ets2-buildings-road-transport-and-additional-sectors_en

European Parliament. (2015, April). Regulation (EU) 2015/757 of the European Parliament and of the Council of 29 April 2015 on the monitoring, reporting and verification of carbon dioxide emissions from maritime transport, and amending Directive 2009/16/EC. Retrieved February 17, 2025, from https://eur-lex.europa.eu/legal-content/EN/TXT/PDF/?uri=CELEX:32015R0757

European Parliament. (2018, December). Directive (EU) 2018/2001 of the European Parliament and of the council of 11 December 2018 on the promotion of the use of energy from renewable sources. Retrieved April 6, 2025, from https://eur-lex.europa.eu/eli/dir/2018/2001/oj/eng

European Parliament & European Council. (2023a). Regulation (EU) 2023/1805 of the European Parliament and of the Council of 13 September 2023 on the use of renewable and low-carbon fuels in maritime transport, and amending Directive 2009/16/EC. Retrieved March 20, 2025, from https://eur-lex.europa.eu/legal-content/EN/TXT/PDF/?uri=CELEX:32023R1805

European Parliament & European Council. (2023b, May). Directive (EU) 2023/959 of the European Parliament and of the Council of 10 May 2023 amending Directive 2003/87/EC establishing a system for greenhouse gas emission allowance trading within the Union and Decision (EU) 2015/1814 concerning the establishment and operation of a market stability reserve for the Union greenhouse gas emission trading system. Retrieved February 17, 2025, from https://eur-lex.europa.eu/legal-content/EN/TXT/PDF/?uri=CELEX:32023L0959

European Parliament & European Council. (2023c, September). Regulation (EU) 2023/1804 of the European Parliament and of the Council of 13 September 2023 on the deployment of alternative fuels infrastructure, and repealing Directive 2014/94/EU.

Federal Ministry for the Environment, Nature Conservations, and Nuclear Safety, German Environmental Agency, Environmental Label Jury, & RAL gGmbH. (2021, January). Blue Angel - The German Ecolable - Eco-Friendly Ship Design. Retrieved April 14, 2025, from https://produktinfo.blauer-engel.de/uploads/criteriafile/en/DE-UZ%20141-202101-en-criteria-V5.pdf

Federal Ministry of Research, Technology and Space. (2022, June). Research vessel SONNE. Retrieved June 2, 2025, from https://www.fona.de/en/measures/research-infrastructures/research-vessels/research-vessel-sonne.php

Fr. Fassmer GmbH & Co.KG. (n.d.-a). 35m Fishery Research Vessel (UTHÖRN). Retrieved November 27, 2024, from https://www.fassmer.de/en/shipbuilding/products/research-and-survey-vessels/35m-fishery-research-vessel

Fr. Fassmer GmbH & Co.KG. (n.d.-b). 75 m Survey-, Wrecksearch- and Research Vessel. Retrieved November 27, 2024, from https://www.fassmer.de/fileadmin/user_upload/1_Schiffbau/20_03_SB_SB_ATAIR_EN_web.pdf

Fu, Z., Lu, L., Zhang, C., Xu, Q., Zhang, X., Gao, Z., & Li, J. (2023). Fuel cell and hydrogen in maritime application: A review on aspects of technology, cost and regulations. *Sustainable Energy Technologies and Assessments*, *57*, 103181. https://doi.org/10.1016/j.seta.2023.103181

Fun-sang Cepeda, M. A., Pereira, N. N., Kahn, S., & Caprace, J.-D. (2019). A review of the use of LNG versus HFO in maritime industry. *Marine Systems & Ocean Technology*, *14*(2), 75–84. https://doi.org/10.1007/s40868-019-00059-y

Gao, Q., Yuan, R., Ertugrul, N., Ding, B., Hayward, J. A., & Li, Y. (2023). Analysis of energy variability and costs for offshore wind and hybrid power unit with equivalent energy storage system. *Applied Energy*, *342*, 121192. https://doi.org/https://doi.org/10.1016/j.apenergy.2023.121192

Gaspar, H. M., Brett, P. O., Erikstad, S. O., & Ross, A. M. (2015). Quantifying value robustness of OSV designs taking into consideration medium to long term stakeholders' expectations, 247–259.

Hahn, E. (2024, April). Liquefied Petroleum Gas LPG in Gas - LP Gas: What is Liquefied Petroleum Gas - Properties. Retrieved April 1, 2025, from https://www.elgas.com.au/elgas-knowledge-hub/residential-lpg/lpg-gag-properties-chemical-physical/

Hansson, J., Brynolf, S., Fridell, E., & Lehtveer, M. (2020). The Potential Role of Ammonia as Marine Fuel - Based on Energy Systems Modeling and Multi-Criteria Decision Analysis. *Sustainability*, *12*(8). https://doi.org/10.3390/su12083265

Holtrop, J., & Mennen, G. (1982). An approximate power prediction method [Publisher: SAGE Publications]. *International Shipbuilding Progress*, *29*(335), 166–170. Retrieved September 29, 2025, from https://www.boatdesign.net/attachments/holtrop-approximate-1982-pdf.144448/

IEA. (2019, June). *The Future of Hydrogen - Seizing today's opportunities* (Report prepared by the IEA for the G20, Japan). IEA. Retrieved April 6, 2025, from https://iea.blob.core.windows.net/assets/9e3a3493-b9a6-4b7d-b499-7ca48e357561/The_Future_of_Hydrogen.pdf

IEA. (2024a). *Global Hydrogen Review 2024* (tech. rep.). IEA. Paris. Retrieved March 18, 2025, from https://www.iea.org/reports/global-hydrogen-review-2024

IEA. (2024b, September). Weighted average net margins of renewable energy companies, large utilities and oil majors, Q1-Q4 2022 and Q1-Q3 2023 – Charts – Data & Statistics - IEA [Licence: CC BY 4.0 Place: Paris]. Retrieved April 7, 2025, from https://www.iea.org/data-and-statistics/charts/weighted-average-net-margins-of-renewable-energy-companies-large-utilities-and-oil-majors-q1-q4-2022-and-q1-q3-2023

Ifremer. (2020, February). Detailed characteristics. Retrieved September 22, 2025, from https://www.flotteoceanographique.fr/en/Facilities/Vessels-Deep-water-submersible-vehicles-and-Mobile-equipments/Deep-sea-vessels/Pourquoi-pas/Detailed-characteristics

IMO. (n.d.-a). International Code for Ships Operating in Polar Waters (Polar Code). Retrieved April 11, 2025, from https://www.imo.org/en/ourwork/safety/pages/polar-code.aspx

IMO. (n.d.-b). Kite: GreenVoyage2050 [Place: London]. Retrieved May 6, 2025, from https://greenvoyage2050.imo.org/technology/kite/

IMO. (1974). *International Convention for the Safety of Life at Sea* (tech. rep.).

IMO. (1978, February). *International Convention for the Prevention of Pullution from Ships* (tech. rep.). London.

IMO. (1997). *MARPOL Annex VI: Prevention of Air Pollution from Ships* (tech. rep.). London.

IMO. (2016). *International Code of Safety for Ship Using Gases or Other Low-flashpoint Fuels* (tech. rep.). Retrieved March 4, 2025, from https://www.imo.org/en/ourwork/safety/pages/igf-code.aspx

IMO. (2017a, January). International Code for Ships Operating in Polar Water (Polar Code).

IMO. (2017b, June). IGF Code - International Code of Safety for Ships Using Gases or Other Low-Flashpoint Fuels.

Institute of Marine Research. (2024, October). Dr. Fridtjof Nansen. Retrieved September 22, 2025, from https://www.hi.no/en/hi/about-us/facilities/our-vessels/dr.-fridtjof-nansen

Interreg. (n.d.). Our fleet, Interreg VB North Sea Region Programme. Retrieved April 7, 2025, from https://northsearegion.eu/wasp/our-fleet/

IOR energy Pty Ltd. (2010, August). List of common conversion factors (Engineering conversion factors) - IOR Energy Pty Ltd. Retrieved March 31, 2025, from https://web.archive.org/web/20100825042309/http://www.ior.com.au/ecflist.html

IRENA. (2024a). *Renewable power generation costs in 2023* (tech. rep.). International Renewable Energy Agency. Abu Dhabi. Retrieved April 7, 2025, from https://www.irena.org/-/media/Files/IRENA/Agency/Publication/2024/Sep/IRENA_Renewable_power_generation_costs_in_2023.pdf

IRENA. (2024b). *Shaping sustainable international hydrogen value chains* (tech. rep.) (ISBN: 978-92-9260-616-9). International Renewable Energy Agency. Abu Dhabi. Retrieved April 6, 2025, from https://www.irena.org/-/media/Files/IRENA/Agency/Publication/2024/Sep/IRENA_Shaping_sustainable_hydrogen_value_chains_2024.pdf

Jacobson, M. Z., Delucchi, M. A., Bazouin, G., Dvorak, M. J., Arghandeh, R., Bauer, Z. A. F., Cotte, A., Moor, G. M. T. H. d., Goldner, E. G., Heier, C., Holmes, R. T., Hughes, S. A., Jin, L., Kapadia, M., Menon, C., Mullendore, S. A., Paris, E. M., Provost, G. A., Romano, A. R., … Yeskoo, T. W. (2016). A 100% wind, water, sunlight (WWS) all-sector energy plan for Washington State. *Renewable Energy*, *86*, 75–88. https://doi.org/https://doi.org/10.1016/j.renene.2015.08.003

Jactio. (2023, September). The cost of structural steel per kg in 2023 [Section: Sourcing]. Retrieved May 22, 2025, from https://jactio.com/en/the-cost-of-structural-steel-per-kg/

Jann, T. (2022). Methanol treibt die „Uthörn" an. *Täglicher Hafenbericht*. Retrieved May 8, 2025, from https://www.thb.info/rubriken/schiffbau/detail/news/methanol-treibt-die-uthoern-an.html

Kang, S., Boshell, F., Goeppert, A., Prakash, S. G., Landälv, I., & Saygin, D. (2021). *Innovation outlook: Renewable methanol* (D. Gielen & G. Dolan, Eds.). International Renewable Energy Agency.

Karatuğ, Ç., & Durmuşoğlu, Y. (2020). Design of a solar photovoltaic system for a Ro-Ro ship and estimation of performance analysis: A case study. *Solar Energy*, *207*, 1259–1268. https://doi.org/https://doi.org/10.1016/j.solener.2020.07.037

Kaya, C. (2024). Sodium Borohydride (NaBH4) as a Maritime Transportation Fuel. *Hydrogen*, *5*(3), 540–558. https://doi.org/10.3390/hydrogen5030030

Kayfeci, M., Keçebaş, A., & Bayat, M. (2019). *Solar Hydrogen Production* (F. Calise, M. D. D'Accadia, M. Santarelli, A. Lanzini, & D. Ferrero, Eds.). Academic Press. https://doi.org/https://doi.org/10.1016/B978-0-12-814853-2.00003-5

Kerlen, H. (1985). *Über den Einfluß der Völligkeit auf die Rumpfstahlkosten von Frachtschiffen* [Doctoral dissertation, Hamburg University of Technology]. https://doi.org/10.15480/882.879

Kisjes, A. S. (2017). *Wind Propulsion for Merchant Vessels* [Master's thesis, Delft University of Technology]. Retrieved January 6, 2025, from https://resolver.tudelft.nl/uuid:a681c8e6-552e-45a1-8657-893123a8e06b

Klebanoff, L. E., Caughlan, S. A., Madsen, R. T., Conard, C. J., Leach, T. S., & Appelgate, T. B. (2021). Comparative study of a hybrid research vessel utilizing batteries or hydrogen fuel cells. *International Journal of Hydrogen Energy*, *46*(76), 38051–38072. https://doi.org/10.1016/j.ijhydene.2021.09.047

Klein Woud, H., & Stapersma, D. (2016, February). *Selected chapters of Design of Auxiliary Systems, Shafting and Flexible Mounting* (Selected chapters) [Course reader MT44050]. Delft University of Technology.

Klein Woud, H., & Stapersma, D. (2019). *Design of Propulsion and Electric Power Generation Systems* (Revised Edition). Institute of Marine Engineering, Science & Technology.

Lange, C. L. (2024). *Assessing Fuel Efficiency: Hydrodynamic Design Investigation and Operational Considerations in Wind-Assisted Cruise Ships* [Master's thesis, Delft University of Technology]. Retrieved January 6, 2025, from https://resolver.tudelft.nl/uuid:910649ec-0684-4b6a-b7ae-c959cb48da8c

Laursen, R., Barcarolo, D., Patel, H., Dowling, M., Penfold, M., Faber, J., Király, J., van der Veen, R., Pang, E., & van Grinsven, A. (2023, September). *Update on potential of Biofuels in Shipping* (tech. rep.). European Maritime Safety Agency. Retrieved March 24, 2025, from https://emsa.europa.eu/publications/reports/item/4834-update-on-potential-of-biofuels-for-shipping.html

Law, A. M. (2015). *Simulation Modeling and Analysis* (5th). McGraw-Hill Education. Retrieved July 24, 2025, from https://industri.fatek.unpatti.ac.id/wp-content/uploads/2019/03/108-Simulation-Modeling-and-Analysis-Averill-M.-Law-Edisi-5-2014.pdf

Lempert, R. J., Popper, S. W., & Bankes, S. C. (2003). *Shaping the Next One Hundred Years: New Methods for Quantitative, Long-Term Policy Analysis* (1st ed.). RAND Corporation. Retrieved May 20, 2025, from http://www.jstor.org/stable/10.7249/mr1626rpc

Lloyd's Register. (2023, April). Guidance Notes on the Installation of Fuel Cells on Ships. Retrieved April 15, 2025, from https://r4s.oneocean.com/regulation/document/264463

Lloyd's Register. (2024a, January). Guidance Notes on Wind Assisted Propulsion Systems. Retrieved April 14, 2025, from https://r4s.oneocean.com/regulation/document/264509

Lloyd's Register. (2024b, July). Guidance Notes for Methyl and Ethyl Alcohol Fuels. Retrieved April 15, 2025, from https://r4s.oneocean.com/regulation/document/264463

Lloyd's Register. (2024c, July). Rules and Regulations for the Classification of Ships. Retrieved April 14, 2025, from https://r4s.oneocean.com/regulation/document/264481

Lloyd's Register. (2024d, July). Rules and Regulations for the Classification of Ships using Gases or other Low-flashpoint Fuels. Retrieved April 14, 2025, from https://r4s.oneocean.com/regulation/document/264449

Lloyd's Register. (2025, January). Guidance Notes for Liquid Hydrogen Systems. Retrieved April 15, 2025, from https://r4s.oneocean.com/regulation/page/287774

Lu, R., & Ringsberg, J. W. (2020). Ship energy performance study of three wind-assisted ship propulsion technologies including a parametric study of the Flettner rotor technology [Publisher: Taylor & Francis _eprint: https://doi.org/10.1080/17445302.2019.1612544]. *Ships and Offshore Structures*, *15*(3), 249–258. https://doi.org/10.1080/17445302.2019.1612544

Madsen, R., Klebanoff, L., Caughlan, S., Pratt, J., Leach, T., Appelgate, T., Kelety, S., Wintervoll, H.-C., Haugom, G., Teo, A., & Ghosh, S. (2020). Feasibility of the Zero-V: A zero-emissions hydrogen

fuel-cell coastal research vessel. *International Journal of Hydrogen Energy*, *45*(46), 25328–25343. https://doi.org/10.1016/j.ijhydene.2020.06.019

Maersk. (2024, November). Maersk completes first large container vessel conversion to dual-fuel methanol engine. Retrieved August 4, 2025, from https://www.maersk.com/news/articles/2024/11/18/maersk-completes-first-large-container-vessel-conversion-to-dual-fuel-methanol-engine

MAN Energy Solutions. (n.d.-a). *Advancing Methanol Propulsion* (tech. rep.). Augsburg, Germany.

MAN Energy Solutions. (n.d.-b). *Hydrogen in Shipping* (tech. rep.). Augsburg, Germany. Retrieved March 12, 2025, from https://www.man-es.com/campaigns/download-Q1-2025/Download/hydrogen-in-shipping/faffa612-4edc-4a2a-a5f9-df89c632a431/Future-Fuels-Hydrogen/A1EDD4298E8D602D68E87E374A2EB7BD49C846FF/?cid=3708b9d4-b688-48a6-9840-8f374e558ce9

MAN Energy Solutions. (n.d.-c). LPG. Retrieved April 1, 2025, from https://www.man-es.com/marine/applications/lpg

MAN Energy Solutions. (n.d.-d). *A Maritime Energy Transition* (tech. rep.). Augsburg, Germany; Copenhagen, Denmark. Retrieved March 12, 2025, from https://www.man-es.com/campaigns/download-Q1-2025/Download/a-maritime-energy-transition/bee9b06b-c251-49b5-9d4c-ddd7f9cd35c0/Maritime-Energy-Transition/A1EDD4298E8D602D68E87E374A2EB7BD49C846FF/?cid=3708b9d4-b688-48a6-9840-8f374e558ce9

MAN Energy Solutions. (n.d.-e). *Methanol in Shipping* (tech. rep.). Augsburg, Germany. Retrieved March 12, 2025, from https://www.man-es.com/campaigns/download-Q1-2025/Download/methanol-in-shipping/d8358bd6-c66e-4dce-8656-4237259c5338/Methanol-Paper-SF/A1EDD4298E8D602D68E87E374A2EB7BD49C846FF/?cid=3708b9d4-b688-48a6-9840-8f374e558ce9

MAN Energy Solutions. (2019, September). *Batteries on board ocean-going vessels* (tech. rep.). Copenhagen, Denmark. Retrieved March 12, 2025, from https://www.man-es.com/docs/default-source/marine/tools/batteries-on-board-ocean-going-vessels.pdf?sfvrsn=deaa76b8_16

Marchau, V. A. W. J., Walker, W. E., Bloemen, P. J. T. M., & Popper, S. W. (Eds.). (2019, April). *Decision Making under Deep Uncertainty - From Theory to Practice* (1st ed.). Springer Cham. Retrieved April 16, 2025, from https://doi.org/10.1007/978-3-030-05252-2

Meinders, L. (2025, March). Re: Anfrage zu Missionsprofilen; Masterarbeit Entkarbonisierung von Forschungsschiffen [Email].

Methanol Institute. (n.d.). Methanol - Technical Data Sheet. Retrieved February 28, 2025, from https://www.methanol.org/wp-content/uploads/2016/06/Methanol-Technical-Data-Sheet.pdf

Methanol Institute. (2025). Bunker, Storage and Storage + Bunkering Facilities. Retrieved April 4, 2025, from https://www.methanol.org/marine/

Moallemi, E. A., Elsawah, S., & Ryan, M. J. (2020). Robust decision making and Epoch–Era analysis: A comparison of two robustness frameworks for decision-making under uncertainty. *Technological Forecasting and Social Change*, *151*, 119797. https://doi.org/https://doi.org/10.1016/j.techfore.2019.119797

Molland, A. F. (2008). *The maritime engineering reference book : A guide to ship design, construction and operation*. Amsterdam ; Boston ; London : Butterworth-Heinemann. Retrieved July 8, 2025, from https://www.sciencedirect.com/book/9780750689878/the-maritime-engineering-reference-book

Mondejar, M. E., Andreasen, J. G., Pierobon, L., Larsen, U., Thern, M., & Haglind, F. (2018). A review of the use of organic Rankine cycle power systems for maritime applications. *Renewable and Sustainable Energy Reviews*, *91*, 126–151. https://doi.org/https://doi.org/10.1016/j.rser.2018.03.074

Muir, S. S., & Yao, X. (2011). Progress in sodium borohydride as a hydrogen storage material: Development of hydrolysis catalysts and reaction systems. *International Journal of Hydrogen Energy*, *36*(10), 5983–5997. https://doi.org/https://doi.org/10.1016/j.ijhydene.2011.02.032

Mylonopoulos, F., Durgaprasad, S., Coraddu, A., & Polinder, H. (2024). Lifetime design, operation, and cost analysis for the energy system of a retrofitted cargo vessel with fuel cells and batteries. *International Journal of Hydrogen Energy*, *91*, 1262–1273. https://doi.org/https://doi.org/10.1016/j.ijhydene.2024.10.235

Nederland Maritiem Land. (2024, May). Greening the Dutch State Fleet - Nederland Maritiem Land. Retrieved April 14, 2025, from https://maritiemland.nl/nieuws/greening-the-dutch-state-fleet/

Nieuwejaar, P., Mazauric, V., Betzler, C., Carapuço, M., Cattrijsse, A., Coren, F., Danobeitia, J., Day, C., Fitzgerald, A., Florescu, S., Ignacio Diaz, J., Klages, M., Koning, E., Lefort, O., Magnifico, G., Mikelborg, Ø., & Naudts, L. (2019, November). *Next Generation European Research Vessels: Current Status and Foreseeable Evolution* (P. Kellett, C. Viegas, B. Alexander, J. Coopman, & A. Muniz Piniella, Eds.) [Publication Title: EPIC3Ostend, Belgium, European Marine Board, 140 p., ISBN: 978-94-92043-79-5]. European Marine Board. Retrieved March 4, 2025, from https://epic.awi.de/id/eprint/50523/

OceanWings. (2024a). History - OceanWings. Retrieved April 7, 2025, from https://www.oceanwings.com/history

OceanWings. (2024b). Lowerable Fixed Wingsail (OW RE). Retrieved April 7, 2025, from https://www.oceanwings.com/product/ow-lf-lowerable-fixed-wingsail

OceanWings. (2024c). Rigid Tiltable Wingsail (OW RT). Retrieved April 7, 2025, from https://www.oceanwings.com/product/ow-rt-rigid-tiltable-wingsail

Papanikolaou, A. (2014, September). *Ship Design Methodologies of Preliminary Design* (1st ed.). Springer Dordrecht. https://doi.org/10.1007/978-94-017-8751-2

Pospiech, P. (2019, April). Fertigstellung der ATAIR im Plan. Retrieved June 2, 2025, from https://veus-shipping.com/2019/04/fertigstellung-der-atair-im-plan/

PowerCell Group. (2023, March). World's Largest Marine Fuel Cell Systems | PowerCell Group. Retrieved April 2, 2025, from https://powercellgroup.com/worlds-largest-marine-fuel-cell-systems/

PowerCell Group. (2025). *Marine System 225* (Product Sheet). PowerCell Group. Retrieved April 2, 2025, from https://25513287.fs1.hubspotusercontent-eu1.net/hubfs/25513287/Marine%20System%20225%20Data%20Sheet.pdf?utm_medium=email&_hsenc=p2ANqtz-9KInfmddklEZopAAe_AkkEqPX4Aiia5ncbws0ug8VIgvfUmb90juztIXNkZTT83gC-NXr2kR72t-ybrUWVjwMAraG_DzNQhRsWLD0oSf2zIUTsgSU&_hsmi=88671217&utm_content=88671217&utm_source=hs_automation

Riaz, A., Zahedi, G., & Klemeš, J. J. (2013). A review of cleaner production methods for the manufacture of methanol. *Journal of Cleaner Production*, *57*, 19–37. https://doi.org/10.1016/j.jclepro.2013.06.017

Ryste, J. A. (2019, September). *Comparison of Alternative Marine Fuels* (tech. rep. No. 2019-09-25). SEA-LNG and DNV GL. Høvik, Norway. Retrieved April 1, 2025, from https://sea-lng.org/wp-content/uploads/2020/04/Alternative-Marine-Fuels-Study_final_report_25.09.19.pdf

Sazali, N. (2020). Emerging technologies by hydrogen: A review. *International Journal of Hydrogen Energy*, *45*(38), 18753–18771. https://doi.org/https://doi.org/10.1016/j.ijhydene.2020.05.021

Scherpenhuijsen Rom, E. P. W. (2023). *Iron Powder as a fuel on Service Vessels* [Master's thesis]. Retrieved March 6, 2025, from https://resolver.tudelft.nl/uuid:2e46edbd-7a41-4841-a341-1a069b65d48f

Schneekluth, H. (1985). *Entwerfen von Schiffen: Vorlesungen* (3rd ed.). Koehler.

Schneekluth, H. (1988). *Hydromechanik zum Schiffsentwurf: Vorlesungen* (3rd ed.). Koehler.

Schneekluth, H., & Bertram, V. (1998). *Ship Design for Efficiency and Economy* (Second edition). Butterworth-Heinemann. https://doi.org/https://doi.org/10.1016/B978-075064133-3/50001-3

Schreuder, W., Slootweg, J. C., & Zwaan, B. v. d. (2025). Techno-economic assessment of low-carbon ammonia as fuel for the maritime sector. *Applications in Energy and Combustion Science*, *22*, 12. https://doi.org/https://doi.org/10.1016/j.jaecs.2025.100330

SEA-LNG. (n.d.). Availability. Retrieved March 21, 2025, from https://sea-lng.org/why-lng/availability/

SEA-LNG. (2025). Rotterdam Marine Fuel LNG Bunker prices. Retrieved April 7, 2025, from https://sea-lng.org/lng-bunker-fuel-prices/rotterdam-marine-fuel-lng-bunker-prices/

Seatech Engineering. (2017, June). Scientific Vessels. Retrieved June 2, 2025, from https://www.seatech.com.pl/scientific-vessels/

Seddiek, I. S., & Ammar, N. R. (2023). Technical and eco-environmental analysis of blue/green ammonia-fueled RO/RO ships. *Transportation Research Part D: Transport and Environment*, *114*, 103547. https://doi.org/https://doi.org/10.1016/j.trd.2022.103547

Shell Deutschland Oil GmbH. (2019). *Shell LNG Study - Liquefied Natural Gas - New Energy for Ships and Trucks?* (Tech. rep.). Shell Deutschland Oil GmbH. Retrieved March 21, 2025, from https:

//www.shell.de/about-us/newsroom/shell-lng-study/_jcr_content/root/main/containersection-0/simple/call_to_action/links/item1.stream/0/8c14ea6b6b92b887fba9026055a12cd0e9b817779cec881fdf3910537b5db666/lng-study-uk-einzelseiten.pdf
ShipFC. (2020). About ShipFC. Retrieved April 6, 2025, from https://shipfc.eu/about/
ShipFC. (2025, February). Temporary Suspension for ShipFC Project - Zpirit. Retrieved April 6, 2025, from https://shipfc.eu/temporary-suspension-for-shipfc-project/
Sigma-Aldrich. (2025, March). Safety Data Sheet according to Regulation (EC) No. 1907/2006. Retrieved March 17, 2025, from https://www.sigmaaldrich.com/DE/en/sds/aldrich/452882?userType=undefined
SkySails Marine. (n.d.). SkySails Marine. Retrieved March 26, 2025, from https://skysails-marine.com/
SkySails Power GmbH. (n.d.-a). How Power Kites Work. Retrieved March 27, 2025, from https://skysails-power.com/how-power-kites-work/
SkySails Power GmbH. (n.d.-b). Onshore Wind Power has a New Face. Retrieved May 6, 2025, from https://skysails-power.com/onshore-unit-pn-14/
SkySails Power GmbH. (2024). Skysails Power - Airborne wind energy. From Germany to the world. - Breakthrough in Airborne Wind Energy: Worldwide First Validated Performance Curve, 2. Retrieved March 26, 2025, from https://skysails-power.com/wp-content/uploads/sites/6/2024/03/Press-Release-SkySails-Breakthrough-in-Airborne-Wind-Energy.pdf
Smeets, M. (2024). *VentoFoil Adoption Model* [Master's thesis, Delft University of Technology]. Retrieved January 6, 2025, from https://repository.tudelft.nl/record/uuid:61556e5d-987c-46aa-9c3c-4b7bfe74f339
S&P Gobal. (2025). Platts global bunker fuel cost calculator - Monthly Average Cost, February 2025. Retrieved April 4, 2025, from https://www.spglobal.com/commodityinsights/PlattsContent/_assets/_files/downloads/053024-interactive-platts-global-bunker-fuel-cost-calculator.html
Stapersma, D. (2010, January). *Part I: Diesel engines A - Performance analysis and turbocharging* (8th, Vol. 1) [Lecture Notes WB4408A]. NLDA & Delft UT.
Statista. (n.d.). Global methanol production 2022. Retrieved February 27, 2025, from https://www.statista.com/statistics/1323406/methanol-production-worldwide/
Streng, J. E. (2021, April). *Alternative Energy Carriers in Naval Vessels* [Master's thesis, Delft University of Technology]. Retrieved January 5, 2025, from https://resolver.tudelft.nl/uuid:47e02b82-5a0f-4eba-8092-f2e10b5c6845
Suy, X. G. (2022, January). *Technical and economical feasibility of zero-emission walk to work vessels* [Master's thesis, Delft University of Technology]. Retrieved January 5, 2025, from https://resolver.tudelft.nl/uuid:9cf2a69b-5a2a-41d8-9daf-d62d26b25931
Svanberg, M., Ellis, J., Lundgren, J., & Landälv, I. (2018). Renewable methanol as a fuel for the shipping industry. *Renewable and Sustainable Energy Reviews*, *94*, 1217–1228. https://doi.org/10.1016/j.rser.2018.06.058
Swedish University of Agricultural Sciences. (2024, February). Ship specifications - Svea. Retrieved March 31, 2025, from https://www.slu.se/en/Collaborative-Centres-and-Projects/research-vessel-svea/ship-specifications/
Taen, J., Otheguy, M., & Hekkenberg, R. (2016). Energy Efficient Maritime Accommodations.
Taphorn, N. (2024, November). Industrialization of high-altidtude wind energy. Retrieved May 6, 2025, from https://windenergietage.de/2024/wp-content/uploads/sites/9/2018/01/32WET07_F22_1000_SkySails-Power-GmbH.pdf
Terün, K. (2020, February). *Assessing Alternative Fuel Types for ULCVs in Face of Uncertainty* [Master's thesis, Delft University of Technology]. Retrieved January 5, 2025, from https://resolver.tudelft.nl/uuid:84f29960-87fd-427b-bc9d-96b46f4bfe3c
Tian, Z., Wang, Y., Zhen, X., & Liu, Z. (2022). The effect of methanol production and application in internal combustion engines on emissions in the context of carbon neutrality: A review. *Fuel*, *320*, 123902. https://doi.org/10.1016/j.fuel.2022.123902
TNO. (2020). *Power-2-Fuel Cost Analysis* (tech. rep.). TNO. Retrieved April 7, 2025, from https://smartport.nl/wp-content/uploads/2020/09/Cost-Analysis-Power-2-Fuel_def_2020.pdf
Traut, M., Gilbert, P., Walsh, C., Bows, A., Filippone, A., Stansby, P., & Wood, R. (2014). Propulsive power contribution of a kite and a Flettner rotor on selected shipping routes. *Applied Energy*, *113*, 362–372. https://doi.org/https://doi.org/10.1016/j.apenergy.2013.07.026

TU/e. (n.d.). Iron Power. Retrieved March 25, 2025, from https://www.tue.nl/en/research/institutes/eindhoven-institute-for-renewable-energy-systems/iron-power

University of Gdansk. (2023, October). Research vessel Oceanograf. Retrieved September 22, 2025, from https://offshore.ug.edu.pl/en/research-vessel-oceanograf/

University of Gothenburg. (2024, November). R/V Skagerak | Ship facts | University of Gothenburg. Retrieved March 31, 2025, from https://www.gu.se/en/skagerak/ship-facts

Valera-Medina, A., Xiao, H., Owen-Jones, M., David, W. I. F., & Bowen, P. J. (2018). Ammonia for power. *Progress in Energy and Combustion Science*, *69*, 63–102. https://doi.org/https://doi.org/10.1016/j.pecs.2018.07.001

van Lynden, C. K. W. (2021). *Offshore Wind Installation Vessels* [Master's thesis, Delft University of Technology]. Retrieved May 13, 2025, from https://resolver.tudelft.nl/uuid:e7d96aa8-bd14-4446-8e78-1d388133c106

VesselFinder. (2025). ONEGO DEUSTO, General Cargo Ship - Schiffsdaten und aktuelle Position - IMO 9399129 - VesselFinder. Retrieved May 6, 2025, from https://www.vesselfinder.com/de/vessels/details/9399129

Viking Line. (2021, April). Test run of rotor sail on Viking Grace completed. Retrieved April 1, 2025, from https://www.vikingline.com/press-room-old/BDD4C986EDFCE9A6/

VPLP Design. (n.d.). About us. Retrieved April 7, 2025, from https://www.vplp.fr/en/about-us/

Wang, Y., Cao, Q., Liu, L., Wu, Y., Liu, H., Gu, Z., & Zhu, C. (2022). A review of low and zero carbon fuel technologies: Achieving ship carbon reduction targets. *Sustainable Energy Technologies and Assessments*, *54*, 102762. https://doi.org/https://doi.org/10.1016/j.seta.2022.102762

Wärtsilä. (2023). The Wärtsilä 32 Methanol Engine. Retrieved April 4, 2025, from https://brandhub.wartsila.com/m/13700176e818aaff/original/W32-Methanol-Brochure.pdf?utm_source=engines&utm_medium=dfengines&utm_term=w32&utm_content=brochure&utm_campaign=mp-engines-and-generating-sets-brochures

Wärtsilä. (2024a). Wärtsilä 20. Retrieved April 7, 2025, from https://brandhub.wartsila.com/m/37d4d432c0137850/original/Wartsila-20-brochure.pdf?utm_source=mcae&utm_medium=redirect&utm_term=marine&utm_content=brochure&utm_campaign=mp-engines-and-generating-sets-brochures

Wärtsilä. (2024b). Wärtsilä 25 - The power to target net zero. Retrieved April 5, 2025, from https://brandhub.wartsila.com/m/6ec1690a9bc01222/original/Wartsila-25-Brochure.pdf?utm_source=engines&utm_medium=dfengines&utm_term=w25&utm_content=brochure&utm_campaign=mp-engines-and-generating-sets-brochures

Xing, H., Stuart, C., Spence, S., & Chen, H. (2021). Alternative fuel options for low carbon maritime transportation: Pathways to 2050. *Journal of Cleaner Production*, *297*, 126651. https://doi.org/10.1016/j.jclepro.2021.126651

Yang, M., & Lam, J. S. L. (2023). Operational and economic evaluation of ammonia bunkering – Bunkering supply chain perspective. *Transportation Research Part D: Transport and Environment*, *117*, 103666. https://doi.org/https://doi.org/10.1016/j.trd.2023.103666

Yi, M. (n.d.-a). A Complete Guide to Box Plots. Retrieved September 4, 2025, from https://www.atlassian.com/data/charts/box-plot-complete-guide

Yi, M. (n.d.-b). A Complete Guide to Violin Plots. Retrieved September 4, 2025, from https://www.atlassian.com/data/charts/violin-plot-complete-guide

Zhaka, V., & Samuelsson, B. (2024). Hydrogen as fuel in the maritime sector: From production to propulsion. *Energy Reports*, *12*, 5249–5267. https://doi.org/https://doi.org/10.1016/j.egyr.2024.11.005

Zhen, X., & Wang, Y. (2015). An overview of methanol as an internal combustion engine fuel. *Renewable and Sustainable Energy Reviews*, *52*, 477–493. https://doi.org/10.1016/j.rser.2015.07.083

A

Input Parameters

Table A.1: Overview of Input Parameters used in Parametric Model.

Category	Parameter	Value	Unit	Source
	ρ	1.025	t/m³	
	K	0.039	t/m³	Schneekluth, 1985
	g	9.810	m/s²	
	N_{PoB}	60		Section 4.4.1
	v_s	12	kn	Section 4.4.1
Converter	$\varphi_{G,\,FC}$	184	kW/t	PowerCell Group, 2025
	$\varphi_{G,\,ICE\ Ammonia}$	92	kW/t	Wärtsilä, 2024b
	$\varphi_{G,\,ICE\ Hydrogen}$	50	kW/t	Stapersma, 2010
	$\varphi_{G,\,ICE\ HVO/MDO}$	150	kW/t	Wärtsilä, 2024a
	$\varphi_{G,\,ICE\ LNG}$	110	kW/t	Wärtsilä, 2024a
	$\varphi_{G,\,ICE\ Methanol}$	107	kW/t	Wärtsilä, 2023
	$\varphi_{V,\,FC}$	104	kW/m³	PowerCell Group, 2025
	$\varphi_{V,\,ICE\ Ammonia}$	52	kW/m³	Wärtsilä, 2024b
	$\varphi_{V,\,ICE\ Hydrogen}$	36	kW/m³	Stapersma, 2010
	$\varphi_{V,\,ICE\ HVO/MDO}$	97	kW/m³	Wärtsilä, 2024a
	$\varphi_{V,\,ICE\ LNG}$	87	kW/m³	Wärtsilä, 2024a
	$\varphi_{V,\,ICE\ Methanol}$	82	kW/t	Wärtsilä, 2023
Efficiencies	η_{EHR}	10	%	Mondejar et al., 2018
	η_{FC}	50	%	Section 4.4.1
	η_{ICE}	45	%	Stapersma, 2010
	$\eta_{relocation}$	50	%	Section 5.6
	η_{tw}	97	%	Section 5.3

(Continued on next page)

(Continued from previous page)

Category	Parameter	TtW	Unit	Source
	η_u	90	%	Section 5.3
	η_{WASP}	10	%	Section 3.3
Fuel	$\rho_{G,\,Ammonia}$	6 250	kWh/t	Chatterjee et al., 2021
	$\rho_{G,\,HVO}$	11 944	kWh/t	Laursen et al., 2023
	$\rho_{G,\,Hydrogen}$	33 889	kWh/t	Xing et al., 2021
	$\rho_{G,\,LNG}$	12 500	kWh/t	Shell Deutschland Oil GmbH, 2019
	$\rho_{G,\,MDO}$	12 472	kWh/t	IOR energy Pty Ltd, 2010
	$\rho_{G,\,Methanol}$	5 556	kWh/t	Zhaka and Samuelsson, 2024
	$\rho_{V,\,Ammonia}$	4 000	kWh/m³	Al-Aboosi et al., 2021
	$\rho_{V,\,HVO}$	8 889	kWh/m³	Laursen et al., 2023
	$\rho_{V,\,Hydrogen}$	2 222	kWh/m³	Xing et al., 2021
	$\rho_{V,\,LNG}$	5 833	kWh/m³	Shell Deutschland Oil GmbH, 2019
	$\rho_{V,\,MDO}$	11 000	kWh/m³	IOR energy Pty Ltd, 2010
	$\rho_{V,\,Methanol}$	4 389	kWh/m³	Kang et al., 2021
Sonne	B_{BCV}	20.600	m	Briese Research, n.d.
	D_{BCV}	6.400	m	Briese Research, n.d.
	f_{port}	15	%	Meinders, 2025
	$f_{transit}$	40	%	Meinders, 2025
	$L_{pp,\,BCV}$	102.860	m	Briese Research, n.d.
	$P_{nR,\,BCV}$	3 200	kW	Meinders, 2025
	$P_{pR,\,BCV}$	6 000	kW	Meinders, 2025
	$P_{transit,\,BCV}$	4 000	kW	Meinders, 2025
	Range	7 500	nm	Briese Research, n.d.
	N_{PoB}	80		Briese Research, n.d.
	$v_{s,\,BCV}$	12	kn	Briese Research, n.d.
	f_{port}	15	%	Meinders, 2025
	$f_{transit}$	40	%	Meinders, 2025

Table A.2: Overview of Input Parameters used in Measure Formulations.

Category	Parameter	Value	Unit	Source
	r	3.010	%	European Central Bank, 2025a

(Continued on next page)

(Continued from previous page)

Category	Parameter	TtW	Unit	Source
Carbon Prices	$C_{Carbon,\,2027}$	45	EUR/t_{CO_2}	Section 4.4.1
	$C_{Carbon,\,2055}$	675	EUR/t_{CO_2}	Section 4.4.1
Emission	f_{CO_2}	1		Climate Change Connection, 2020
	f_{CH_4}	25		Climate Change Connection, 2020
	f_{N_2O}	298		Climate Change Connection, 2020
	$c_{f\,CH_4,\,HVO}$	0.00005	g CH_4/g Fuel	European Parliament and European Council, 2023a
	$c_{f\,CH_4,\,MDO}$	0.00005	g CH_4/g Fuel	European Parliament and European Council, 2023a
	$c_{f\,CO_2,\,HVO}$	3.115	g CO_2/g Fuel	European Parliament and European Council, 2023a
	$c_{f\,CO_2,\,LNG}$	2.750	g CO_2/g Fuel	European Parliament and European Council, 2023a
	$c_{f\,CO_2,\,MDO}$	3.206	g CO_2/g Fuel	European Parliament and European Council, 2023a
	$c_{f\,CO_2,\,Methanol}$	1.375	g CO_2/g Fuel	European Parliament and European Council, 2023a
	$c_{f\,N_2O,\,HVO}$	0.00018	g N_2O/g Fuel	European Parliament and European Council, 2023a
	$c_{f\,N_2O,\,LNG}$	0.00011	g N_2O/g Fuel	European Parliament and European Council, 2023a
	$c_{f\,N_2O,\,MDO}$	0.00018	g N_2O/g Fuel	European Parliament and European Council, 2023a
	$c_{slip,\,LNG}$	3.100	%	European Parliament and European Council, 2023a
	$CO_{2eq\,WtT\,Ammonia,\,green}$	0.605	g $CO_{2\,eq}$/kWh	Seddiek and Ammar, 2023
	$CO_{2eq\,WtT,\,Ammonia,\,grey}$	475.200	g $CO_{2\,eq}$/kWh	European Parliament and European Council, 2023a
	$CO_{2eq\,WtT,\,HVO}$	−74.504	g $CO_{2\,eq}$/kWh	European Parliament, 2018
	$CO_{2eq\,WtT,\,LNG}$	66.600	g $CO_{2\,eq}$/kWh	European Parliament and European Council, 2023a
	$CO_{2eq\,WtT,\,MDO}$	51.840	g $CO_{2\,eq}$/kWh	European Parliament and European Council, 2023a
	$CO_{2eq\,WtT,\,Methanol,\,green}$	−210.060	g $CO_{2\,eq}$/kWh	European Parliament, 2018
	$CO_{2eq\,WtT,\,Methanol,\,grey}$	31.300	g $CO_{2\,eq}$/kWh	European Parliament and European Council, 2023a

(Continued on next page)

(Continued from previous page)

Category	Parameter	TtW	Unit	Source
Fuel Prices	$C_{Ammonia,\,Green,\,2025}$	648	EUR/t	IRENA, 2024b
	$C_{Ammonia,\,Green,\,2050}$	279	EUR/t	IRENA, 2024b
	$C_{Ammonia,\,Grey}$	270	EUR/t	Yang and Lam, 2023
	C_{HVO}	1 760	EUR/t	Argus O.M.R., 2025
	$C_{Hydrogen,\,2025}$	4 500	EUR/t	DNV, 2022b
	$C_{Hydrogen,\,2050}$	1 800	EUR/t	DNV, 2022b
	C_{LNG}	750	EUR/t	SEA-LNG, 2025
	$C_{Methanol,\,Green,\,2025}$	923	EUR/t	S&P Gobal, 2025
	$C_{Methanol,\,Green,\,2050}$	450	EUR/t	Kang et al., 2021
	$C_{Methanol,\,Grey}$	344	EUR/t	S&P Gobal, 2025
	C_{MDO}	456	EUR/t	S&P Gobal, 2025
Hull	C_{ST2}	30	EUR/h	Jactio, 2023
	C_{ST1}	1 000	EUR/t	Jactio, 2023
	C_{FR}	32	h/t	Kerlen, 1985
Inst. Cost	C_{EHR}	1 800	EUR/kW	Mondejar et al., 2018
	$C_{FC,\,Ammonia}$	1 836	EUR/kW	Seddiek and Ammar, 2023
	$C_{FC,\,Hydrogen}$	1 440	EUR/kW	IEA, 2019
	$C_{FC,\,Methanol}$	1 836	EUR/kW	
	$C_{ICE,\,Ammonia}$	900	EUR/kW	Seddiek and Ammar, 2023
	$C_{ICE,\,HVO/MDO}$	636	EUR/kW	TNO, 2020
	$C_{ICE,\,Hydrogen}$	900	EUR/kW	
	$C_{ICE,\,LNG}$	923	EUR/kW	TNO, 2020
	$C_{ICE,\,Methanol}$	655	EUR/kW	TNO, 2020
	$C_{Tank,\,Ammonia}$	28	EUR/GJ	Schreuder et al., 2025
	$C_{Tank,\,Hydrogen}$	1 180	EUR/GJ	TNO, 2020
	$C_{Tank,\,LNG}$	100	EUR/GJ	TNO, 2020
	C_{WASP}	325 000	EUR	Chica et al., 2023
Main.	$C_{Main.,\,WASP}$	535	EUR/month	Chica et al., 2023
	$t_{Main.,\,FC}$	25 000	h	Mylonopoulos et al., 2024